OPTIMAL SWITCHING CONTROL OF FLOW IN PV/T SYSTEMS WITH FORCED CIRCULATION

By

JUAN SIECKER

Master of Engineering in Electrical Engineering

In the Department of Electrical, Electronic and Computer Engineering

Faculty of Engineering and Information Technology

Central University of Technology, Free State

Supervisor: **Prof. K. Kusakana**

Co-supervisor: **Dr. B.P. Numbi**

May 2018

Declaration

I, JUAN SIECKER, student number   , do hereby declare that this research project which has been submitted to the Central University of Technology Free State, for the degree Master of Engineering in Electrical Engineering, is my independent work and complies with the Code of Academic Integrity, as well as other relevant policies, procedures, rules and regulations of the Central University of Technology, Free State, and has not been submitted before by any person in fulfilment (or partial fulfilment) of the requirements for the attainment of any qualification.

J. Siecker   Date: 12th of May 2018 (South Africa)

I

Dedication

This Dissertation is dedicated to the Lord Jesus Christ, my source of inspiration.

Acknowledgments

Firstly, I would like to thank God for giving me the strength and ability to complete this work, without Him none of this would be possible. His guidance and inspiration made it possible to complete this work.

To Professor Kanzumba Kusakana, my supervisor, I am truly thankful for the motivation and guidance that he bestowed upon me. I am also thankful to him for always pushing me to improve and never give up.

To Doctor Bubele Papy Numbi, my co-supervisor, I would like to thank for his outstanding guidance during the course of this research. I am also sincerely thankful for his support in completing this work.

I would like to thank my parents, Doctor Adriaan Siecker and Mrs. Christa Siecker, as well as my brother and sister, Rudie Siecker and Marianka Knox, for their support and encouragement.

List of abbreviations

Ac	collector surface area (m²)
As	tank surface area (m²)
ASHP	air source heat pump
BCR	benefits-to-cost ratio
C	specific heat capacity (J/kg°C)
CPV	concentrated photovoltaic
ELM	extreme learning machine
Fr	heat removal factor
G	solar global irradiance (W/m²)
GC-CPCS	ground coupled-central panel cooling system
h	surface heat transfer coefficient (W/m²K)
IPA	isopropyl alcohol
IRR	internal rate of return
k	thermal conductivity (W/m.K)
LCC	lifecycle cost
LSC	luminescent solar concentrators
PBP	payback period
PCM	phase-change materials
PMMA	polymethyl methacrylate
Ppv	generator output power (W)
Ppv,stc	rated power at STC (W)
PV	photovoltaic
PV/T	photovoltaic/thermal
SPP	simple payback period
STC	standard test conditions
Ta	ambient temperature (°C)

$T_{c,i}$	collector inlet water temperature (°C)
$T_{c,o}$	collector outlet water temperature (°C)
$T_{d,i}$	demand inlet cold water temperature (°C)
$T_{d,o}$	demand outlet cold water temperature (°C)
TE	thermoelectric
T_j	cell temperature (°C)
TRNSYS	transient system simulation tool
T_s	storage tank temperature
T_o	initial temperature (°C)
t_s	sampling time (hour)
$\dot{T}$	derivative of temperature
U_l	collector overall heat loss coefficient
$U(t)$	control variable switching status
Δx	thickness of insulation layer (m)
Υ	power temperature coefficient (0.043%/°C)
τ	transmittance factor
a	absorbance factor

Abstract

Cooling the operating surface is a key operational factor to take into consideration to achieve higher efficiency when operating solar photovoltaic systems. Appropriate cooling may improve the electrical efficiency and decrease the rate of cell degradation with time, resulting in maximization of the life span of photovoltaic modules. The excessive heat removed by the cooling system can be used in domestic, commercial or industrial applications.

The hybrid photovoltaic/thermal (PV/T) system cooled by forced water circulation is one of the most efficient methods used to improve the electrical performance of a PV module. These systems operate mostly on the principle in cooling the PV module at a constant flow rate. However, the optimal PV output power cannot be achieved due to the circulating water not absorbing most of the heat on the surface of the PV module.

In order to solve this problem, a mathematical model dealing with the optimal switching of flow in PV/T systems with forced circulation has been developed, with the aim of controlling the surface operating temperature whilst increasing the conversion efficiency.

The optimal switching control model is used to reduce the surface operating temperature of the PV module, where it is simulated by making use of the SCIP (Solving Constrained Integer Programs) solver in the optimization toolbox in MATLAB. The simulation results illustrate that the optimal switching control of flow may improve the electrical output power of a PV module, as well as effectively reducing the surface temperature thereof. Furthermore, an economic feasibility study was performed to compare these systems, where the optimal switching control strategy has a significantly higher initial capital cost compared to the standard PV system. However, when studying both systems over their predicted lifetime, the optimal switching control strategy generates a significantly higher profit, regardless of its extortionate initial capital cost, and is, therefore, the ultimately efficient system.

Keywords: Photovoltaic/thermal (PV/T) system, optimal switching control, cooling technologies, flat plate collector.

Content

VIII

IX

List of figures

XI

List of tables

Chapter I: Introduction

1.1. Background

Globalisation and economic growth led to an increase in the consumption of conventional methods in generating electricity, which have some negative environmental impacts, such as greenhouse gas emissions. Therefore, there was a need for investigating alternative energy sources, such as solar photovoltaic (PV) energy, which is currently the fastest growing renewable energy technology in the world [1].

However, solar PV energy systems still have the matter of low conversion efficiency. The surface operating temperature is one of the most important factors that affect the performance of a PV module. Due to the temperature raise, not all of the solar energy absorbed by the photovoltaic cells is converted into electrical energy. To satisfy the law of conservation of energy, the remaining solar energy is converted or wasted into heat. To solve this undesirable effect, heat extraction by forced water circulation has been proposed and implemented. The use of forced circulation will therefore result in reducing the panel temperature, hence improving its efficiency and in the meanwhile, producing hot water. Since the system produces both electrical and heat energy, it is referred to as a hybrid solar PV/Thermal system. However, the efficiency of the hybrid PV/T system will depend on the surface operating temperature and fluid flow at which the system operates. Hence, a higher electrical efficiency will be achieved if the fluid circulation pump is optimally switched to obtain the desired consuming temperature.

The aim of this work, therefore, is to develop an optimal switching control model that improves the efficiency of the hybrid solar PV/T system through a forced circulation.

1.2. Problem statement

The electrical efficiency of the PV panel decreases with an increase in its operating temperature (beyond 25 °C, depending on the material the solar cells are made of). The energy from the sun, which is not converted into electricity, is wasted as heat on the surface of the PV panel.

Therefore, wasted heat on the surface of the PV panel results in a decrease in the electrical efficiency of the PV panel.

1.3. Objective of the study

The aim of this work is to improve the operation efficiency of the PV system using a hybrid PV/T configuration. Therefore, the main objective of this work is to develop an optimal switching control model that improves the electrical efficiency of the hybrid solar PV/T system by collecting excess heat from the PV panel through a forced circulation.

1.4. Delimitations of the study

The study will be conducted with the following delimitations:
- The study will concentrate specifically on maximizing the hybrid PV/T power output through optimal switching control of a circulating fluid.
- The research will exclude the designing of the hybrid PV/T system with all of the components.
- The study will focus mainly on mathematical model developments and simulations.
- The study will exclude how a higher output power drawn by the motor can affect the output power of the PV panel, but will focus solely on the electrical output and thermal output of the PV panel.

2

1.5. Expected outcomes

- Scientific outcomes:
  - A mathematical model for optimal switching control of a hybrid solar photovoltaic/thermal system with forced circulation.
  - Conference presentations, journal articles as well as a Master's Dissertation.
- Social impact:
  - Energy and water saving awareness with renewable energy system.

1.6. Research methodology

The following methodology will be issued in this research:

- **Literature review**: The literature related to photovoltaic and previous researches on various cooling strategies used for hybrid photovoltaic/thermal systems will be reviewed.
- **System model development**: After reviewing the various cooling strategies, the mathematical model (objective function and subjected constraints) of the photovoltaic/thermal system will be developed.
- **Simulation of developed model:** The developed mathematical model will be optimized and simulated with MATLAB software.

1.7. Hypothesis

- The output power of the hybrid PV/T system will be increased significantly if the fluid flow rate is optimally controlled.
- An increase in the overall system efficiency will be observed with a mathematical model which maximizes the output power of the hybrid PV/T system.

3

1.8. Publications during the study

Journal papers:

- Siecker J., Kusakana K., Numbi B.P. 2017. "A review of solar photovoltaic systems cooling technologies." Renewable and Sustainable Energy Reviews, 79:192-203.

- Siecker J., Kusakana K., Numbi B.P. 2018. "Optimal Switching Control in PV/T Systems with Forced Circulation: Model Development." (Accepted to be published in advanced science letters).

- Siecker J., Kusakana K., Numbi B.P. 2018. "Optimal switching control of PV/T systems with water storage system using forced circulation". (Submitted).

Conferences papers:

- Siecker J., Kusakana K. 2017. "Cooling Photovoltaic Systems: A Survey of Available Technologies." 25th Southern African Power Engineering Conference (SAUPEC 2017), Stellenbosch, South Africa, 30 January-1 February, 194-199.

- Siecker J., Kusakana K., Numbi B.P. 2018. "Economic Analysis of Photovoltaic/Thermal Systems with Forced Circulation under Optimal Switching Control." International Conference on Domestic Use of Energy Conference (DUE 2018), Cape Town, South Africa, 03 April-05 April, 105-111.

- Siecker J., Kusakana K., Numbi B.P. 2018. "Optimal Switching Control of PV/T Systems with Energy Storage Using Forced Water Circulation: Case of South Africa". (Submitted).

1.9. Dissertation structure

This dissertation has been structured as follows:

Chapter I: comprise of the research background, problem statement and give the objective of the study and research methodology.

4

Chapter II: literature review on different cooling strategies used for hybrid photovoltaic/thermal systems.

Chapter III: present the proposed on/off control operation model with the detailed optimization algorithm.

Chapter IV: present and discuss the simulated optimization results obtained in MATLAB.

Chapter V: present the economic analysis.

Chapter VI: work of this dissertation and indicates the next level for future studies to be made.

Chapter II: Literature review

2.1. Introduction

One of the most widespread technologies of renewable energy generation is the use of photovoltaic (PV) systems which convert sunlight into usable electrical energy [1-2]. This type of renewable energy technology, which is pollutant free during operation, diminishes global warming issues, lowers operational cost and offers minimal maintenance and the highest power density compared to the other renewable energy technologies; highlights the advantages of solar photovoltaic (PV) energy [3-4].

Apart from the several advantages displayed by the PV technology, this conversion system has a few general problems such as hail, dust and surface operating temperature which can negatively affect the efficiency of the conversion system [5]. Exogenous climatic parameters such as wind speed, ambient temperature, relative humidity, accumulated dust and solar radiation are the most common natural factors which influence the surface temperature of a PV module [6]. Every 1°C surface temperature rise of the PV module causes a reduction in efficiency of 0.5% [7]. Therefore, due to the temperature rise, not all of the solar energy absorbed by the photovoltaic cells is converted into electrical energy. To satisfy the law of conservation of energy, the remaining solar energy is converted into heat. The consequences of this wasted heat bring about a reduction in the overall conversion efficiency.

Efficiency improvements in solar energy conversion systems need to be made in order for this renewable energy technology to be a viable solution. To make it a viable solution, there is a need to find different means of solving this temperature problem, which needs to result in an increase of the overall conversion efficiency.

Very few authors have tried to put together and conduct an extensive review of different technologies that can be used to cool the operating surface of solar panels, with the aim of increasing the overall efficiency of the solar conversion system.

The authors of the paper cited in reference [8] have briefly discussed various solar PV panel cooling technologies. However, only a few technologies were introduced, while the main focus of the paper was on the testing and performance of a developed ground-coupled central panel cooling system (GC-CPCS).

In reference to [9], the authors presented an overview of various methods that can be employed for cooling photovoltaic cells. However, when studied closely, it can be observed that the focus of the paper was only on examining the passive, forced air and liquid forced convection cooling methods applied to different solar concentrator systems.

Unlike the above-mentioned review studies, this research provides a comprehensive review of how different technologies can be used to minimize the negative effects of increased temperature, while trying to improve the performance of a PV panel, operating beyond the recommended temperature of the standard test conditions (STC). For this purpose, an extensive number of research papers from different authors are used to achieve the objectives of the current study. Different tools (schematic diagrams, pictures, tables and figures) are used to enhance the content and to offer an effective and simple presentation.

The following technologies will be discussed and analysed in this work:

- Floating tracking concentrating cooling system (FTCC)
- Hybrid solar photovoltaic/thermal system cooled by water spraying
- Hybrid solar photovoltaic/thermoelectric (PV/TE) system cooled by heat sink
- Hybrid solar photovoltaic/thermal (PV/T) cooled by forced water circulation
- Improving the performance of solar panels through the use of phase-change materials
- Solar panel with water immersion cooling technique
- Solar PV panel cooled by transparent coating (photonic crystal cooling)
- Hybrid solar photovoltaic/thermal system cooled by forced air circulation
- Solar panel with thermoelectric cooling

This chapter is organized as follows: in Section 2.2, the basic operational principle of a PV cell is presented. The problem caused by an increase of temperature is clearly explained using graphs and equations. In section 2.3, the various cooling technologies are described based on

their operational principle using a suitable visual representation. In section 2.4, an extensive tabular list of reviewed works is provided. Information such as the authors, research focus, review contribution and the technology used to address the temperature problem, can be obtained from this table. A discussion of this paper's main findings on the various technologies reviewed is available in section 2.5 and the last section is the Conclusion.

2.2. Description of a solar photovoltaic system operation

When a PV cell is exposed to solar radiation, the photon is absorbed by the P-N junction, which creates a potential difference across the junction. The charge-carriers start to flow and the resulting photocurrent is denoted as I_{PV}, which is paralleled by a P-N junction diode.
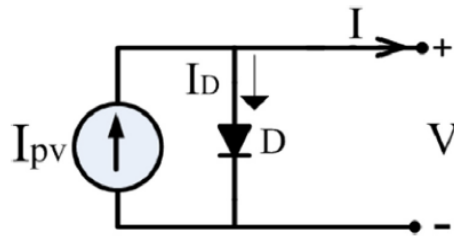
Figure 2.1: Equivalent circuit of a PV cell [10]

Investigating the performance of a PV cell presents that the surface operating temperature plays a crucial part during the PV energy conversion process. High ambient temperatures and high PV panel surface operating temperatures cause overheating of the PV panel, which reduces the efficiency radically [11].

Fig. 2.2 presents the preferred operating temperature ranges between 0°C and 75°C. The P-V characteristics are the relation between the output power and the output voltage, while the solar irradiance E, and module temperature Tm, are kept constant.

8
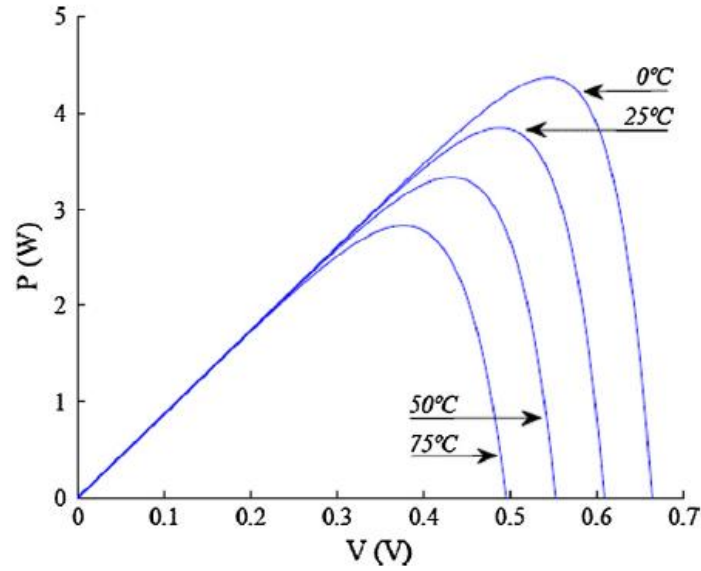
Figure 2.2: The ideal P-V characteristics of a solar cell [12].

The effect of temperature on the solar panel's electrical efficiency can be analysed using the following equation:

$$\eta_{PV} = \eta_{TR}[1 - \beta_R(T_C - T_R) + \gamma \log_{10} I_{PV}] \tag{2.1}$$

where: η_{PV} is the PV module efficiency measured at reference cell temperature; T_R (25°C). β_R is the temperature coefficient for cell efficiency (typically 0.004-0.005/°C) [13]; I_{PV} is the average hourly irradiation incident on the PV module at nominal operating temperature, NT. T_C is the PV module temperature, and γ is the radiation-intensity coefficient for cell efficiency, which is mostly assumed to be zero [14, 15], reducing the equation to:

$$\eta_{PV} = \eta_{TR}[1 - \beta_R(T_C - T_R)] \tag{2.2}$$

By adding and subtracting the ambient temperature, T_A, to and from the two temperature terms respectively, the following expression is obtained [13]:

9

$$\eta_{PV} = \eta_{TR}[1 - 0.9\beta\left(\frac{I_{PV}}{I_{PV,NT}}\right)(T_{C,NT} - T_{A,NT}) - \beta(T_A - T_C)] \qquad (2.3)$$

where: $T_{C,NT}$ (typically 45°C) and $T_{A,NT}$ (typically 20°C) are the cell and ambient temperatures respectively. When using equation (2.3), it is clearly observed that when $T_{A,NT}$ increases, the efficiency decreases.

2.3. Technologies used to increase the efficiency of the PV by solving the temperature problem

In this section, the general operational principle of the different technologies that can be used to minimize the effect of the increased temperature, while attempting to improve the performance of a PV panel operating beyond the recommended temperature of the Standard Test Conditions (STC), will be explained technically in order to understand the relevant researches from different authors gathered, reviewed and summarized in section 2.4 as well as the discussion in section 2.5.

2.3.1. Floating tracking concentrating cooling (FTCC)

One method to achieve optimal output power of a PV module, makes use of artificial basins for installing PV floating plants. These floating plants consist of a platform with PV modules, a set of reflectors and a solar tracking system. Cooling of the PV module is achieved via water sprinklers. Reflectors are used to concentrate the solar radiation to increase the energy harvesting. The floating platform allows for a one-axis tracking system for the positioning of reflectors and also for increasing the solar radiation on the PV modules. These plants are called FTCC, the acronym of floating, tracking, concentrating and cooling. Fig. 2.3 shows an FTCC system with its main components, where the following numbering represents: (1) PV modules

10

(2) Sprinklers

(3) Solar reflectors
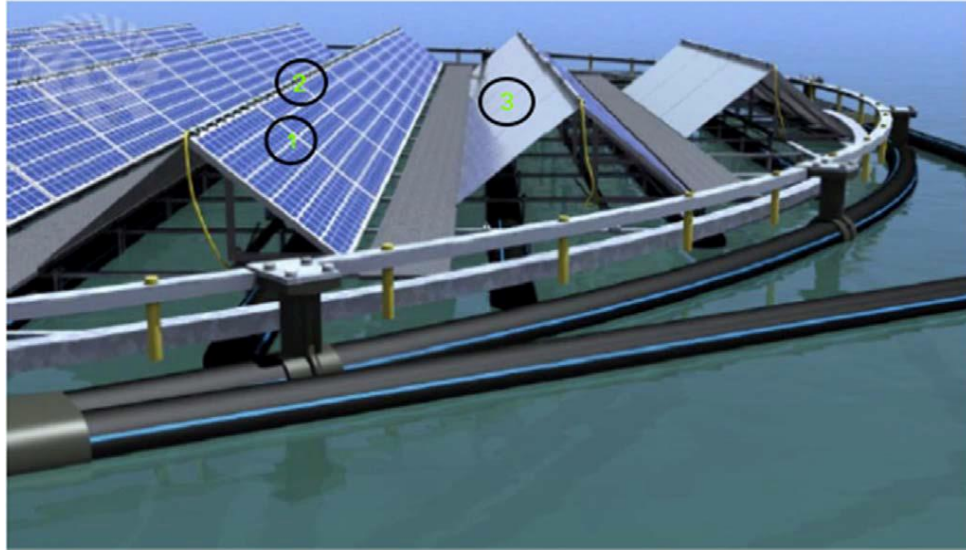
Figure 2.3: Floating tracking concentrating cooling (FTCC) [16]

2.3.2. Hybrid photovoltaic/thermal (PV/T) system cooled by water spraying

In this system, a centrifugal pump is used to force water flow through the spraying nozzles from the tank via a suction pipe. The suction pipe consists of a non-return valve and strainer to avoid the sucking in of large particles and to protect the centrifugal pump. Beyond the strainer, water is transferred to the spraying nozzles with the intention to cool the PV module via an industrial transparent water filter. A hybrid photovoltaic/thermal (PV/T) system, as seen in the figure below, consists of PV modules and a cooling system. The cooling agent, i.e. water, is sprayed on the surface area of the PV panel by using a fan [10]. When spraying water on the surface of the PV module, the temperature decreases and the electrical efficiency increases.

11
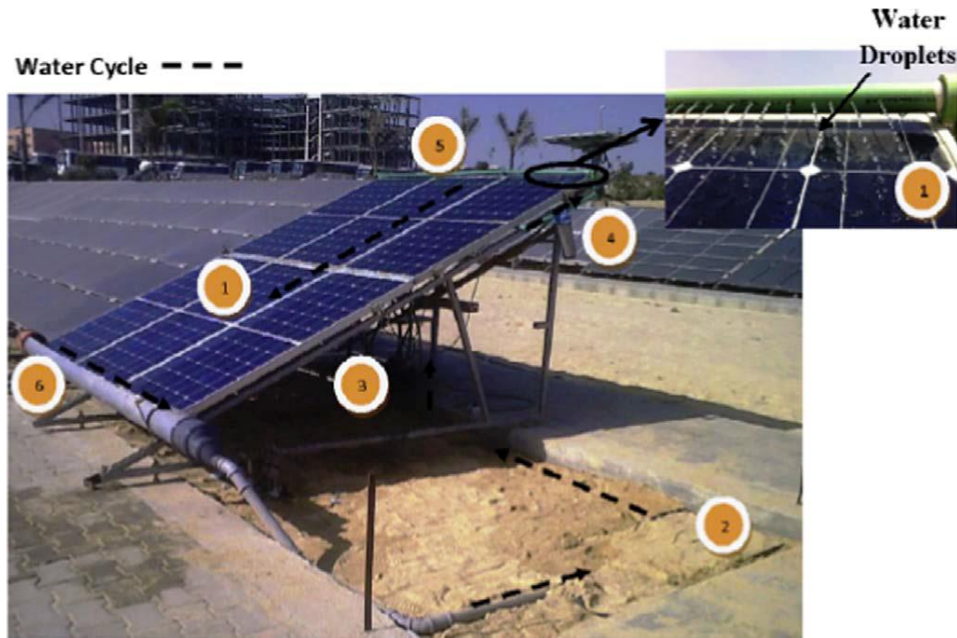
Figure 2.4: Hybrid solar photovoltaic/thermal (PV/T) system cooled by water spraying [10]

The numbers on the figure above represent the following components:

(1) PV modules

(2) Aluminium water tank

(3) Centrifugal pump

(4) Industrial transparent water filter

(5) Water spraying nozzles

(6) Drain pipe for water collection

2.3.3. Hybrid photovoltaic/thermoelectric (PV/TE) system cooled by heat sink

Advancements have been made in PV conversion systems by combining them with a thermoelectric module (TE) and heat sink as seen in Fig. 2.5 [17]. The TE module is used to absorb heat from the surface of the PV module, which is generated by thermalization loss of photons containing high energy and transmission loss of photons containing low energy. The thermoelectric module is placed at the centre of the back part of the PV module. One thermal resistor is placed on top of the TE module and other thermal resistors in the remaining

12

surrounding areas of the TE module. When exposing the PV/TE system to solar radiation, the temperature increases with time. There is a slight temperature difference between the thermal resistor above and the thermal resistors placed below, due to the diffusion of charge carriers within the thermoelectric materials when the top and bottom surfaces have a temperature variance. The collected power from the PV module is dissipated into the resistor and stored in a battery. The heat sink is used for heat dissipation of the PV module, which cools down the surface of the PV module [18].
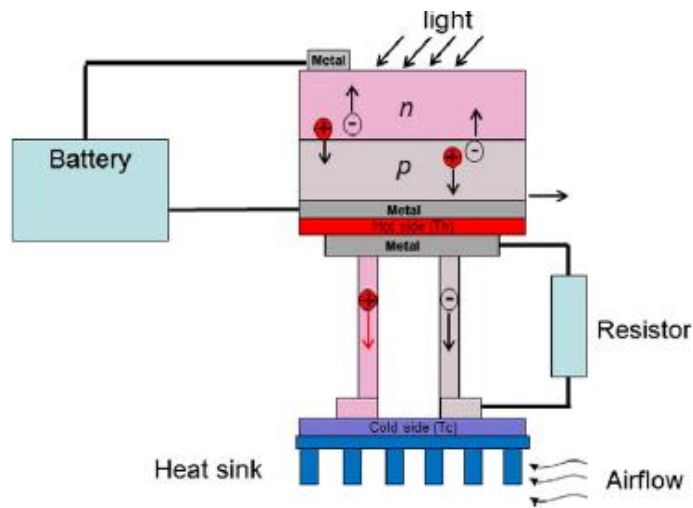
Figure 2.5: Hybrid PV/TE system with heat sink [17].

2.3.4. Hybrid solar photovoltaic/thermal (PV/T) system cooled by forced water circulation

With the aim of increasing the PV systems' efficiency, a hybrid photovoltaic/thermal (PV/T) system generates electrical energy and thermal energy simultaneously [19]. The system consists of a PV module and thermal collecting pipes, which are mounted to the back part of the PV module, as seen in Fig. 2.6 [20]. Rectangular collecting pipes are used to improve the contact area between the PV module and the thermal collecting pipes. Water is used as the circulating fluid, which flows through the paralleled thermal collecting pipes via a DC pump, which may be powered by the PV module or other sources. When the hybrid system is exposed to solar radiation, waste heat is transferred to the circulating water flowing through the thermal

13

collecting pipes. The heated water flows back to the hot water insulated tank for domestic or other applications.

Figure 2.6: Hybrid photovoltaic/thermal (PV/T) system cooled by forced water circulation [20].

The numbers on the figure above represent the following components:

(1) PV modules
(2) Circulation pump
(3) Water storage tank

2.3.5. Improving the performance of solar panel through the use of phase-change materials

One technique that can be used to reduce the surface operating temperature of a PV panel in order to reach a higher electrical efficiency, is by incorporating phase-change materials (PCM), such as tungsten photonic crystals. PCM is a latent heat storage material, which is situated behind the PV panel as seen in Fig. 2.7. When the temperature increases, the chemical bonds within the PCM separate as phase-changing from solid to liquid occurs. The PCM

14

absorbs heat, due to the phase-change being a endothermic process. When the heat stored within the storage material reaches the phase-change temperature, the material starts to melt [21]. The temperature then stabilises until the melting process is completed. It is called latent heat storage material, as the heat is stored during the melting process (phase-change process).

Figure 2.7: PV panel with phase-change materials [22]

The numbers on the figure above represent the following components:

(1) PV module

(2) PCM module.

2.3.6. Water immersion cooling technique

Another technique that may be used to reduce the temperature of a PV panel involves implementing the water immersion cooling technique as seen in Fig. 2.8. With the water immersion cooling technique, a PV module is placed in large water bodies like rivers, oceans, lakes, canals, etc. Water is used as the immersing fluid, which absorbs the heat from the PV module and maintains the surface temperature of the PV module. Therefore, when water absorbs the heat from the PV module, the electrical efficiency increases [23].

15
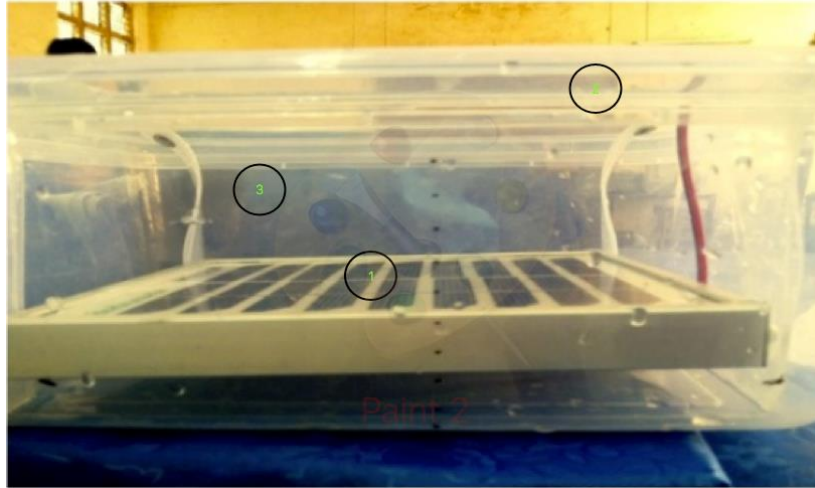
Figure 2.8: Water immersion cooling technique applied to PV panel [23]

The numbers on the figure above represent the following components:

(1) PV modules

(2) Plastic container

(3) Water

2.3.7. Transparent coating (photonic crystal cooling)

A technique that may be used to reduce the surface operating temperature of a PV panel in order to reach a higher electrical efficiency involves incorporating transparent coating (photonic crystal cooling). This visible transparent thermal blackbody is based on silica photonic crystals and is placed on the upper surface of the PV cells, and it has the capability to reflect heat generated by the PV cells in the form of infrared light (thermal long infrared transparency window, which is in the 8-30 microns range) under solar irradiance back into space [24]. Simultaneously, the PV cells are slightly enhanced by anti-reflection and light-trapping effects. Therefore, the PV cells are cooled by enabling more photons to be absorbed by the PV module. A PV module cooled by transparent coating (photonic crystal cooling), is shown in Fig. 2.9 below.

16
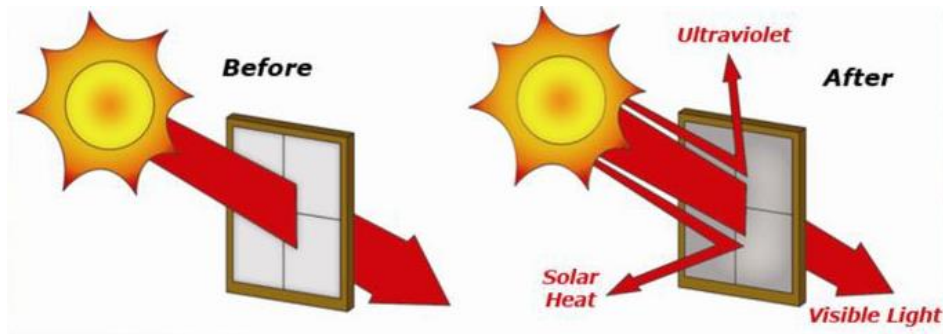
Figure 2.9: PV panel cooled by transparent coating (photonic crystal cooling) [25]

2.3.8. Hybrid photovoltaic/thermal (PV/T) system cooled by forced air circulation

An alternative technique that may be used to reduce the surface operating temperature of a PV panel in order to reach a higher electrical efficiency makes use of forced air circulation. This system consists of a photovoltaic module, which is placed on top of a steel plate with an air channel underneath, as seen in Fig. 2.10. Air is used as the working fluid, which is forced through the channels by a fan with a nozzle. The fan is powered by the PV module, where the energy consumption thereof increases as the cavity velocity increases, and also as the channel width and the heat exchanging surface increase. The heat from the PV panel is transferred to the air in the channels via convection, therefore reducing the surface operating temperature in order to reach a higher electrical efficiency [26].

17

Figure 2.10: Hybrid solar photovoltaic/thermal (PV/T) system cooled by forced air circulation [8]

The numbers on the figure above represent the following components:

(1) PV module

(2) Forced circulation fan

(3) Air channel

2.3.9. Thermoelectric cooling system

Thermoelectric devices comprise of an n-type semiconductor and p-type semiconductor. Under a temperature gradient, the majority charge carriers diffuse from the hot section (positively charged electrode), to the cold section (negatively charged electrode), due to the Peltier effect, which in turn creates a voltage resulting in current flow. When the voltage is applied across the material, it forces a current through it, which causes the heat pump to cool the one section and heat the other, which should be connected to a heat sink for excess heat dissipation. The thermoelectric cooling system described, can be seen in Fig. 2.11 [8].

18
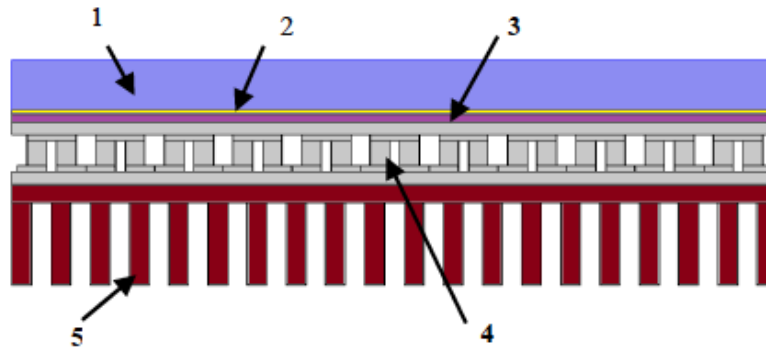
Figure 2.11: Thermoelectric cooling system for PV cells [27]

The numbers on the figure above represent the following components:

(1) Glass cover

(2) PV cells

(3) Insulator

(4) TEG module

(5) Fin heat sink

2.4. Relevant literature review

Several authors have attempted to improve the efficiency of solar panels by attending to the problem linked to the PV surface's operating temperature. Table 2.1 summarizes various papers by authors in which attempts have been made to increase the efficiency of the PV module, using the various techniques explained above. The table provides the source authors, the focus area of the study; a summary of the review contribution and the technology used to address the temperature problem.

19

Table 2.1: Highlights of selected studies on cooling of PV modules in terms of technology/Contribution

Authors	Highlights/Contribution	Technology
Carlotti M, Ruggeri G, Bellina F. and Pucci A. [28]	• Investigation improving optical efficiency of solar concentrators was made. • PMMA layers increased light concentration effectively.	FTCC
Vishwanathan B, Reinders A.H.M.E, de Boer D.K.G, Desmet L, Ras A.J.M, Zahn F.H. and Debije M.G. [29]	• Performance comparison between flat and cylindrically bent PMMA light guide sheets was done. • Results showed cylindrically bent PMMA to be superior.	FTCC
Shaltout M.A.M, Ghettas A. and Sabry M. [30]	• Performance of PV module combined with V-trough concentrator was evaluated. • V-trough concentrators showed increased efficiency in hot desert climate.	FTCC
Andrade L.A, Barrozo M.A.S. and Vieira L.G.M. [31]	• Study on dynamic heating in solar dish concentrators was done. • Results show validity to provide high thermal energy demands.	FTCC
Parel T.S, Pistolas C, Danos L. and Markvart T. [32]	• Model developed showing angular distribution light	FTCC

	• escaping from luminescent solar concentrator (LSC) edge. • Can be applied to PV modules, which enhances efficiency.	
Wu Y, Connelly K, Liu Y, Gu X, Gao Y. and Chen G.Z. [33]	• Smart solar concentrators lightweight, low cost and generate electricity. • 3-D tracing technique used to analyse optimal optical performance, where results show output power increased.	FTCC
Rabl A. [34]	• Acceptance angle, sensitivity to mirror errors, reflector area and average reflections of parabolic concentrators were evaluated. • Advantageous for high thermal applications.	FTCC
Correia S.F.H, Lima P.P, Andre P.S, Ferreira M.R.S. and Carlos L.A.D. [35]	• High efficiency LSC for flexible wave-guiding photovoltaics proposed showing optimal optical and power conversion efficiency. • Cost-effectiveness and negligibility of self-absorption and transfer losses validated.	FTCC
Akbarzadeh A. and Wadowski T. [36]	• Cooling PV module can increase output power by around 50%.	Sprinkler

	• Results show PV panel does not allow PV panel surface temperature to go beyond 46°C.	
Alonso Garcia M.C. and Balenzategui J.L. [37]	• Nominal operation cell temperature (NOCT) effective method to estimate PV module performance. • Applied to different types of PV modules to estimate temperature and performance [38].	Sprinkler
Dubey S. and Tiwari G.N. [38]	• Model derived for PV/flat plate solar collector. • Results show an increase in thermal efficiency.	Sprinkler
Hashim H. , Bomphrey J.J. and Min G. [39]	• Model derived for geometry optimisation of thermoelectric modules. • Simulation results show an increase in electrical efficiency.	Hybrid PV/TE
Popovici C.G., Hudisteanu S.V., Mateescu T.D. and Chereches N.C. [40]	• Angle between ribs and base plate of heat sink modified to evaluate performance. • Cooling method reduced PV surface temperature by 10°C.	Hybrid PV/TE
Verma V., Kane A., and Singh B. [41]	• Dynamic model developed to simulate thermal and electrical characteristics of TEM material.	Hybrid PV/TE

22

	• Simulation results show maximum energy harvesting where hybrid system endured dynamic perturbation and solar radiation.	
Ali H., Yilbas B.S., and Al-Sulaiman F.A. [42]	• Performance of pin shaped thermoelectric generator is analysed. • Simulation results show increased output power of PV module when air flow is utilised more efficiently.	Hybrid PV/TE
Soprani S., Haertel J.H.K., Lazarov B.S., Sigmund O. and Engelbrecht K. [43]	• Model developed for hybrid PV/thermoelectric modules integrated with heat sink specific design constraints. • Simulation and experimental results indicate good compatibility with one another.	Hybrid PV/TE
Kalogirou S.A. and Tripanagnostopoulos Y. [44]	• Models tested and evaluated according to their electrical and thermal efficiencies. • Increased electrical and thermal efficiency, and economic viability improved.	Hybrid PV/T
Ali H.H., Ahmed M. and Abdel-Gaied S.M. [45]	• Investigated how convection heat transfer and fluid flow affect PV module efficiency.	Hybrid PV/T

23

	• Model results show different Reynolds number values in laminar flow with both optimum plate thickness and length increase heat transfer.	
Wu S.Y., Zhang Q.L., Xiao L., Guo F.H. [46]	• Model developed to predict thermal-electrical performance of heat pipe. • Results show overall thermal, electrical and exergy efficiencies increased to 63.65%, 8.45% and 10.26%.	Hybrid PV/T
Michael J.J., Iniyan S., Goic R. [47]	• Flat plate solar collector used to increase PV module efficiency. • An investigation is done on the different solar flat plate collector PV/T, efficiencies, advantages and disadvantages.	Hybrid PV/T
Hu M., Zheng R., Pei G., Wang Y., Li J. and Ji J. [48]	• Wickless heat pipe compared with wire-meshed heat pipe. • Thermal efficiency on wickless heat pipe and wire-meshed heat pipe was 52.8% and 51.5%, respectively.	Hybrid PV/T
Jouhara H., Szulgowska-Zgrzywa M., Sayegh M.A., Milko J., Danielewicz	• Experiments done on hybrid PV/T systems to analyse hot water to consumer.	Hybrid PV/T

J., Nannou T.K. and Lester S.P. [49]	• Results show systems able to supply 60% of consumer's hot water needs on cloudy days and 100% on sunny days.	
Ntsaluba S., Zhu B. and Xia X. [50]	• Model developed to maximize the energy extracted from solar collectors by optimizing flow rate. • 7.82% increased extracted energy, where thermal efficiency decreased between 5.54% and 7.34% using connecting pipes.	Hybrid PV/T
Tang X., Quan Z. and Zhao Y. [51]	• Micro-heat pipe array used for PV panel cooling, by making use of evaporator and condenser for heat transfer. • Experiments show air cooling increased electrical efficiency by 2.6% and water cooling by 3%, which indicates water cooling to be superior.	Hybrid PV/T
Sotehi O., Chaker A., Maalouf C. [52]	• Hybrid PV/T solar collector for net zero energy buildings proposed. • Results indicate produced solar electricity is high and covers hot water needs, air conditioning,	Hybrid PV/T

	lighting and household appliances.	
Aste N., Leonforte F. and Del Podro C. [53]	• Water glazed PV/T system, where roll-bond flat plate absorber is used. • Model developed to evaluate performance of PV/T collectors, where results validated enhancements in electrical efficiency.	Hybrid PV/T
Kroi A., Prabst A., Hamberger S., Spinnler M., Tripanagnostopoulos Y. and Sattelmayer T. [54]	• Seawater-proof hybrid PV/T solar collector developed and applied to reverse osmosis (RO) desalination plant. • Seawater utilized to cool PV modules, where results show increased electrical efficiency.	Hybrid PV/T
Tonui J.K. and Tripanagnostopoulos Y. [55]	• PV/T solar collector cooled via natural airflow, where two methods improving heat transfer are evaluated. • Thin metal sheet suspended at middle or fins attached to back part of PV panel, where modelling and outdoor test show good agreement.	Hybrid PV/T

Tonui J.K. and Tripanagnostopoulos Y. [56]	• PV/T system cooled by forced/natural air circulation with suspended metallic sheets or fins attached to back part of PV panel. • Compared with typical PV/T air cooling system, where results show increased electrical and thermal outputs.	Hybrid PV/T
Tripanagnostopoulos Y, Yianoulis P. and Patrikios D. [57]	• Hybrid PV/T system, where water circulates through connecting pipes with fins attached to back part of PV module. • Electrical performance improved.	Hybrid PV/T
Tripanagnostopoulos Y. [58]	• Hybrid action extraction system developed, which cools PV panel either by air or water. • Experiment results show increased efficiency and cost-effectiveness.	Hybrid PV/T
Tripanagnostopoulos Y, Nousia T, Souliotis M. and Yianoulis P. [59]	• Hybrid PV/T solar collector cooled. • Outdoor tests performed to evaluate, where results show electrical efficiency improved.	Hybrid PV/T

Tripanagnostopoulos Y. [60]	• Flat absorber, static parabolic absorber and Fresnel lens compared. • Design and application aspects discussed, where results show electrical efficiency increased.	Hybrid PV/T
Rahul S.R. and Hariharan R. [61]	• PV/T collector integrated with blower passing air to back part of PV panel to increase efficiency and reduce surface temperature. • Results show electrical efficiency increase and surface temperature reduced.	Hybrid PV/T
Hosseini R, Hosseini N. and Khorasanizadeh H. [62]	• PV system cooled by thin film of water using another system to transfer heat to water. • Results show electrical efficiency improved.	Hybrid PV/T
Tan W.C., Chong K.K. and Tan M.H. [63]	• Multiple-channel heat sink for CPV cells. • 91.4°C cell temperature and 0.6m/s flow rate optimized conversion efficiency to 31.8% and net power to 4064W.	Hybrid PV/T
Huang M.J, Eames P.C. and Norton B. [63]	• 2-D finite volume heat transfer model developed for building-	Phase-change materials (PCM) used to decrease the operating

28

	integrated PV/phase-change materials. • The simulation and experimental results indicate an increase in efficiency.	temperature of solar panels
Huang M.J, Eames P.C. and Norton B. [64]	• Internal fins for bulk PCM thermal conductivity compared with datum single flat aluminium plate used in buildings. • Internal fins reduced PV/PCM system temperature by 30°C compared to single flat aluminium plate.	Phase-change materials (PCM) used to decrease the operating temperature of solar panels
da Cunha J.P. and Eames P. [65]	• PCM phase transition temperatures between 0 and 250°C presented. • Organic compounds and salt hydrates effective below 100°C, where eutectic mixtures vary from 100 to 250°C.	Phase-change materials (PCM) used to decrease the operating temperature of solar panels
Liu L., Su D., Tang Y. and Fang G. [66]	• Thermal conductivity enhancement of phase-change materials for thermal energy storage presented [67]. • Models developed to improve PCM thermal conductivity and discussed for in-depth investigation.	Phase-change materials (PCM) used to decrease the operating temperature of solar panels

Wang T., Wang S., Luo R., Zhu C., Akiyama T. and Zhang Z. [68]	• Microencapsulation of phase-change materials with binary cores and calcium carbonate shells for thermal energy storage proposed. • Results show binary cores ranges between 55.7% and 59.4%. When heated to 400°C mass loss of microcapsules between 5% and 28%. • The conductive calcium carbonate shell enhances PV efficiency.	Phase-change materials (PCM) used to decrease the operating temperature of solar panels
Hachem F., Abdulhay B., Ramadan M., El Hage H., El Rab M.G. and Khaled M [69]	• Pure and combined PCM enhances electrical performance of PV panel, where transient energy balance presented to analyse thermal behaviour. • Combined PCM increased electrical efficiency by an average of 5.8%.	Phase-change materials (PCM) used to decrease the operating temperature of solar panels
Hasan A., Sarwar J., Alnoman H. and Abdelbaqi S. [70]	• Yearly energy performance of paraffin based PV/PCM system presented. • Model developed to predict melting and solidification fractions, where electrical energy	Phase-change materials (PCM) used to decrease the operating temperature of solar panels

	yield improved by 5.9% and cost-effectiveness increased.	
Sardarabadi M., Passandideh-Fard M., Maghrebi M.J. and Ghazikhani M [71]	• Experiments done on ZnO/water nanofluid (0.2 wt%) and paraffin wax. • PVT with PCM/Nanofluid increased thermal energy output by 48%.	Phase-change materials (PCM) used to decrease the operating temperature of solar panels
Chandel S.S. and Agarwal T [72]	• Research must be focused on inorganic PCM and only economically viable in high insolation throughout the year. • Due to high system costs and only a 5% electrical efficiency increase, further research must be done.	Phase-change materials (PCM) used to decrease the operating temperature of solar panels
Su D., Jia Y., Alva G., Liu L and Fang G [73]	• Dynamic model developed to do comparative performance analysis of PV/PCM. • Upper phase-change material ensured improved performance.	Phase-change materials (PCM) used to decrease the operating temperature of solar panels
Chinamhora T., Cheng G., Tham Y. and Irshad W. [74]	• Performance of PV panel analysed when submerged in water at various depths. • Results show surface temperature reduced effectively, which enhances electrical efficiency tremendously.	PV panel with water immersion cooling

Zhu L., Boehm R.F., Wang Y., Halford C. and Sun Y. [75]	• De-ionised water used as immersion fluid to cool PV cells in two-axis dish concentrator tracking system presented. • Results show CPV module cooled to 45°C at a 920W/m² irradiance, 17°C ambient temperature and 30°C water inlet temperature.	PV panel with water immersion cooling
Abrahamyan Y.A., Serago V.I., Aroutiounian V.M., Stafeev V.I., Karamian G.G., Martoyan G.A. and Mouradyan A.A. [76]	• Efficiency of solar cells immersed in isotropic liquid dielectric, where analysis was done on current/voltage characteristics and fill factor. • Efficiency increased by 40-69% of reference value.	PV panel with water immersion cooling
Wang Y., Fang Z., Zhu L., Huang Q., Zhang Y. and Zhang Z. [77]	• PV cells immersed in liquids evaluated performance under simulated sunlight, where non-polar silicon oil showed best performance. • PV cells submerged in liquid improve performance thereof.	PV panel with water immersion cooling
Rosa-Clot M., Rosa-Clot P., Tina G.M. and Scandura P.F. [78]	• Performance of PV panel submerged in water evaluated at different submersion depths.	PV panel with water immersion cooling

32

	• Results show lower electrical efficiency when submerged in deeper water.	
Han X., Wang Y. and Zhu L. [79]	• De-ionized (DI) water, isopropyl alcohol (IPA), ethyl acetate, and dimethyl silicon oil chosen as submerging liquids. • 3-D model developed where results show direct-immersion cooling keeps PV cells at low temperature, improving electrical efficiency.	PV panel with water immersion cooling
Sun Y., Wang Y, Zhu L, Yin B., Xiang H. and Huang Q. [80]	• Direct liquid-immersion cooling of concentrator PV cells, where dimethyl silicon oil is used as immersing fluid. • Results show temperature controllable from 20°C to 31°C at 920W/m² irradiance and Reynolds number varying between 13,602 and 2720.	PV panel with water immersion cooling
Xiang H., Wang Y., Zhu L, Han X., Sun Y. and Zhao Z. [81]	• Two structural models developed and tested under actual weather conditions. • Heat transfer performance of two structural models at axial and lateral direction in agreement with simulations.	PV panel with water immersion cooling

33

Arpin A. K., Losego M.D., Cloud A.N., Ning H., Mallek J., Sergeant N. P., Zhu L., Yu Z., Kalanyan B., Parsons G.N., Girolami G.S., Abelson J.R., Fan S. and Braun P.V. [82]	• 3-D metallic photonic crystals modified to be within emission spectrum for useful solar thermo-photovoltaics. • High quality tungsten photonic crystals maintain stability to 1400°C.	PV panel cooled by transparent coating (photonic crystal cooling)
Zhu L, Raman A., Wang K.X., Anoma M.A. and Fan S. [83]	• Micro-photonic design approaching ideal performance scheme used to cool PV panel via radiative cooling. • Results show micro-photonic design effectively cools PV cells.	PV panel cooled by transparent coating (photonic crystal cooling)
Cao C. , Li H. , Feng G. , Zhang R. and Huang K. [84]	• PV/T system is applied to air source heat pump (ASHP) heating systems in cold climatic conditions. • TRNSYS transient simulation software used, where results show outlet temperature reaches 76.6°C, which improves heating efficiency.	Hybrid solar Photovoltaic/Thermal system cooled by forced air circulation
Tiwari A., Sodha M.S. , Chandra A and Joshi J.C. [85]	• Performance of PV module integrated with air duct evaluated by developing a model to determine overall efficiency.	Hybrid solar Photovoltaic/Thermal system cooled by forced air circulation

34

	• Results show good compatibility with developed model, which indicates increased overall efficiency reached.	
Mojumder J.C., Ong H.C., Chong W.T., Izadyar N. and Shamshirband S. [86]	• Extreme learning machine (ELM) applied to PV/T air cooled system. • ELM model compared with genetic programming and artificial neural networks models, where results show ELM model to be most accurate.	Hybrid solar Photovoltaic/Thermal system cooled by forced air circulation
Kasaeian A., Khanjari Y., Golzari S., Mahian O and Wongwises S [87]	• Investigate effects of forced convection on thermal and electrical efficiencies of PV/T system. • Reducing depth of channel and Reynolds number increases thermal efficiency, but has no considerable effect on electrical efficiency. • Thermal efficiency ranges from 15–31% while electrical efficiency ranges from 12-12.4%.	Hybrid solar Photovoltaic/Thermal system cooled by forced air circulation
Saygin H., Nowzari R., Mirzaei N., and	• Model developed to determine effect on thermal and electrical	Hybrid solar Photovoltaic/Thermal

35

Aldabbagh L.B.Y [88]	performances when PV module position changed inside collector. • Maximum thermal and electrical performance measured when distance between PV module and cover is 3cm and 5cm, respectively. • Analysis of variance used to compare electrical efficiency of PV/T system with standard PV system, where hybrid system is superior.	system cooled by forced air circulation
Senthil Kumar R., Puya Priyadharshini N. and Natarajan E [89]	• Heat rejected by heat sink used for domestic applications [90]. • Geometric model developed and compared with experimental results, showing good compatibility.	Hybrid PV/TC
Borkar D.S., Prayagi S.V. and Gotmare J [91]	• Hybrid PV/TC system presented to increase overall efficiency by keeping temperature constant within limits. • Model developed to evaluate performance, where results show overall efficiency improvement.	Hybrid PV/TC

Benghanem M, Al-Mashraqi A.A. and Daffalla K.O. [92]	• TEC module used to cool PV panel in hot climatic areas. • Efficiency increased by using TEC in hot areas.	Hybrid PV/TC
Najafi H and Woodbury K. [93]	• Model developed to determine temperature in different sections and calculate required power for TEC and excess heat generated. • Simulation results validate efficiency improvements.	Hybrid PV/TC
Ahadi S, Hoseini H.R. and Faez R. [94]	• Thermoelectric power generation using large pn-junction is discussed. • Results show efficiency increase from 6.8% to 10.92% at 83°C.	Hybrid PV/TC
Najafi H and Woodbury K [95]	• Model developed to determine temperatures of system and required power [96]. • Results show temperature kept within limits and produced maximum output power.	Hybrid PV/TC
van Sark W.G.J.H.M [97]	• Thermoelectric (TE) converters attached to back part of PV panels. • Developed model shows 24.9% energy yield obtained, where experimental results show 10% increase.	Hybrid PV/TC

37

Yang D and Yin H [98]	• Water pipelines used for more effective heat transfer and theoretical conversion efficiency limit of system evaluated. • Results show PV/TE/HW system superior to PV/HW and conventional PV systems as electrical efficiency increased by 30%.	Hybrid PV/TC
Kane A, Verma V and Singh B [99]	• Temperature based maximum power point tracking (MPPT) scheme presented to find optimal temperature of PV system. • The performance improvement of PV system with thermoelectric cooling is presented through simulated results.	Hybrid PV/TC
Irshad K., Habib K., Basrawi F. and Saha B.B [100]	• Fifteen TEC air duct modules assisted by a 300Wp PV system to cool a 9.45m^3 test room investigated through experiments and simulations. • Experimental and simulation results showed good compatibility with one another,	Hybrid PV/TC

	where combined system saves 1806.75kWh/year.	
Enescu D. and Spertino F [101]	• Formulate equations for cooling capacity, heat rejection rate and input power, and model developed PV generator. • Technical, economic and environmental research must be done in future.	Hybrid PV/TC

2.5. Discussion

After investigating the various technologies used to deal with the temperature problem with the aim of increasing efficiency, it is imperative to summarise the findings in an easy and accessible way for any party interested in these technologies; this is done in Table 2.2 below. This table indicates the advantages, disadvantages and the comments for justification of the use of these different technologies.

After analysing the table, it may be concluded that any cooling arrangement selected should be used to keep the photovoltaic cell temperature low and constant, with the aim of increasing electrical efficiency. It should furthermore, if feasible, allow the use of extracted thermal heat to be implemented in other relevant functions.

Table 2.2: Technical discussion of different PV module cooling technologies

Technology	Advantages	Disadvantages	Comments
Floating tracking concentrating cooling (FTCC)	1. Avoid energy dispersion problems. 2. Avoid electric grid stress when using a pumping scheme. 3. Operates highly efficiently.	1. Evaporation causes water wastage. 2. Sprinklers cannot spray whole surface of PV module. 3. High capital cost.	The FTCC system operates efficiently. However, when water is sprayed, the whole surface area is partially cooled.
Hybrid solar photovoltaic/ thermal PV/T system cooled by water spraying	1. Increased energy yield. 2. More efficient than air cooling.	1. Whole surface area of PV panel partially cooled. 2. Heat wastage.	Experimental results show efficiency increased. However, water is wasted and heat could be utilised to harvest more solar radiation.
Hybrid solar photovoltaic/ thermoelectric PV/TE system cooled by heat sink	1. Average temperature with heat sink lowered to 8.29%. 2. Electrical efficiency improved. 3. Alleviates hot spotting.	1. Heat conduction loss between hot and cold parts through semiconductors. 2. Heat is wasted. 3. Turbulent airflow with pin fin heat sink.	Experimental results show heat sink can decrease surface temperature. However, turbulent airflow makes heat sink highly unstable. Also, wasted heat rather utilised to increase electrical efficiency.

40

Hybrid solar photovoltaic/ thermal (PV/T)	1. Electrical efficiency increased. 2. Supplies hot water for domestic applications. 3. More efficient combined than separated.	1. Cannot achieve optimal efficiency, due to constant flow rate. 2. High initial cost. 3. Subsidies needed for these systems.	Hybrid PV/T system increases electrical efficiency effectively. However, cannot reach optimal efficiency, due to flow rate being kept constant. By adjusting the flow rate, optimal efficiency may be achieved.
Phase-change materials (PCM) used to decrease the operating temperature of solar panels	1. Able to store large amounts of heat with small temperature changes. 2. Phase-change occurs at a constant temperature. 3. Heat absorbed may be used to heat buildings.	1. Paraffin has low thermal conductivity in its solid state. 2. Segregation reducing active volume available for heat storage. 3. Less efficient in colder areas.	PCM operates effectively. System stores heat from PV panel during melting process, however absorptive capabilities of material degrades over time. Furthermore, superior performance during hot climatic conditions.
PV panel with water immersion cooling	1. Highly efficient. 2. Economic. 3. Environmentally friendly. 4. Electrical efficiency	1. Efficiency is low during cloudy days. 2. Submersion depth influences efficiency. 3. Ionised water affects the electrical	Temperature reduced and efficiency increased. However, efficiency low during cloudy days. Further, ionised water exposure affects the

	increased during clear days. 5. Land requirements unnecessary.	efficiency over time.	electrical efficiency over time.
PV panel cooled by transparent coating (photonic crystal cooling)	1. Economic solution. 2. No space requirement necessary. 3. PV cell temperature reduced drastically.	1. Heat reflected into space is wasted and could instead be utilised for domestic applications.	Temperature problem eliminated, which enhances PV panel efficiency. However, heat is wasted and could rather be utilised for domestic applications.
Hybrid solar photovoltaic/ thermal system cooled by forced air circulation	1. Overall efficiency increased. 2. Economically viable. 3. Heated air can be used to heat buildings.	1. Efficiency of cooling with air is lower than water cooling. 2. Water cooling is more effective in hot climatic conditions than air cooling.	System very effective, but most effective in cold climatic conditions. Also, forced air circulation not as efficient as forced water circulation.
Hybrid PV/TC system	1. Clean source of energy. 2. Waste heat changed into useful energy.	1. Slow technological progression. 2. Requires relatively constant heat source. 3. Low conversion efficiency rate.	System efficiently uses waste heat for higher efficiency but has low conversion efficiency rate and technology progression is slow.

42

	3. Increasing life span of PV modules.

2.6. Summary

Extensive reviews of various cooling techniques used to enhance the performance of a PV system are discussed in detail in this research. Appropriate cooling of PV systems improves the thermal, electrical and overall efficiency, which in turn also reduces the rate of cell degradation and maximizes the life span of the PV module. Different tools, such as equations, schematic diagrams and pictures have been used to clearly illustrate, analyse and compare these technologies used to address the undesirable influence of temperature on PV efficiency in terms of their advantages and disadvantages, as well as their techno-economic and environmental implications.

Several papers from various research fields have been reviewed and classified based on their focus, contribution and the form of technology used to achieve cooling, while trying to increase the efficiency of the panel. Future research should be focused on harvesting heat from the surface of a PV module effectively and the cooling thereof in a higher controlled and stable manner. As learned from the reviewed studies, the following cooling technologies are found to be promising based on materials used, capital cost and performance:

- Floating tracking concentrating cooling sprinklers cannot spray the whole surface area of the PV module, which means that only sections are cooled. Water is also wasted during evaporation.

- A Hybrid solar photovoltaic/thermal (PV/T) system cooled by water spraying demonstrated, through experiments, that an efficiency increase was obtained and viable. However, water is wasted and heat could be utilised to harvest more solar radiation.

43

- A Hybrid solar photovoltaic/thermoelectric (PV/TE) system cooled by heat sink is able to reduce the surface temperature of the PV module effectively. However, the turbulent airflow present causes the heat sink to be highly unstable. In addition, the wasted heat could alternatively be utilised to increase the electrical efficiency.

- A Hybrid solar photovoltaic/thermal (PV/T) cooled by forced water circulation increases the electrical efficiency effectively; however, it cannot reach optimal efficiency, due to the flow rate being kept constant. It is preferable to adjust the flow rate according to the temperature change to achieve optimal efficiency.

- Improving the performance of solar panels through the use of phase-change materials reduced the surface temperature, therefore, increased the electrical efficiency drastically. The system stores the heat from the PV panel during the melting process, however, the absorptive capabilities of the material degrades over time. This system will further not achieve the same performance during cold and hot climatic conditions.

- The Water immersion cooling technique reduced PV module temperature and increased efficiency adequately when the exact submersion depth is applied. In addition, ionised water exposure affects the electrical efficiency over time.

- Transparent coating (photonic crystal cooling) eliminated the temperature problem completely, which enhances the efficiency of the PV panel. However, heat is wasted and could instead be utilised for domestic applications.

- A Hybrid solar photovoltaic/thermal system cooled by forced air circulation is highly effective, but more so in cold climatic conditions than in hot climatic conditions. Forced air circulation is further not as efficient as forced water circulation.

- A Thermoelectric cooling system effectively uses the waste heat for higher efficiency; it has a low conversion efficiency rate and the progression of this technology is slow.

Chapter III: Mathematical model development and optimization algorithm formulation

3.1. Introduction

In this chapter, the mathematical model of the hybrid PV/T system and all the main components thereof are presented in section 3.2. Section 3.3 presents the optimal control model of the hybrid PV/T system. The study is summarized in section 4.4.

3.2. Mathematical model of the hybrid PV/T system

3.2.1. Dynamic model of the hybrid PV/T system

Mathematical modelling of hybrid systems' operation can be developed for simulation purposes, when conducting experiments on an actual system, would be impossible or impractical [102].

Figure 3.1 presents the schematic of the hybrid PV/T system cooled by forced water circulation. The dynamic model of the hybrid PV/T system consists of the variation of the storage tank temperature with the solar irradiance and ambient temperature. A flat plate solar collector is used in this setup to absorb heat from the surface of the PV panel. The flat plate solar collector supplies heat to the water storage tank (thermodynamic system) and is modelled in this section.

45
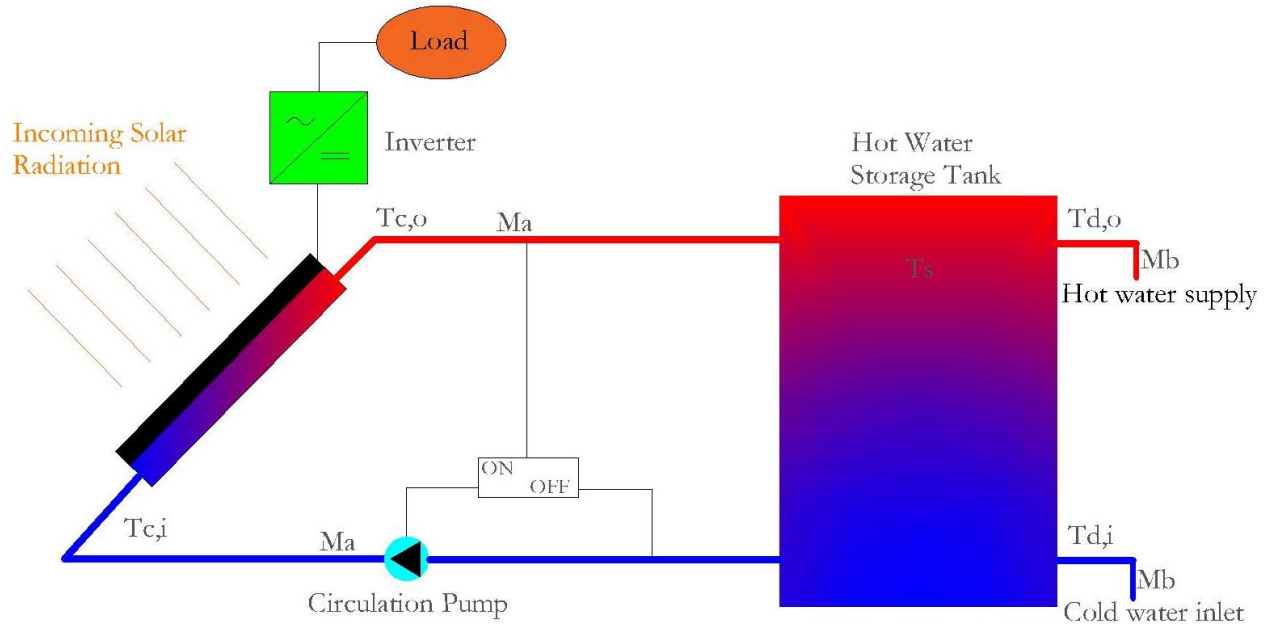
Figure 3.1: Schematic model layout of the PV/T system

The first law of thermodynamics is applied to the circulation fluid storage tank, in order to obtain the energy balance in the tank. The following equation describes the energy balance equation:

$$M.C.\frac{dT_s}{dt} = Q_{in} - Q_{load} + Q_{cw} - Q_{loss}$$ (3.1)

where:

$$Q_{in} = \dot{M}_a.C.(T_{c,o} - T_{c,i})$$ (3.2)

$$Q_{load} = \dot{M}_b.C.T_{d,o}$$ (3.3)

$$Q_{cw} = \dot{M}_b.C.T_{d,i}$$ (3.4)

46

$$Q_{loss} = \frac{(T_s - T_a).A_s}{\frac{\Delta x}{k} + \frac{1}{h}}$$

(3.5)

where: $\beta = \dfrac{A_s}{\dfrac{\Delta x}{k} + \dfrac{1}{h}}$

(3.6)

Q_{in} is the useful heat gained by the thermodynamic system,

Q_{load} is the heat removed from the tank to the load,

Q_{cw} is the heat removed from the tank through the addition of cold water at a flow rate, $\dot{M}_b$,

Q_{loss} is the heat lost in the tank due to its thermal properties,

T_s is the storage tank temperature and C is the water specific heat capacity (J/k°C),

In this model, the heat losses due to the connecting pipes are neglected.

By substituting Eqs. (3.2), (3.3), (3.4), (3.5) and (3.6) into Eq. (3.1) yields:

$$M.C.\frac{dT_s}{dt} = \dot{M}_a.C.(T_{c,o} - T_{c,i}) - \dot{M}_b.C.T_{d,o} + \dot{M}_b.C.T_{d,i} - \beta(T_s - T_a)$$

(3.7)

where:

$\dot{M}_a$ is the mass flow rate of the circulation fluid,

$T_{c,o}$ and $T_{c,i}$ are the outlet and inlet temperatures of the thermal collector pipes, respectively,

$T_{d,o}$ and $T_{d,i}$ are the demand outlet and demand inlet at the consumer's side, respectively,

T_a, A_s, Δx, k and h are the ambient temperature, tank surface area, insulation thickness, thermal conductivity, and surface heat transfer coefficient.

The thermal performance of a collector under steady state conditions is presented in the following equation [20]:

47

$$Q_{in} = A_c.F_r\left((\tau.\alpha)G - U_l(T_{c,o} - T_{c,i})\right) \tag{3.8}$$

where:

A_c is the area of the collector,

Fr is the collector heat removal factor,

τ and α are the transmittance and absorbance factors,

G is the global irradiance and

U_l is the collector overall heat loss coefficient.

Combining Eq. (3.2) and Eq. (3.8) yields:

$$\dot{M}_a.C.(T_{c,o} - T_{c,i}) = A_c.F_r\left((\tau.\alpha)G - U_l(T_{c,o} - T_{c,i})\right) \tag{3.9}$$

Eq. (3.9) can be rewritten as:

$$T_{c,o} - T_{c,i} = \frac{A_c.F_r.\tau.\alpha.G}{\dot{M}_a.C + A_c.F_r.U_l} \tag{3.10}$$

The outlet temperature of the thermal collector fluid, $T_{c,o}$ may be controlled by switching on/off the pump in such a way to control the effect of solar radiance on $T_{c,o}$. This is obtained by multiplying the second term of Eq. (3.10) by a switching status, $U(t)$, which is a control variable. Hence, Eq. (3.10) becomes:

$$T_{c,o} - T_{c,i} = \frac{A_c.F_r.\tau.\alpha.G.U(t)}{\dot{M}_a.C + A_c.F_r.U_l} \tag{3.11}$$

If it is assumed that temperature of the water to the user is equal to the temperature inside the storage tank, that is $T_{d,o} = T_s$.

48

The substitution of Eq. (3.11) in Eq. (3.7) yields:

$$M.C.\frac{dT_s}{dt} = \dot{M}_a.C.\left(\frac{A_c.F_r.\tau.\alpha.G.U(t)}{\dot{M}_a.C + A_c.F_r.U_l}\right) - \dot{M}_b.C.T_s + \dot{M}_b.C.T_{d,i} - \beta.T_s + \beta.T_a \qquad (3.12)$$

Eq. (3.12) can be rearranged as follows:

$$T(t) = \left(\frac{\dot{M}_a(t)}{M}\right).\psi.G(t).U(t) + T_s(t).\left(\frac{-\dot{M}_b(t).C + \beta}{M.C}\right) + T_{d,i}(t).\left(\frac{\dot{M}_b(t)}{M}\right) + T_a(t).\left(\frac{\beta}{M.C}\right) \qquad (3.13)$$

where: $\psi = \dfrac{A_c.F_r.\tau.\alpha}{\dot{M}_a.C + A_c.F_r.U_l}$

Eq. (3.13) can be written in a state space form as:

$$\dot{T}(t) = A(t).T_s(t) + B(t).U(t) + C(t) \qquad (3.14)$$

where:

$\dot{T}(t)$ is the temperature derivative,

$$A = -\left(\frac{\dot{M}_b(t).C + \beta}{M.C}\right),$$

$$B = \frac{\dot{M}_a(t)}{M}.\psi.G(t),$$

49

$$C = T_{d,i}(t).\left(\frac{\dot{M}_b(t)}{M}\right) + T_a(t)\left(\frac{\beta}{M.C}\right)$$

In Eq. (3.14), *A(t)* is the state matrix, *B(t)* is the input matrix, *C(t)* is the disturbance, $T_s(t)$ is the state variable (vector), and *U(t)* is the control (input) variable, which is the switch status of the pump circulating the fluid.

3.2.2. Discretized hot water temperature model

Since the numerical approach is easier than the analytical approach, Eq. (3.14) is discretized at each kth sampling interval at a sample period of t_s.

The general discrete formulation of Eq. (3.14), in terms of the kth hot water temperature, is given in the following equation:

$$T_s(k+1) = (1 + t_s.A(k)).T(k) + t_s B(k).U(k) + t_s.C(k) \tag{3.15}$$

Since the state variable, T_{k+1}, should be expressed in terms of its initial value, T_0 and the control variable, *U(t),* of the initial, T_{k+1} at each interval is first derived as:

$$T_1 = (1 + t_s.A_0).T_0 + t_s.B_0.U_0 + t_s.C_0 ,$$

$$T_2 = (1 + t_s.A_1).(1 + t_s.A_0).T_0 + t_s.[(1 + t_s.A_1).B_0.U_0 + B_1.U_1] + t_s[(1 + t_s.A_1).C_0 + C_1] ,$$

$$T_3 = (1 + t_s.A_2).(1 + t_s.A_1).(1 + t_s.A_0).T_0 + t_s.[(1 + t_s.A_2).(1 + t_s.A_1).B_0.U_0 + (1 + t_s.A_2).B_1.U_1 + B_2.U_2] + t_s.[(1 + t_s.A_2).(1 + t_s.A_1).C_0 + (1 + t_s.A_2).C_1 + C_2]$$

Then, the discrete differential temperature equation in terms of its initial value and control variable is expressed as:

50

$$T_{k+1} = T_0 \cdot \prod_{j=0}^{k}(1+t_s.A_j) + \sum_{j=0}^{k} B_j.U_j \cdot \prod_{i=j+1}^{k}(1+t_s.A_i) + \sum_{j=0}^{k} C_j \prod_{i=j+1}^{k}(1+t_s.A_i) \qquad (3.16)$$

where:

T_0 and T_k are the initial and k[th] water temperatures inside the tank respectively,

t_s is the sampling time and,

U_j is the jth switching status, which can either be 1 or 0.

3.3. Control optimization formulation

3.3.1. Proposed optimization solver and algorithm

 The objective function as shown in Eq. (3.23), is a non-linear function with an integer binary control variable that should be solved in order to obtain the optimal switching status of the fluid circulation pump. This problem is a mixed integer nonlinear optimization problem (MINLP) and can be solved using the SCIP (solving constrained integer programs) solver in the optimization toolbox of MATLAB.

$$\min_x f(x)$$
$$subject\ to: Ax \le b$$
$$A_{eq}x = b_{eq}$$
$$l_b \le x \le u_b$$
$$c(x) \le d$$
$$c_{eq}(x) = d_{eq}$$
$$x_i \in Z$$
$$x_j \in \{0,1\}$$

where:

$f(x)$ is the objective function, which is a scalar function,

$A.x \le b$ is the linear inequality constraint,

51

$A_{eq}.x = b_{eq}$ is the linear equality constraint,

$lb \leq x \leq ub$ is the lower boundary and upper boundary of the decision variable,

$c(x) \leq d$ is the nonlinear inequality constraints,

$c_{eq}(x) = d_{eq}$ is the nonlinear equality constraints,

x_i is a decision variable that only takes integer values,

x_j is a decision variable that only takes binary values.

3.3.2. Algorithm formulation

- Output power maximization

The first objective is to maximize the energy output of the PV module by controlling the pump switching status, *U(t)*. The PV power output varies with solar irradiance and cell temperature, as shown in [103].

$$J_e = P_{pv,stc}.\frac{G(t)}{1000}.\left[1 - \gamma(T_j - 25)\right] \tag{3.17}$$

where:

J_e is the PV generator output power at Maximum Power Point (MPP),

$P_{pv,stc}$ is the rated power at STC,

γ is the power temperature coefficient and,

T_j is the cell temperature.

$T_{c,o}$ equals T_j.

To express the PV power output in terms of the control variable, *U(t)*, Eq. (3.11) is substituted in Eq. (3.17) to become:

$$J_e = \frac{P_{pv,stc}.G(t)}{1000}.\left[1 - \gamma(\psi.G(t).U(t) + T_{c,i}(t) - 25)\right] \tag{3.18}$$

52

Hence, the control optimization model to maximize the PV energy output is expressed as follows:

$$\max J_e = \sum_{k=1}^{N} \left(\frac{P_{pv,stc}.G(k)}{1000} \cdot \left[1 - \gamma(\psi.G(k).U(k) + T_{c,i}(k) - 25) \right] \right).t_s \tag{3.19}$$

- Discomfort level

A load profile is obtained, known as the function $F(t)$. This is a function of time and defined as the desired output temperature of the consumer. The comfort level of the consumer is addressed, where the difference between the output temperature $T(t)$ of the hot water storage tank and the desired temperature $F(t)$ should not be excessive. That is, the value of $(T(t) - F(t))^2$ should be minimized. The function $L(t)$ in Eq. (3.20) denotes the discomfort level, which is the second objective function to be minimized.

$$L = \int_{to}^{tf} (T(t) - F(t))^2 .dt \tag{3.20}$$

The output temperature $T(t)$ is known as the discrete differential temperature equation and is shown in the following equation:

$$T_{k+1} = T_0.\prod_{j=0}^{k}(1+t_s.A_j) + \sum_{j=0}^{k} B_j.U_j.\prod_{i=j+1}^{k}(1+t_s.A_i) + \sum_{j=0}^{k} C_j \prod_{i=j+1}^{k}(1+t_s.A_i) \tag{3.21}$$

The final objective function containing both objective functions is expressed as follows:

$$J = J_e + \mu.L \tag{3.22}$$

53

where : μ is the weighting factor for the final objective function.

Therefore, substituting Eq. (3.19) and Eq. (3.20) into Eq. (3.22), yields the final objective function:

$$J = W_1 . \sum_{k=1}^{N} \left(\frac{P_{pv,stc} . G(k)}{1000} . \left[1 - \gamma(\psi . G(k) . U(k) + T_{c,i}(k) - 25) \right] \right) t_s + W_2 . \int_{to}^{tf} (T(t) - F(t))^2 . dt \qquad (3.23)$$

where :
W_1 is the weighting factor to set priority to maximize the PV module output power
W_2 is the weighting factor to set priority to maximize the storage tank temperature

In this study, the main objective is to maximize the PV module output power, where the hot water is merely a by-product. Therefore, the weighting factor to maximize the output power of the PV module will have priority over the weighting factor to minimize the level of discomfort inside the hot water storage tank.

- Constraints

The discrete switching function, U_k, which is used to switch the circulating fluid pump, can either be 1 or 0. This is illustrated below:

$$U_k \in \{0,1\} \qquad (3.24)$$

The control variable can either be 1 or 0, which is the upper bound and lower bound of the switch. This is shown in the following equation:

$$lb \le x \le ub \qquad (3.25)$$

54

The lower boundary and upper boundary are expressed as follows:

$$lb = zeros(1, N),$$ (3.26)

$$ub = ones(1, N).$$ (3.27)

3.4. Summary

Sufficient cooling of PV systems improves the thermal, electrical and overall efficiency, which in turn reduces the rate of cell degradation and maximizes the life span of the PV module.

In this chapter, a mathematical model with the optimal switching of flow in PV/T systems with forced circulation has been developed, with the aim of controlling the surface operating temperature, while increasing the conversion efficiency. This may be achieved by maximizing the electrical energy generated from the PV module and harvesting heat absorbed by the solar collector, which can be utilized for hot water applications.

The objective function, control variable, state variable, disturbances, are identified and mathematically expressed in the developed model. For any PV/T with a different design variable, as well as operating conditions (solar radiation, ambient temperature, surface temperature), the developed model's decision variables may be optimized using any suitable advanced algorithm adept in solving such a problem.

The model developed in this work can be seen as a valuable tool for researchers and operators who would like to optimize the operation of their PV/T, using forced circulation whilst they operate above the temperature, under standard testing conditions.

Chapter IV: Simulation results and discussion

4.1. Introduction

In this chapter, the optimal switching control of the hybrid energy system is simulated using the SCIP (solving constrained integer programs) solver in the optimization toolbox of MATLAB. The main objective is to maximize the energy output of the PV module by decreasing its surface temperature through the switching of the fluid circulation pump. Load profiles and data resources are used for hybrid energy system simulations.

4.2. Case study

A case study is conducted using meteorological data obtained at the University of Free State, Bloemfontein, South Africa, on a hybrid PV/T system cooled by forced water circulation [107]. The main objective is to maximize the energy output of the PV module by decreasing its surface temperature through the switching of the fluid circulation pump. The sampling time ts =1 hour will be implemented to simplify the simulations.

4.2.1. Data presentation

Table 4.1 (values adopted from [104]) indicates the parameters of a PV module used in this study. The PV module EnerSol 250 was used, with a rated capacity of 250W.

Table 4.1: PV specifications

PV specifications	Figure
Type	Poly-crystalline
Ppv at STC	250W
Vmp	30.83V
Imp	8.11A
Voc	38.10V
Isc	8.71A
Operating temperature	-40°C to 85°C
Weight	19kg
Dimensions	1640x990x40mm

The system's flat plate collector and mass flow rate are shown in table 4.2 (values adopted from [105]).

Table 4.2: Flat plate collector parameters

Parameters	Symbol	Value	Unit
Collector surface area	Ac	0.7839	m²
Transmittance-absorptance factor	τa	0.88	-
Heat removal factor	Fr	0.8	-
Overall heat loss coefficient	Ul	5.46	W/m²K

Table 4.3 shows the parameters of the hot water storage tank (values adopted from [106]). The storage tank is used to store the heat absorbed by the flat plate collector where the size was taken as 150 litres.

57

Table 4.3: Storage tank parameters

Parameters	Symbol	Value	Unit
Storage tank surface area	As	1.677	m²
Tank volume	V	150	L
Specific heat capacity	C	4186	J/kg°C
Surface heat transfer coefficient	h	6.3	W/m²K
Mass flow rate	Ma	0.09	kg/s
Thermal conductivity	k	0.055	W/mK
Thickness of insulation layer	dx	0.07	m
Initial inlet water temperature	Ti	25	°C

Table 4.4 presents the parameters of the fluid circulation pump (values adopted from [106]). The BLDC50K-1260A fluid circulation pump is used to circulate water behind the PV module in order to cool it, which is rated at 24W.

Table 4.4: Fluid circulation pump parameters

Parameters	Symbol	Value	Unit
Operating voltage	V_{pump}	12	V
Maximum current	I_{pump}	2	A
Rated power	P_{pump}	24	W
Operating power	P_{op}	8.64	W
Maximum flow rate	m_{max}	900	l/h
Maximum operating temperature	Tcp_{max}	100	°C

Data for global horizontal irradiance and ambient air temperature of a typical summer day in January and winter day in June are plotted in Figs. 4.1, 4.2 and Figs. 4.3, 4.4 respectively.

Meteorological data during a summer day in January (2017-01-30) and a winter day in June (2017-06-22) utilized in this study have been collected over a 24 hour period from the weather

58

station located at the University of Free State, Bloemfontein (latitude: -29.11º, longitude: 26.185º and elevation: 1491m) [107].

Referring to Fig. 4.1 and Fig. 4.2, it is eminent that the majority of summer days in Bloemfontein are overcast or cloudy, compared to the apparent clear skies experienced during winter. Furthermore, it may be clearly observed that the solar irradiance is larger in magnitude during summer, in comparison with the winter data.
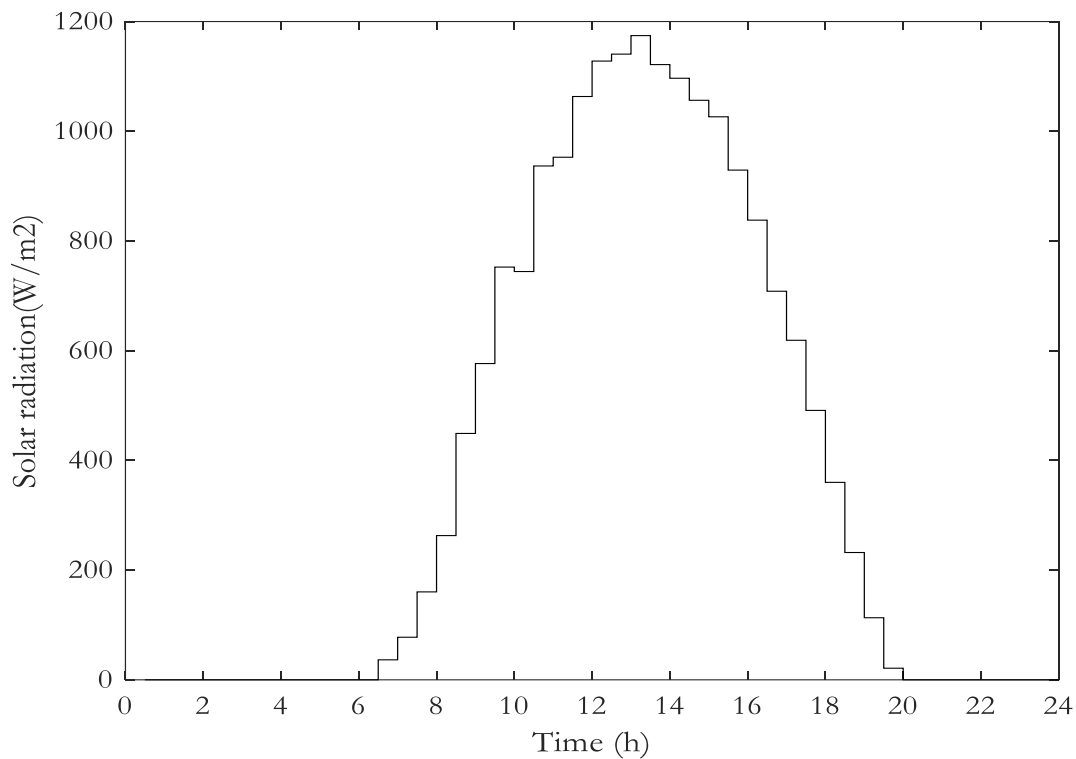
Figure 4.1: Solar radiation during summer
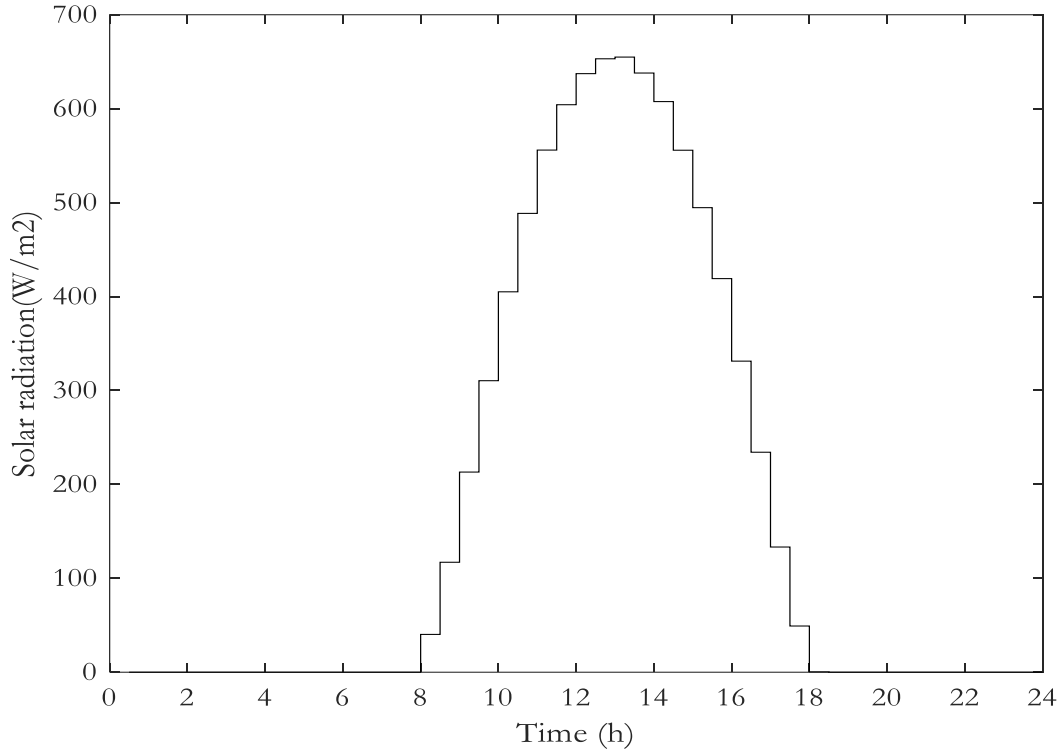
Figure 4.2: Solar radiation during winter

The inlet water temperature and ambient air temperature for summer and winter are illustrated in Figs. 4.3 and 4.4 respectively. Referring to Fig 4.3, it should be noted that the inlet water temperature during the summer months does not vary significantly throughout the day and appears to be consistent. However, the air ambient temperature varies significantly in comparison with the inlet water temperature. In Fig. 4.4, the inlet water temperature during winter also seems to be fairly consistent throughout the day. The ambient temperature during winter further fluctuates significantly in comparison with the inlet water temperature. For this case study location, there is a non-existent hour averaged data for inlet water temperature. Therefore, the inlet water temperature applied to this case study is based on assumptions, where the average inlet water temperature of summer and winter was taken as 24.1°C and 14.2°C, respectively.

60
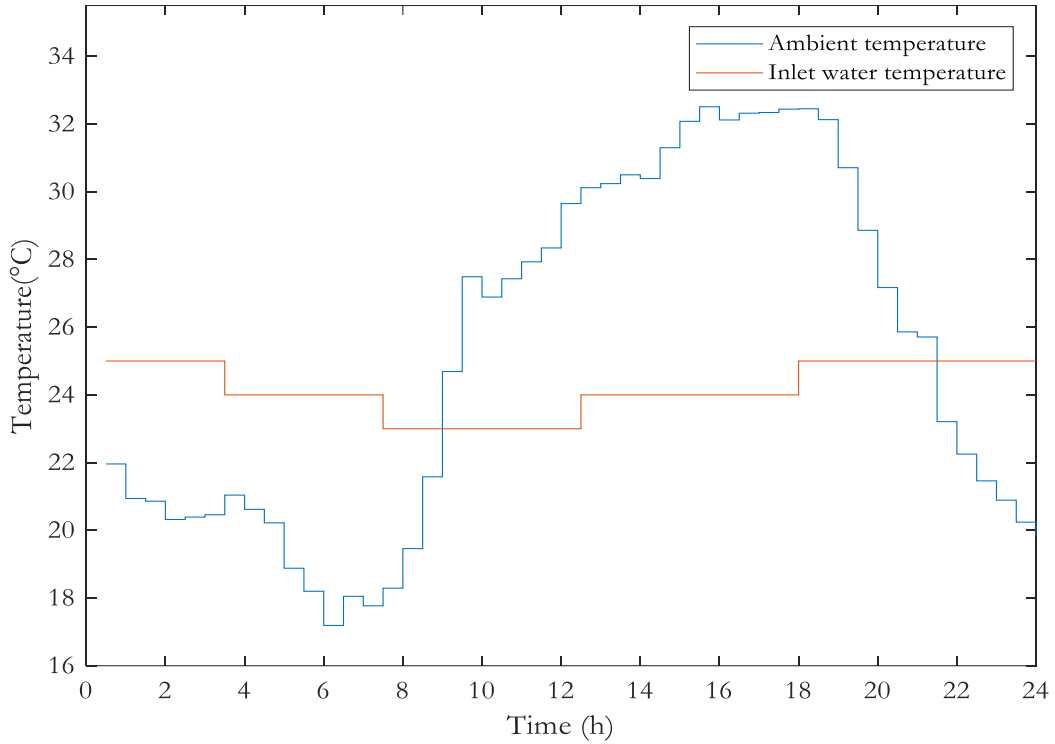
Figure 4.3: Ambient and inlet water temperature during summer
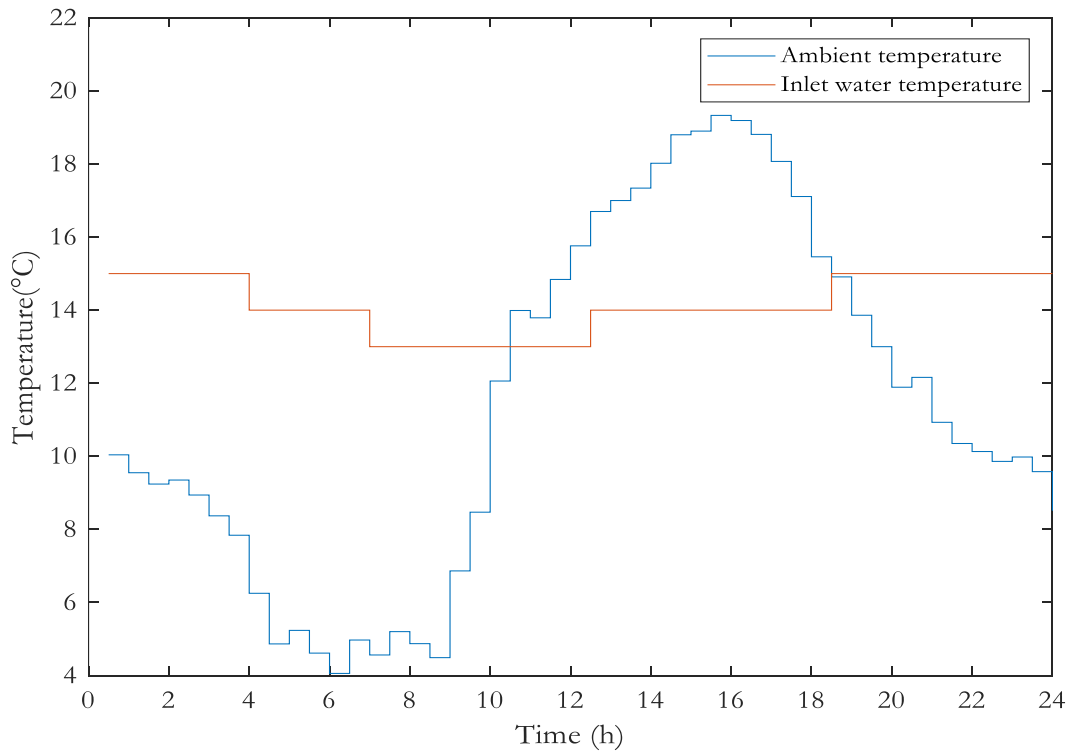
Figure 4.4: Ambient and inlet water temperature during winter

61

The hot water demand profile shown in Fig. 4.5 and Fig. 4.6 is not considered to be a realistic demand load profile. The hot water is merely a by-product of cooling the PV module. Therefore, hot water can solely be supplied to the occupant at specific times, to assist with the domestic hot water demand and is not the main objective.

The water demand profile during summer is demonstrated in Fig. 4.5, where the hot water demand during the day is at zero until 13:00. At 13:00, the dishwasher demands hot water at a flow rate of 3.07 litres per minute until 13:30. From 18:30 until 19:00 there is a hot water demand at a flow rate of 4 litres per minute when two occupants require hot water to shower. From 19:30 until 20:00 there is a hot water demand at a flow rate of 4 litres per minute when another pair of occupants require hot water to shower. Thereafter, the hot water demand for the washing machine and the occupants' minor hygienic purposes ie. washing hands and face, is at 21:00.

The hot water demand profile during winter is shown in Fig. 4.6, where the hot water demand during the day is at zero until 13:00. At 13:00, the dish washer demands hot water at a flow rate of 2.33 litres per minute until 13:30. From 17:00 until 17:30 there is a hot water demand at a flow rate of 4 litres per minute when two occupants require hot water to shower. From 18:00 until 18:30, the hot water demand is at a flow rate of 4 litres per minute, when another pair of occupants require hot water to shower. Thereafter, the hot water demand for the washing machine and the occupants' minor hygienic purposes ie. washing hands and face, is at 19:30.
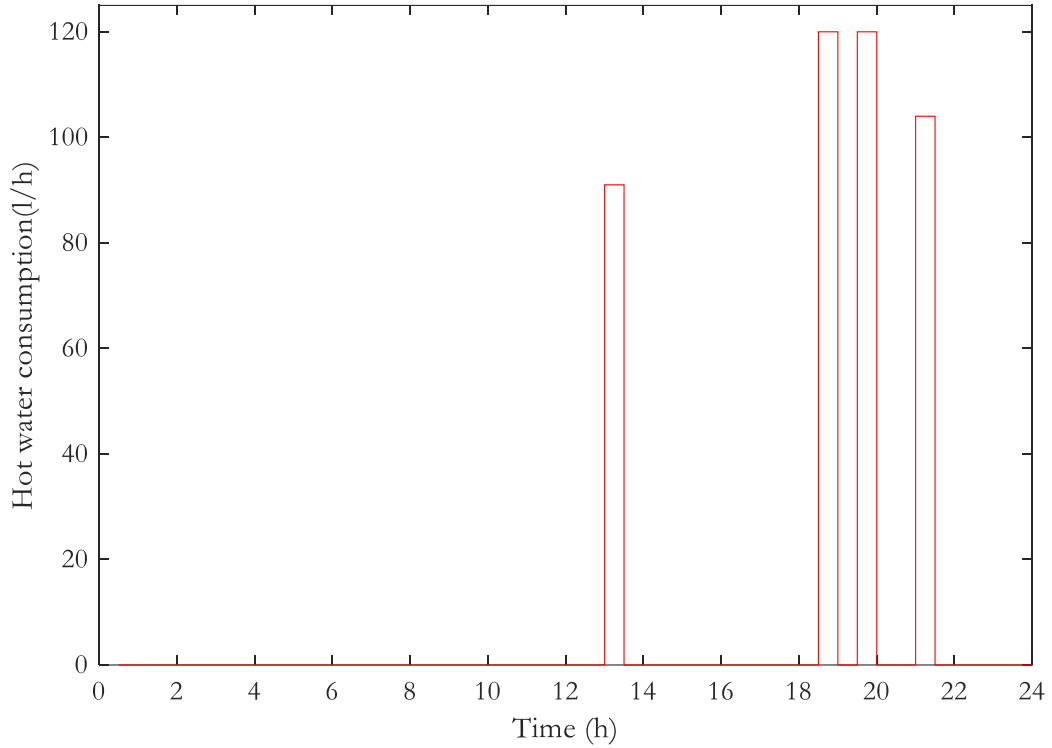
Figure 4.5: Hot water demand during summer
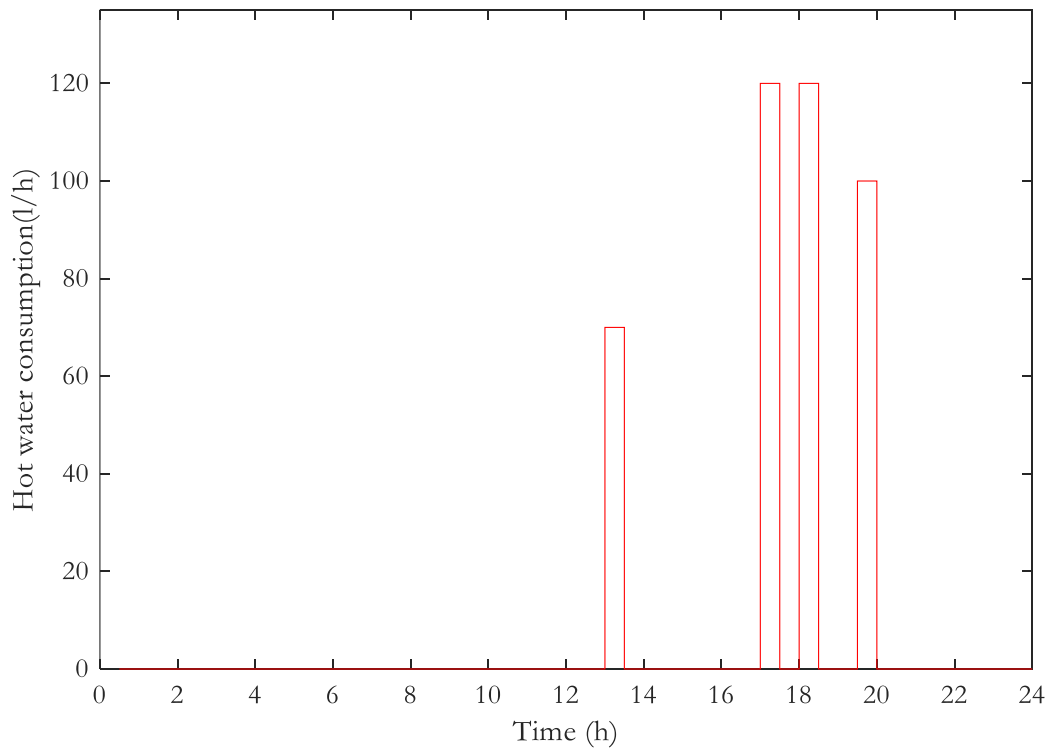
Figure 4.6: Hot water demand during winter

63

Table 4.5 presents the simulation parameters of this study.

Table 4.5: Simulation parameters

Parameters	description	Value
t	Sampling time	30min
Hours	Optimization interval	24h
N	Control horizon samples	48

4.3. Simulation results and discussion

4.3.1 Baseline

A standard EnerSol 250W PV module without any cooling technique is utilized as the baseline in order to evaluate the optimal switching control strategy. The simulations illustrate how the PV output power, PV cell temperature and PV cell efficiency react without a cooling system.

4.3.1.1 Baseline: Summer case

In Fig. 4.7, the cell temperature of the PV module is presented. Initially, the temperature of the PV module starts at 22°C, which is the equivalent as the ambient temperature and decreases until 6:30. From 6:30, the temperature of the PV module begins to increase due to the presence of solar radiation. Between 7:45 and 8:00, the temperature of the PV module reaches 25°C and continues to increase. From 13:00 to 13:30, the temperature of the PV module reaches a maximum temperature of 46°C. From 13:30 it decreases significantly until 20:00, which is when solar radiation is absent and thereafter reduces gradually, until it reaches approximately the equivalent temperature as ambient air temperature at 24:00.

64

In Fig. 4.8, the output power of the PV module is presented. For the specific solar radiation and ambient air temperature described in section 4.2.1, the energy output of the PV module is significantly influenced by the heat generated on its surface. Initially, the output power is at zero due to no solar radiation present. After 6:30, the PV module begins to produce energy and increases up until 13:00. From 13:00 to 13:30, the output power reaches its maximum of 262W, due to extremely high solar radiation present. From 13:30, the output power decreases in value until 20:00, the moment where solar radiation is absent.

The cell efficiency of the PV module is illustrated in Fig. 4.9. Initially, the efficiency of the panel is approximately 15.4% at 6:30. From this time of the day, solar radiation is present and the temperature of the PV module begins to increase. The cell efficiency reduces significantly up until 13:00, reaching a minimum of 13.75% at a surface temperature of 46°C. This is due to a high solar radiation of 1173W/m² and ambient temperature of 30°C, causing the surface temperature of the PV module to increase until it reaches 46°C. From 13:30, a significant cell efficiency increase is observed up until 20:00, when solar radiation is absent. Therefore, a reduction in cell efficiency correlates to a decrease in output power and an increase in cell temperature, as seen in eq. 2.2.

In Fig. 4.10, the cumulative energy produced by the PV module is illustrated. Initially, the cumulative energy is at zero until 6:30, which is due to the absence of solar radiation. Therefore, no energy can be produced during this time. After 6:30, the module begins to produce energy and accumulate during the day until 20:00, reaching 2083.20Wh energy produced.

Figure 4.7: PV module cell temperature during summer without cooling

Figure 4.8: PV module output power during summer without cooling

66

Figure 4.9: PV module cell efficiency during summer without cooling
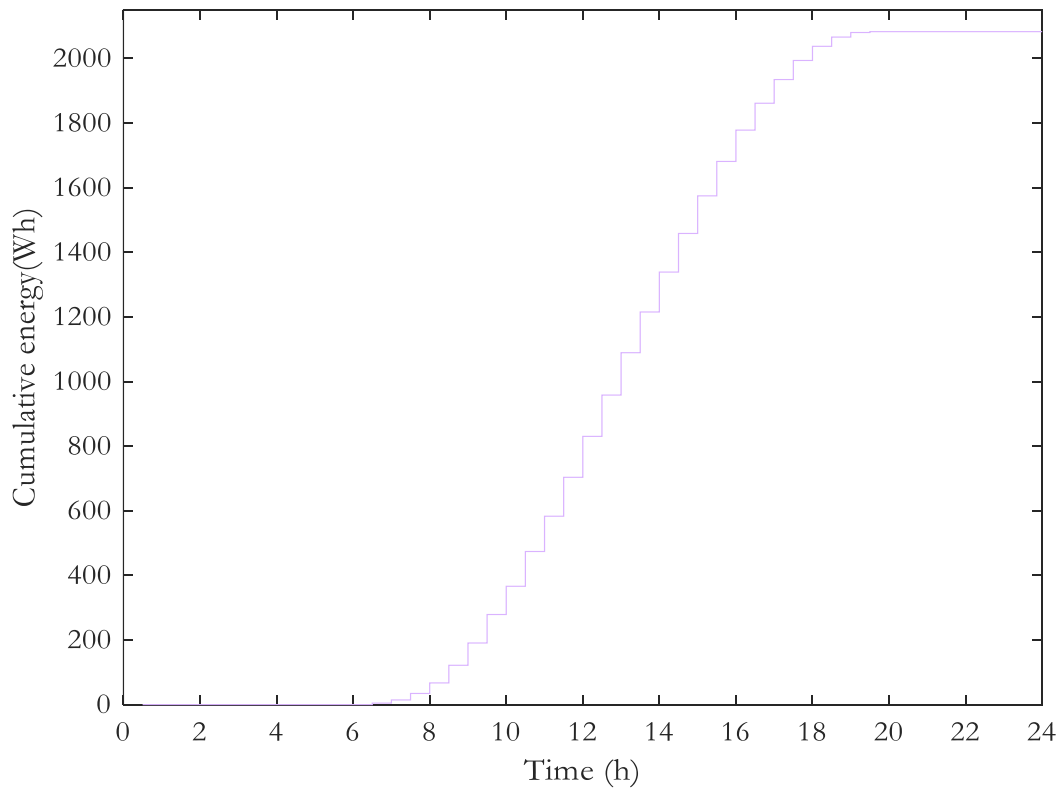
Figure 4.10: Cumulative energy during summer without cooling

67

4.3.1.2 Baseline: Winter case

In Fig. 4.11, the cell temperature of the PV module during winter is shown. Initially, the temperature of the PV module starts at 10°C, which is approximately the same as ambient temperature and decreases until 6:30. From 6:30, the temperature of the PV module begins to increase, due to the presence of solar radiation. From 8:00, the temperature of the PV module increases drastically up to 13:00, where it reaches a maximum temperature of 24°C. From 13:30 it begins to decrease significantly until 18:00, which is when solar radiation is absent and reduces gradually until it reaches the same temperature as ambient air temperature at 24:00.

In Fig. 4.12, the output power of the PV module during winter is presented. Initially, the output power is zero due to no solar radiation present. After 8:00, the PV module begins to produce energy and increases until 13:00. From 13:00 to 13:30, the output power reaches its maximum of 164W, which is due to low solar radiation and ambient temperature present. After 13:30, the output power decreases in value until 18:00, which is the moment where solar radiation is absent.

The cell efficiency of the PV module is illustrated in Fig. 4.13. Initially, the efficiency of the panel is approximately 16.5% at 8:00, when solar radiation is present. The cell efficiency reduces significantly until 13:00, reaching a minimum of 15.47% at 24°C surface temperature. This is due to a solar radiation of 654.92W/m² and ambient temperature of 17°C, causing the surface temperature of the PV module to increase until it reaches 24°C. After 13:30, a significant cell efficiency increase is observed until 18:00, which is when solar radiation is absent.

In Fig. 4.14, the cumulative energy produced by the PV module is illustrated. Initially, the cumulative energy is at zero until 8:00, which is due to the absence of solar radiation. Therefore, no energy can be produced during this time. After 8:00, the module begins to produce energy and accumulate during the entire day until 18:00, reaching 1037.10Wh energy produced.
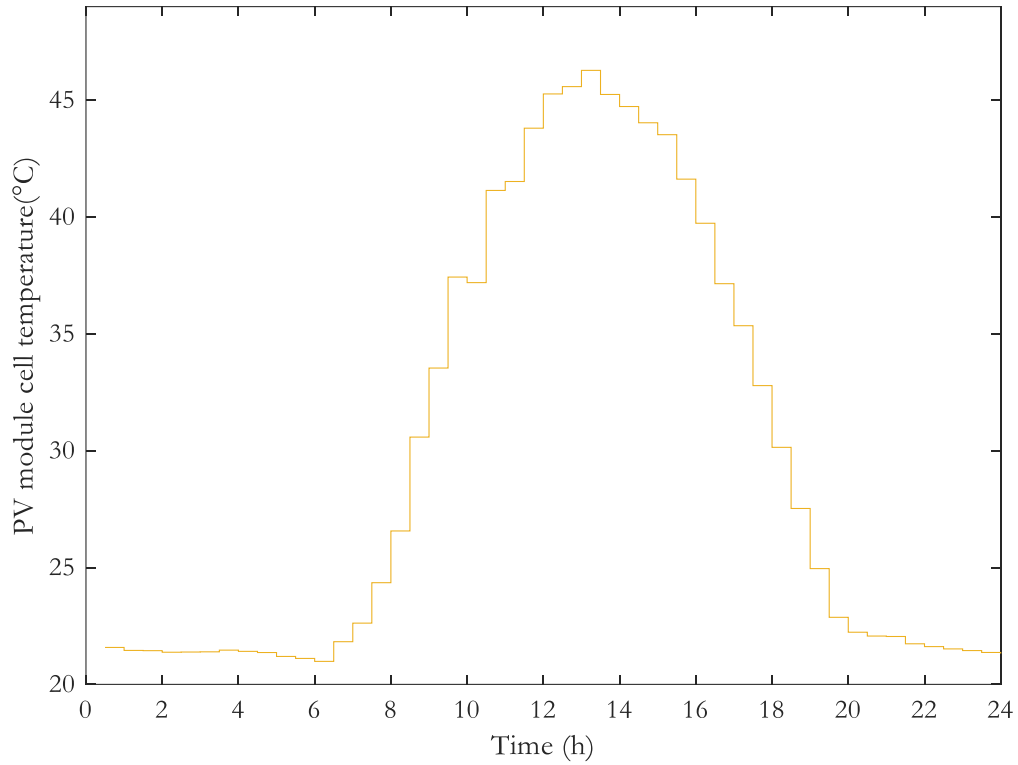
68
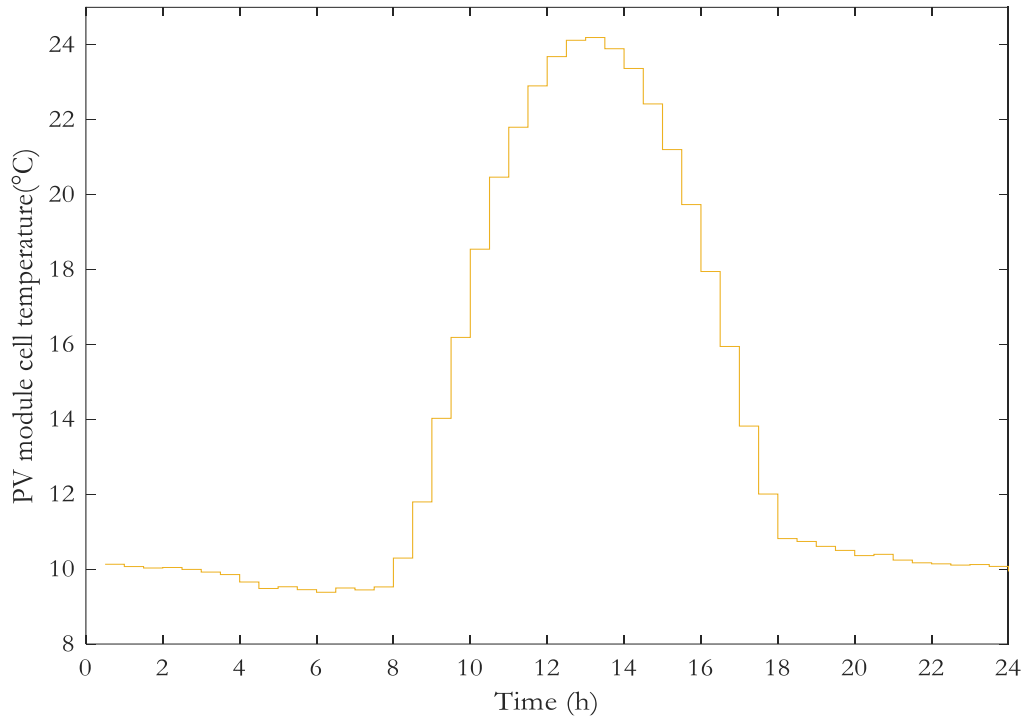
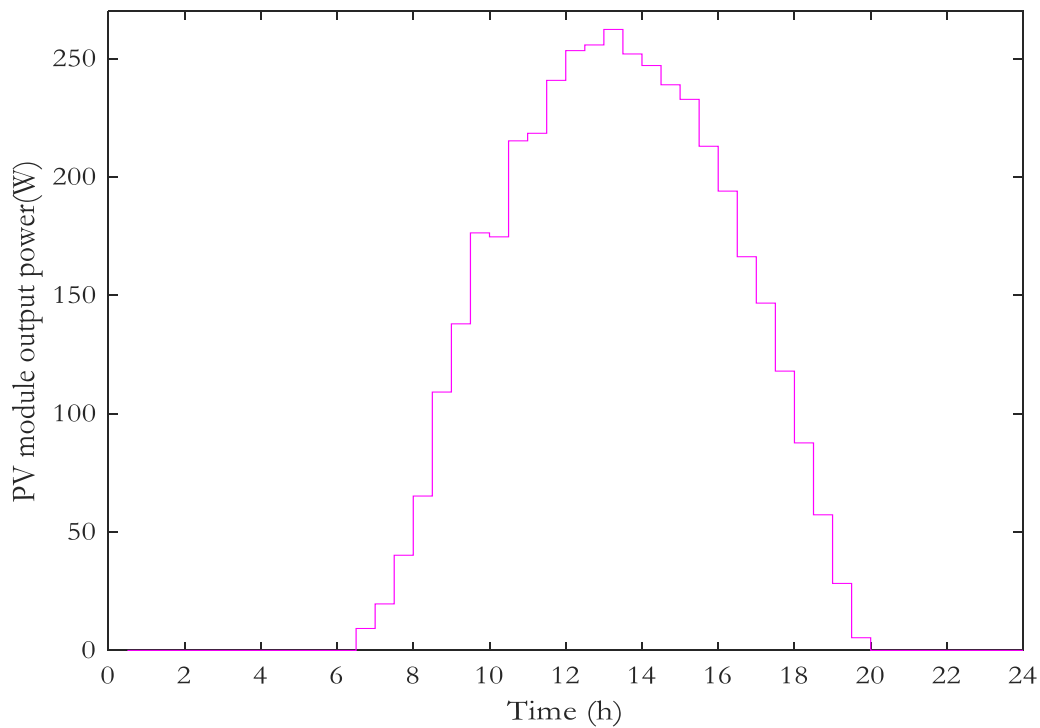Figure 4.11: PV module cell temperature during winter without cooling
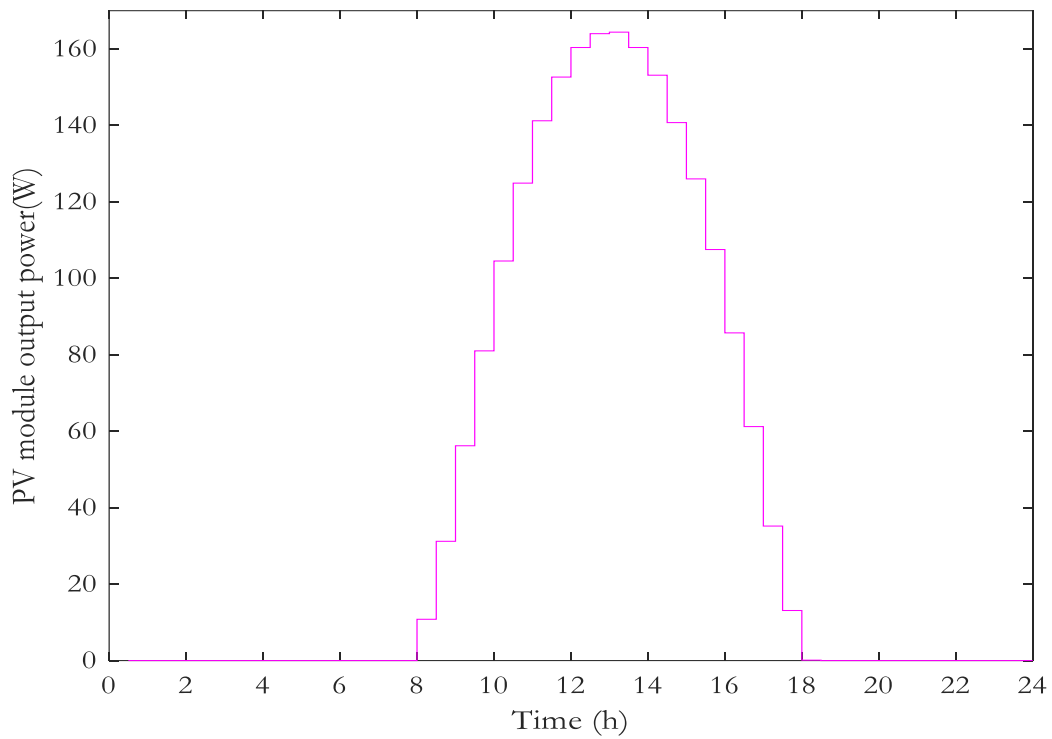
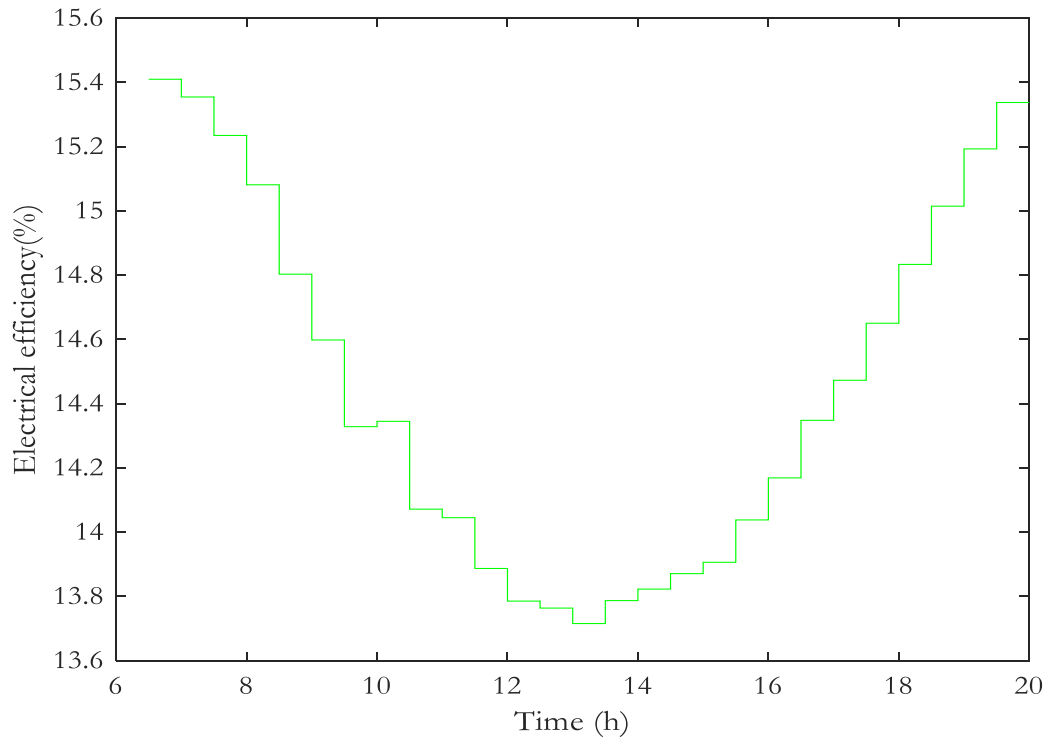Figure 4.12: PV module output power during winter without cooling

69
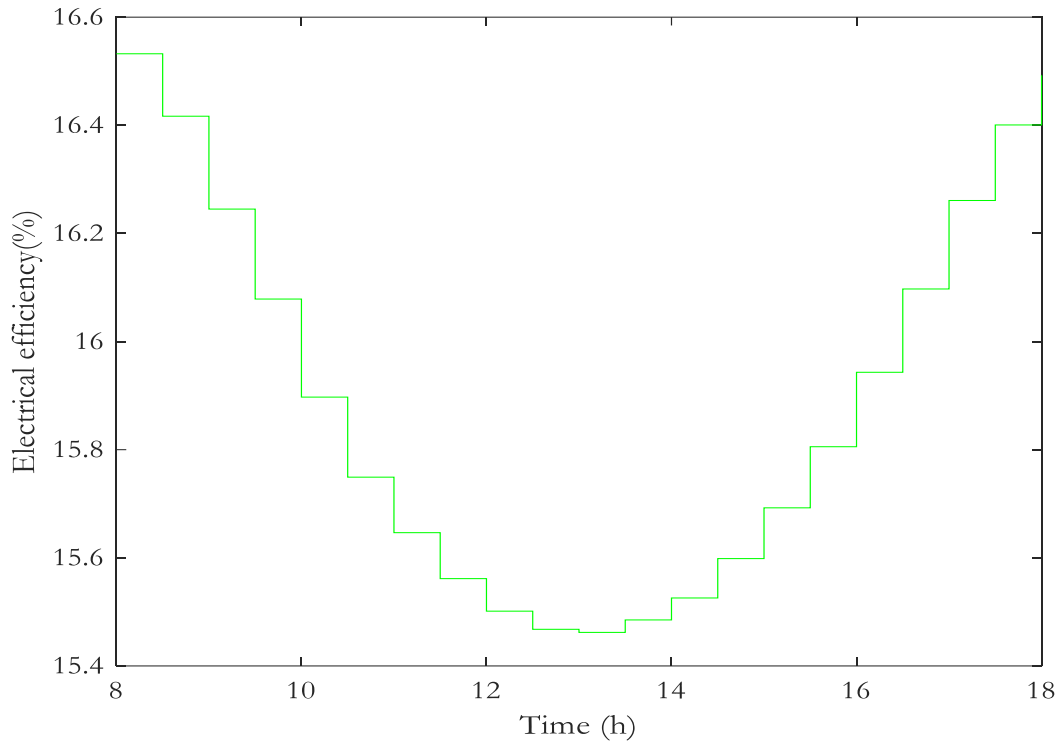
Figure 4.13: PV module cell efficiency during winter without cooling
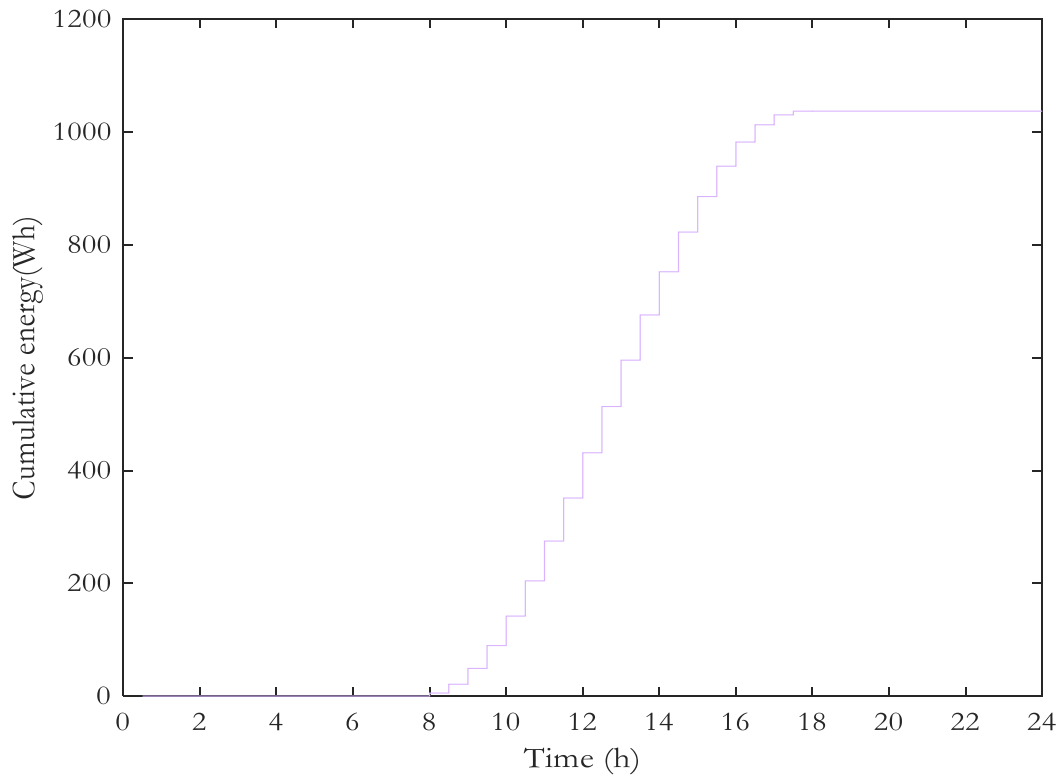
Figure 4.14: Cumulative energy during winter without cooling

70

4.3.2 Optimal switching control model

The optimal switching control of flow in hybrid PV/T systems, with forced circulation, is used to reduce the surface operating temperature of the PV module. Essentially, the fluid circulation pump is controlled by the optimal switching control model, where it is simulated by making use of the SCIP (solving constrained integer programs) solver in the optimization toolbox of MATLAB.

4.3.2.1 Optimal switching control model: Summer case

In Fig. 4.15, the cell temperature of the PV module with cooling is presented. Initially, the temperature of the PV module starts at 24.89°C, which is almost the same as the inlet water temperature at 6:30. The reason as to why the temperature of the PV module and the inlet water temperature are approximately is due to the water being stored in the flat plate collector pipes is attached to the back section of the PV module. After 7:30, the temperature of the PV module decreases to 24.8°C. This is due to the inlet water temperature changing to 23°C at the time and solar radiation being present at the time. From 8:00, the temperature increases slightly until it reaches a maximum of 25.27°C at 13:00, due to a high solar radiation of 1173W/m². From 13:30 to 20:00, the temperature decreases slightly until it reaches 25°C again, due to the absence of solar radiation and the inlet temperature changed to 25°C.

In Fig. 4.16, the output power of the PV module with cooling is presented. It may be observed that the output power begins at zero, due to the lack of solar radiation present until 6:30. After 6:30, the output power of the PV module starts to increase significantly. From 13:00 to 13:30, the output power reaches a maximum of 293W, due to the heat absorbed from the surface of the PV module, via the flat plate collector, leading to higher solar energy being converted to electrical energy, instead of heat energy. After, 13:30, the output power begins to decrease significantly due to a reduced magnitude of solar radiation present during that time until 20:00, the moment in which solar radiation is absent.

71

The cell efficiency of the PV module is illustrated in Fig. 4.17. At 6:30, the efficiency of the panel is 15.48% until 7:30 and slightly increases to a maximum of 15.414% due to the temperature of the PV module decreasing slightly at that time, as seen in Fig. 4.8. At 8:00, the efficiency begins to decrease slightly due to a slight temperature increase on the surface of the PV module up until 13:00 where the efficiency of the PV module is 15.381%. After 13:30, the efficiency increases until 18:00, due to the inlet water temperature increased to 24°C and the ambient temperature being 32°C during this time. After 18:00, the efficiency reaches 15.4% once more when the temperature of the PV module is 25°C and solar radiation is absent.

In Fig. 4.18, the cumulative energy produced by the PV module is illustrated. Initially, the cumulative energy is at zero until 6:30, due to the absence of solar radiation. After 6:30, the module begins to produce energy and accumulate during the entire day up to 20:00, reaching 2256.6Wh energy produced.

In Fig. 4.19, the switching function of the circulation pump, controlling the water flow to the PV module, is presented. The pump is initially switched off due to the solar radiation only begins to be present at 6:30, where the circulation pump is switched on to absorb maximum heat from the surface of the PV module. At 20:00, the circulation pump is switched off due to the absence of solar radiation. The reason for switching the circulation pump on when solar radiation is present, is due to the PV module being cooled optimally, in order to obtain the most output power at all times with the optimal switching control of flow model.

In Fig. 4.20, the hot water storage tank output temperature is presented. The initial temperature inside the tank is 25°C. From 06:00, the temperature begins to increase, due to the flat plate collector absorbing the heat from the surface of the PV module, when solar radiation is present and transferring that heat to the hot water storage tank via the fluid circulation pump. From 13:00 to 13:30, the dishwasher demands hot water, where the temperature reduces slightly and afterwards reaching a maximum of 69°C at 18:30. From 18:30 to 19:00, the temperature decreases to 50°C, due to the two occupants using the show during this period. From 19:30 to 20:00, the temperature decreases to 34°C, due to the two occupants using the shower during this period. From 21:00 to 21:30, the temperature decreases to 25°C,

72

due to the washing machine and the occupants' minor hygiene purposes. After 20:00, the temperature is kept at 25°C, which is the initial temperature for the next day.

In Fig. 4.21, the cumulative heat gained inside the hot water storage tank is illustrated. Initially, the cumulative heat gain is at zero until 6:30, due to the absence of solar radiation. After 6:30, the module begins to produce energy and accumulate heat during the day until 20:00, reaching 9.37 x10^{7}J heat gain, which is 26.03kWh.

Figure 4.15: PV module cell temperature during summer with cooling

Figure 4.16: PV module output power during summer with cooling

Figure 4.17: PV module cell efficiency during summer with cooling

74

Figure 4.18: Cumulative energy during summer with cooling

Figure 4.19: Optimal switching function of fluid circulation pump during summer

75
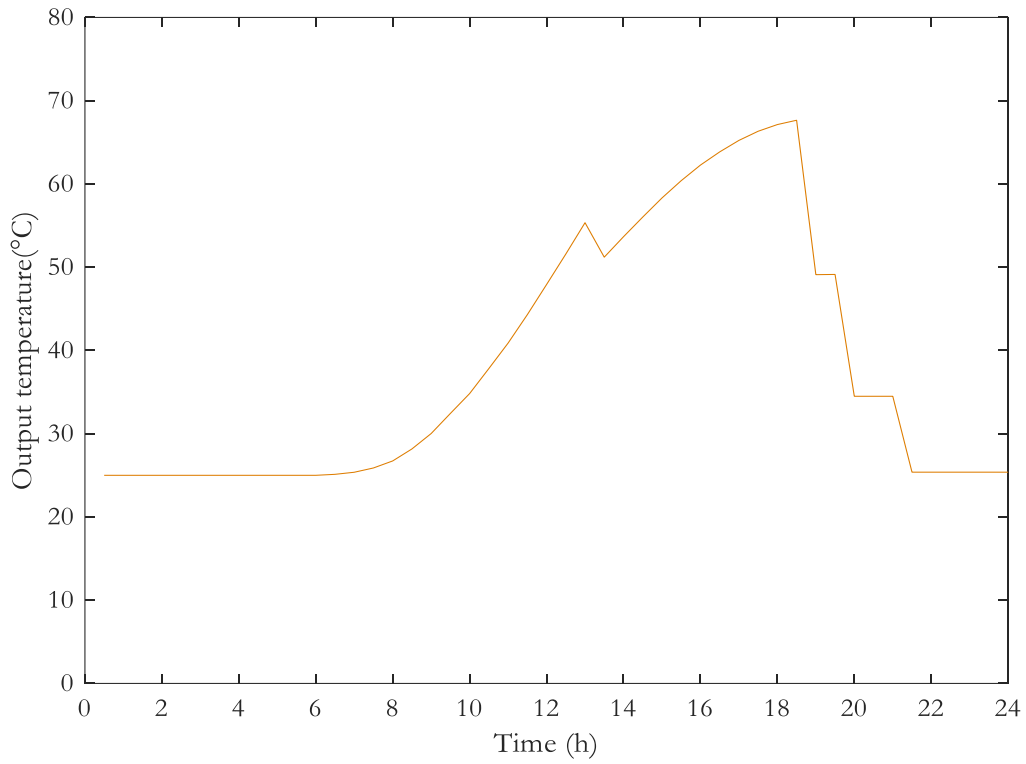
Figure 4.20: Hot water storage tank output temperature during summer

Figure: 4.21: Cumulative heat gain inside the hot water storage tank during summer

4.3.2.2 Optimal switching control model: Winter case

In Fig. 4.22, the cell temperature of the PV module with cooling is presented. Initially, the temperature of the PV module begins at 14.75°C, which is essentially proportionate to the inlet water temperature. The reason why the temperature of the PV module and the inlet water temperature are approximately even is due to the water stored in the flat plate collector pipes, that are attached to the back section of the PV module. After 4:00, the temperature of the PV module decreases to 14.62°C. This is due to the inlet water temperature altering to 14°C at the time. From 7:00, the temperature decreases marginally to 14.5°C, due to the inlet water temperature altering to 13°C. From 8:00, the temperature increases until it reaches a maximum of 14.87°C at 13:00 due to a higher solar radiation of 654.92W/m². From 13:30 to 18:00, the temperature decreases slightly until it drops to 14.62°C, due to the absence of solar radiation. After 18:30, the cell temperature alters back to 14.75°C, which is almost equivalent to the inlet water temperature at the time.

In Fig. 4.23, the output power of the PV module with cooling during winter is presented. It may be observed that the output power begins at zero due to no solar radiation present until 8:00 in the morning. After 8:00, the output power of the PV module starts to increase significantly. From 13:00 to 13:30 the output power reaches a maximum of 172W, due to the heat absorbed from the surface of the PV module via the flat plate collector, causing increased solar energy to be converted into electrical energy, instead of heat energy. After 13:30, the output power begins to decrease significantly, due to a reduced magnitude of solar radiation present during that time up until 18:00, the moment when solar radiation is absent.

The cell efficiency of the PV module is illustrated in Fig. 4.24. At 8:00, the efficiency of the panel is 16.207% and continues to decrease until 13:00, which is where the cell temperature is 14.87°C. After 13:30, the efficiency increases until 18:30, due to the cell temperature decreasing. After 18:00, the efficiency reaches 16.198%, when the temperature of the PV module is 14.75°C and solar radiation is absent.

In Fig. 4.25, the cumulative energy produced by the PV module is illustrated. Initially, the cumulative energy is at zero until 8:00, which is due to the absence of solar radiation. After

77

8:00, the module begins to produce energy and accumulate during the day up until 18:00, reaching 1070Wh energy produced.

In Fig. 4.26, the switching function of the circulation pump controlling the water flow to the PV module is portrayed. The pump is initially switched off due to the absence of solar radiation up until 8:00, where the circulation pump is switched on to absorb the maximum amount of heat from the surface of the PV module. At 18:30, the circulation pump is switched off due to the absence of solar radiation and the hot water demand at the time. The reason for the circulation pump being switched on when solar radiation is present is due to the PV module being cooled to the maximum in order to obtain optimal output power at all times with the optimal switching control of flow model.

In Fig. 4.27, the hot water storage tank output temperature is presented. The initial temperature inside the tank is 15°C. From 08:00, the temperature begins to increase, due to the flat plate collector absorbing the heat from the surface of the PV module and transferring that heat to the hot water storage tank via the fluid circulation pump. From 13:00 to 13:30, the temperature decreases somewhat, due to the dishwasher requiring hot water. The temperature increases until 17:00, where it reaches a maximum of 36°C. From 17:00 to 17:30, the temperature decreases to 27°C, due to the two occupants requiring hot water to shower. From 18:00 to 18:30, the temperature decreases further to 20°C, due to the two other occupants required hot water to shower. From 19:30 to 20:00, the temperature decreases to 15°C, due to the demand for both the washing machine and dishwasher. The temperature is consequently kept at 15°C, the initial temperature for the following day.

In Fig. 4.28, the cumulative heat gained inside the hot water storage tank is illustrated. Initially, the cumulative heat gain is at zero up until 8:00, due to the absence of solar radiation. After 8:00, the module begins to produce energy and accumulate heat during the day until 18:00, reaching 2.61×10^7J heat gain, which is 7.25kWh.
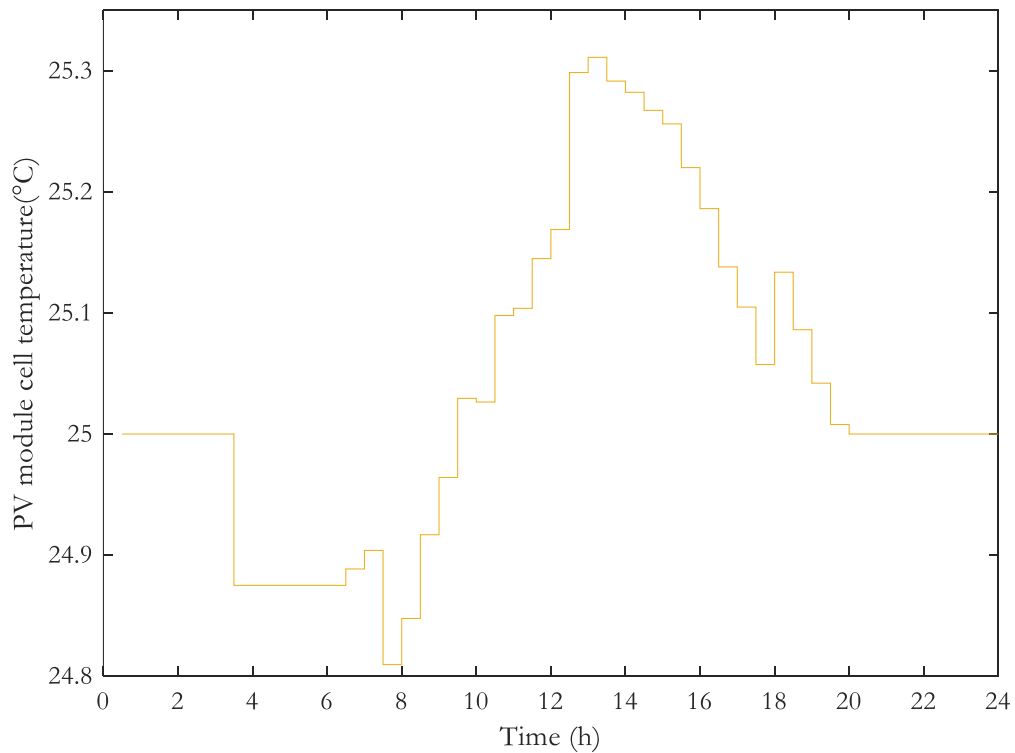
78
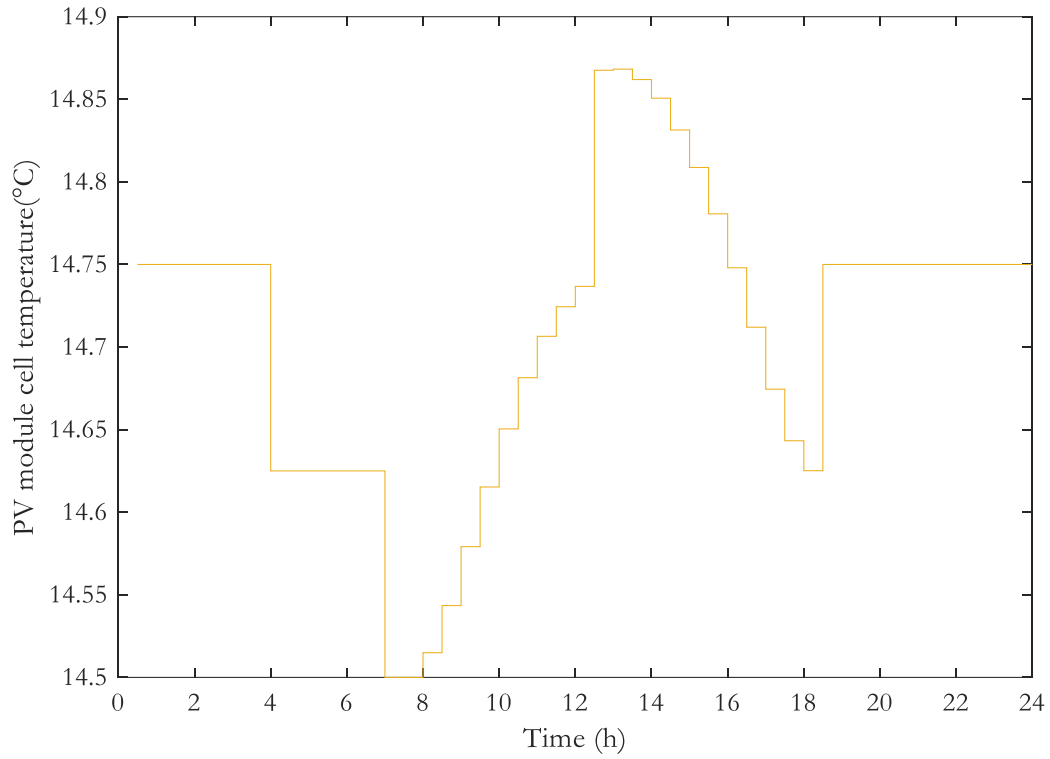
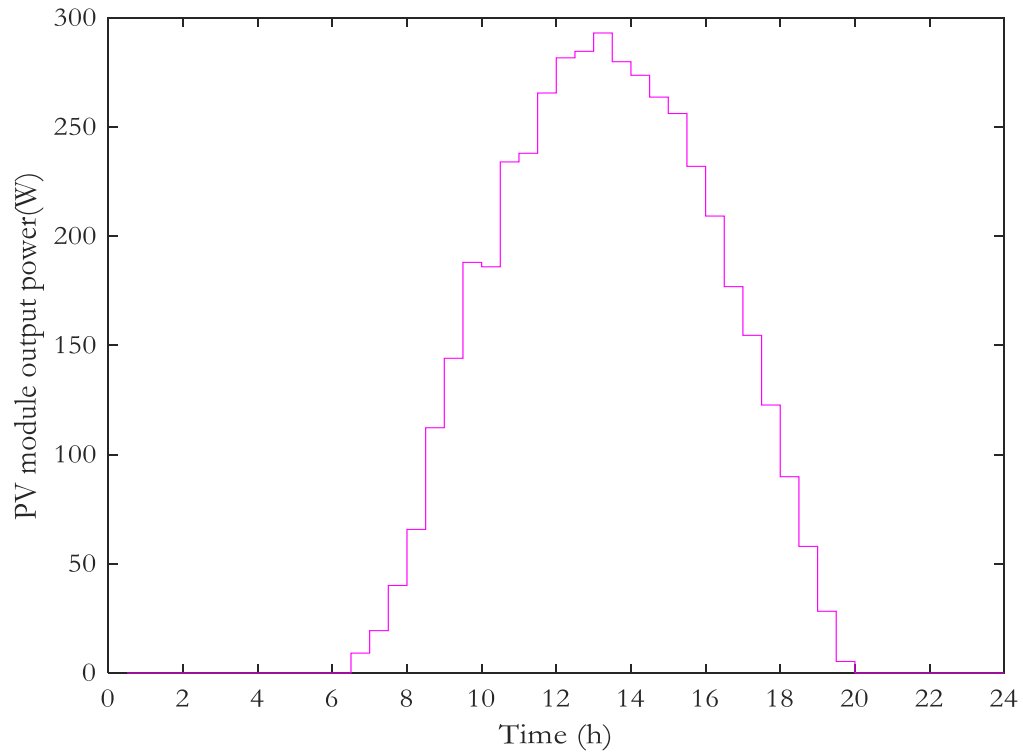Figure 4.22: PV module cell temperature during winter with cooling
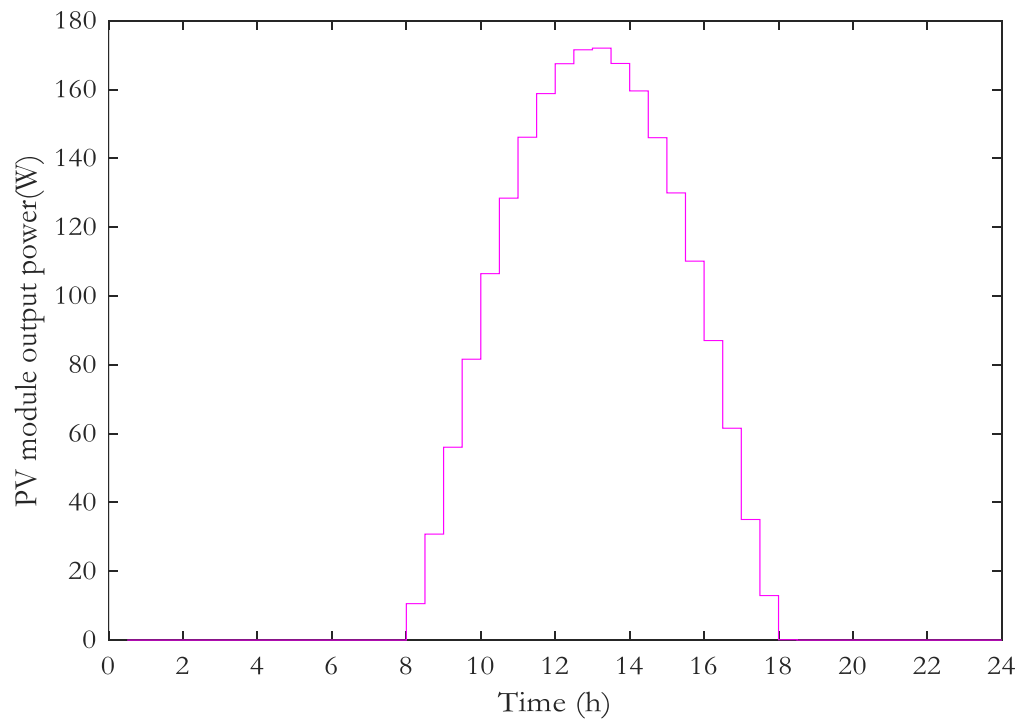
Figure 4.23: PV module output power during winter with cooling
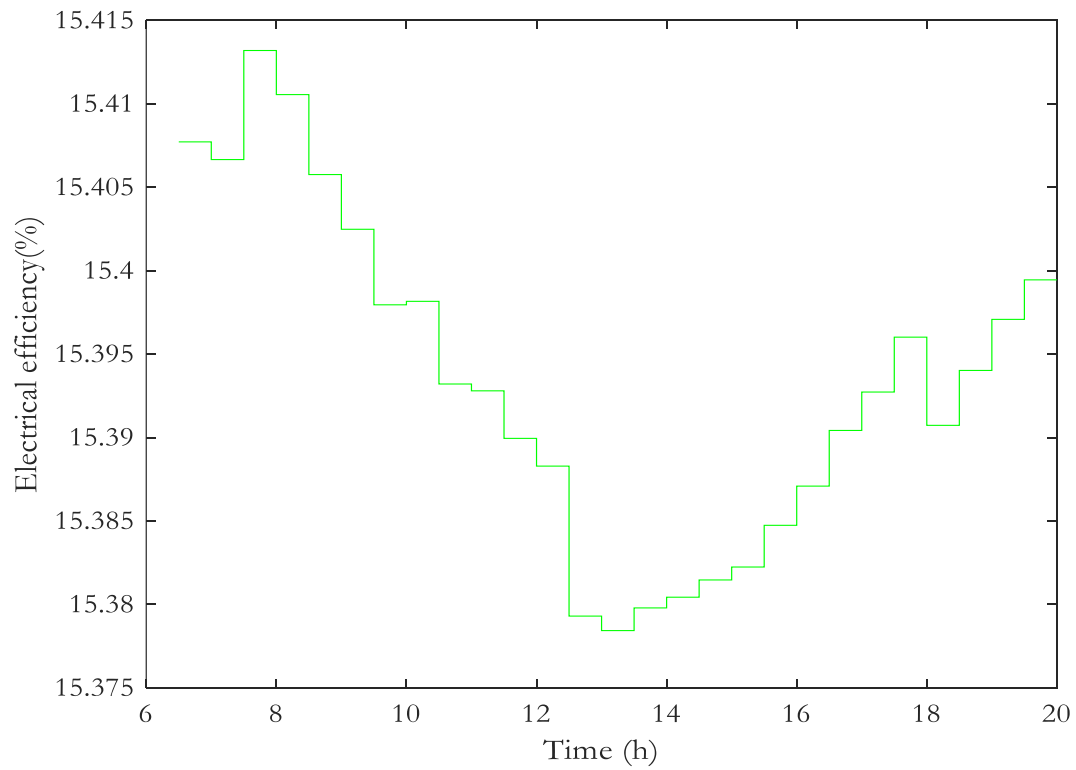
79
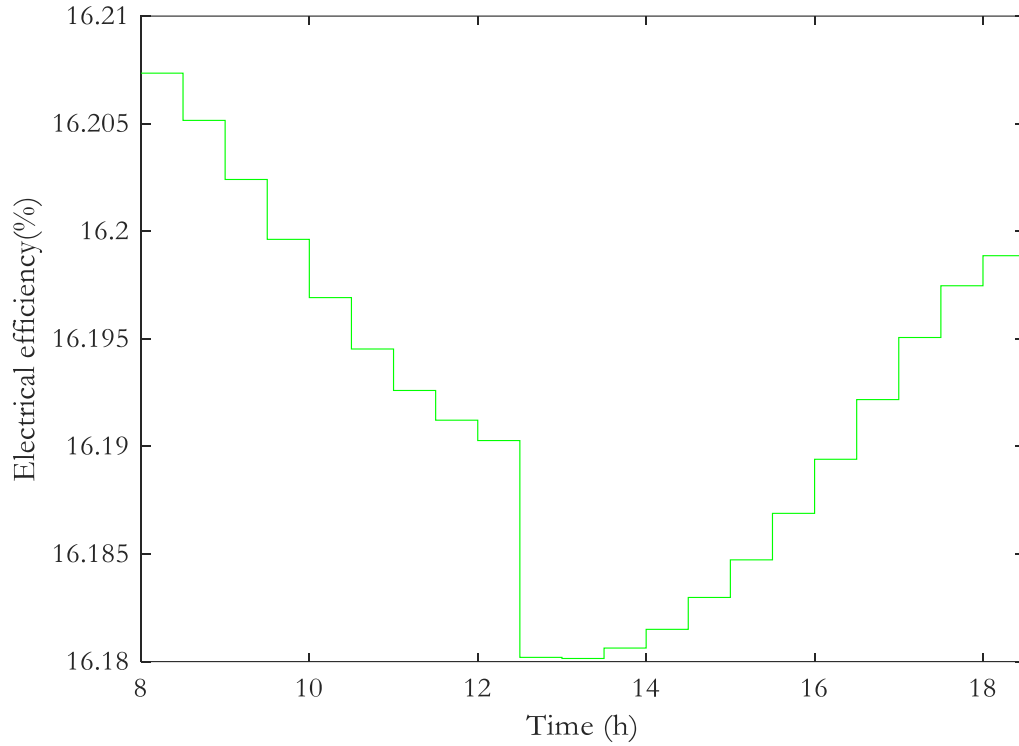
Figure 4.24: PV module cell efficiency during winter with cooling
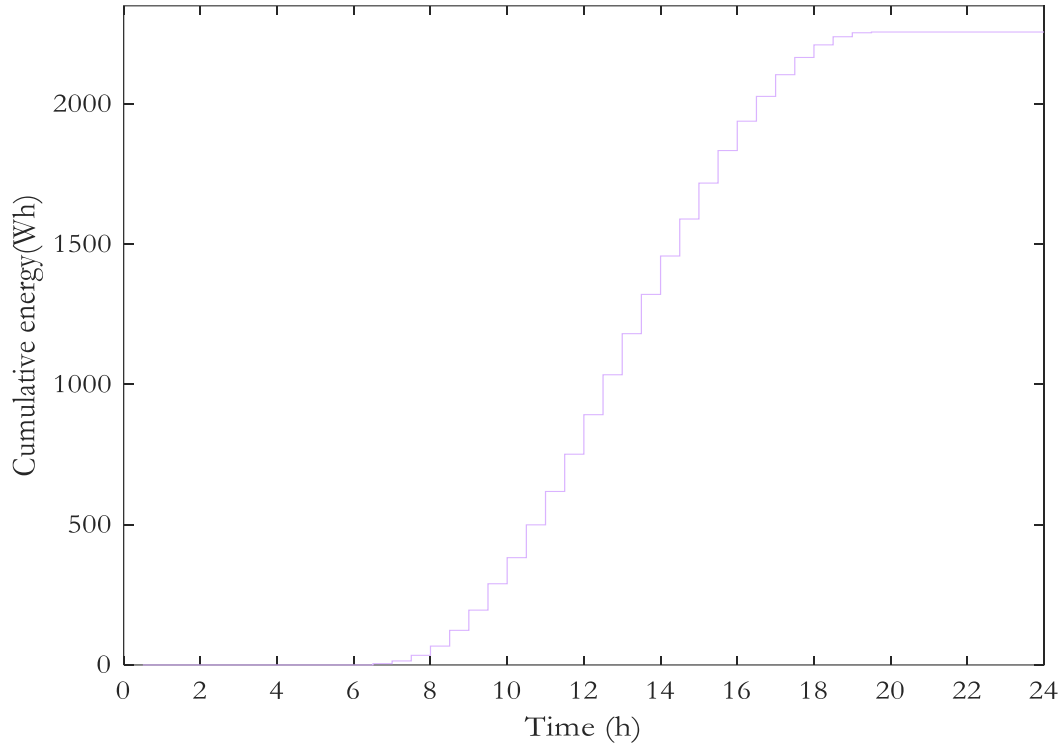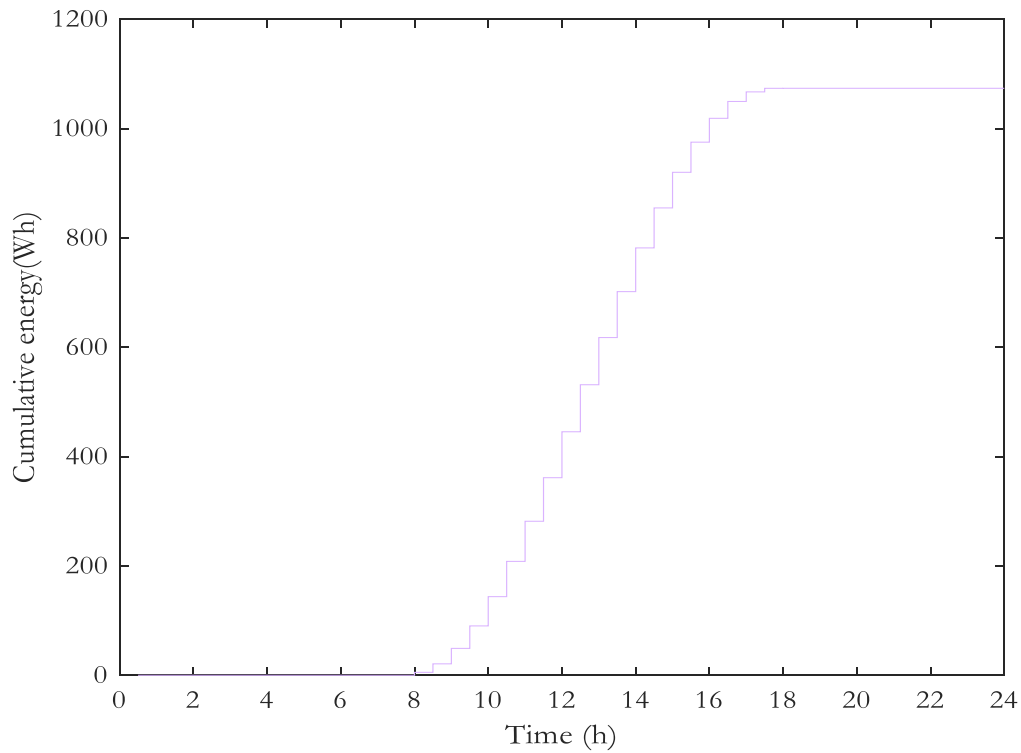

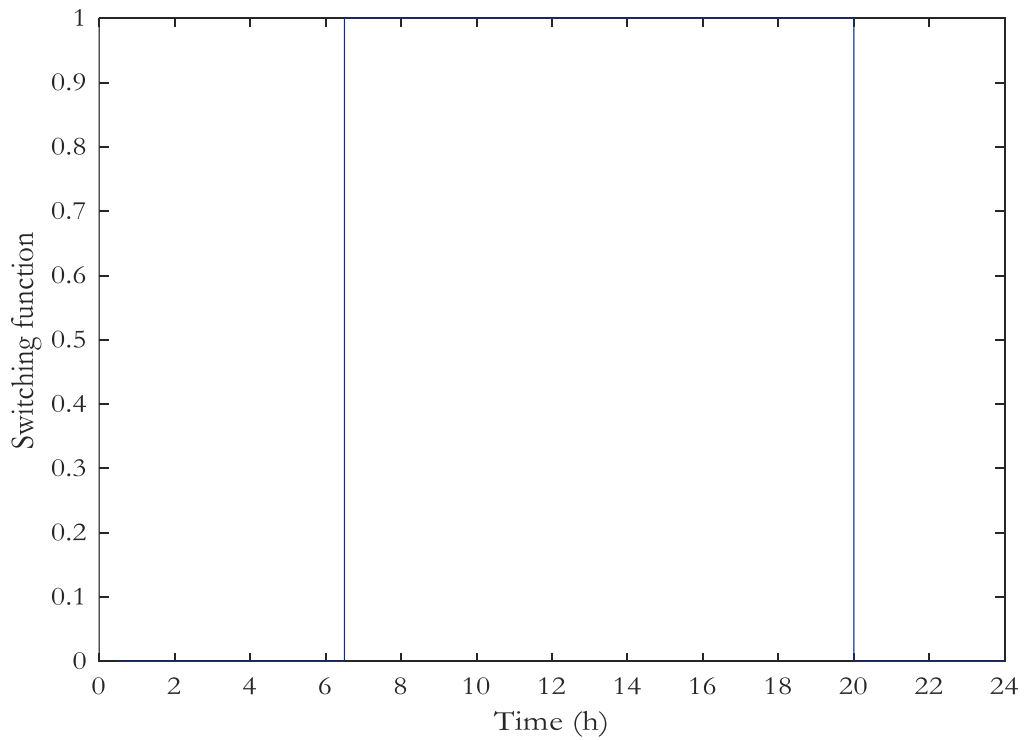Figure 4.25: Cumulative energy during winter with cooling

80
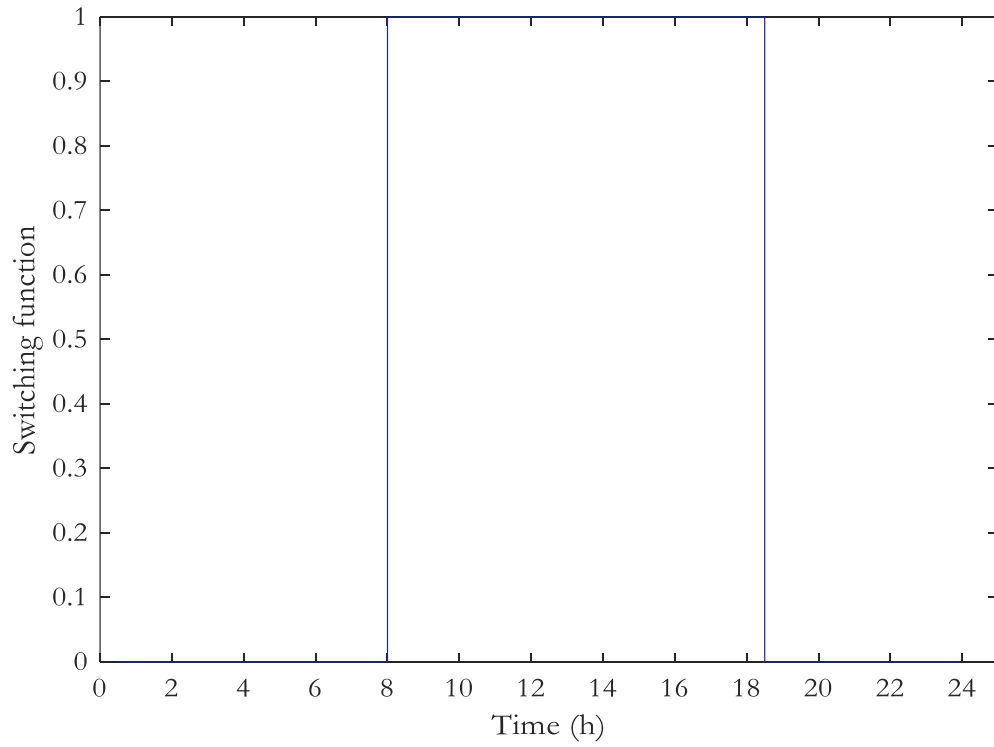
Figure 4.26: Optimal switching function of fluid circulation pump during winter

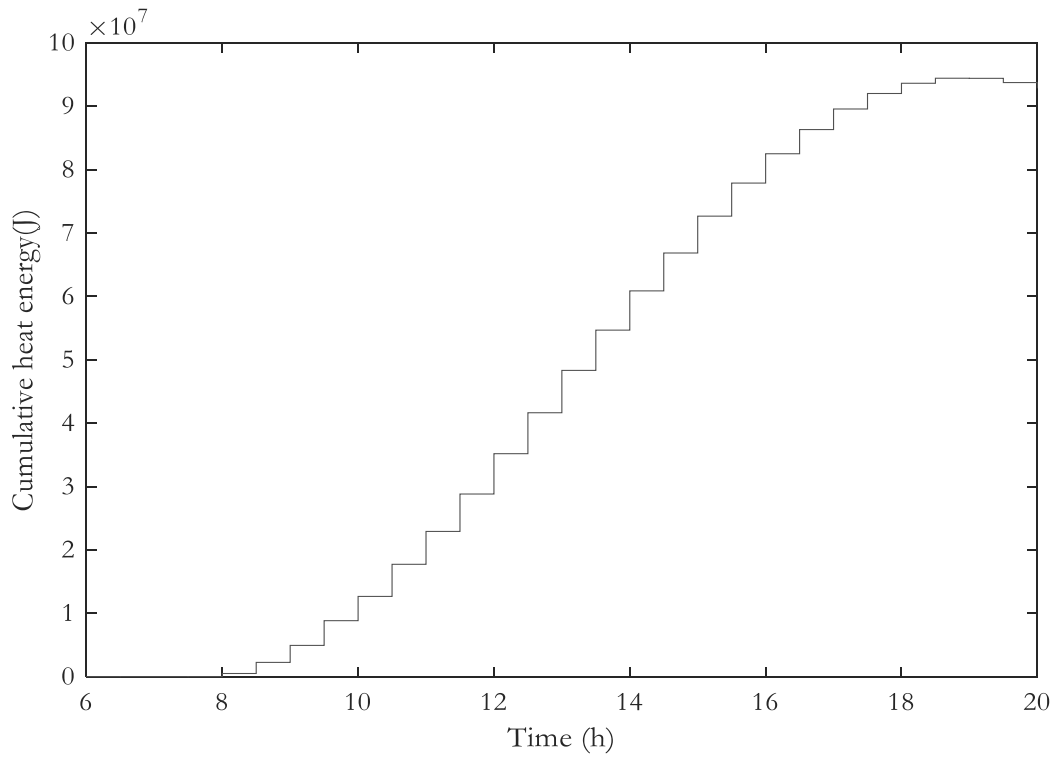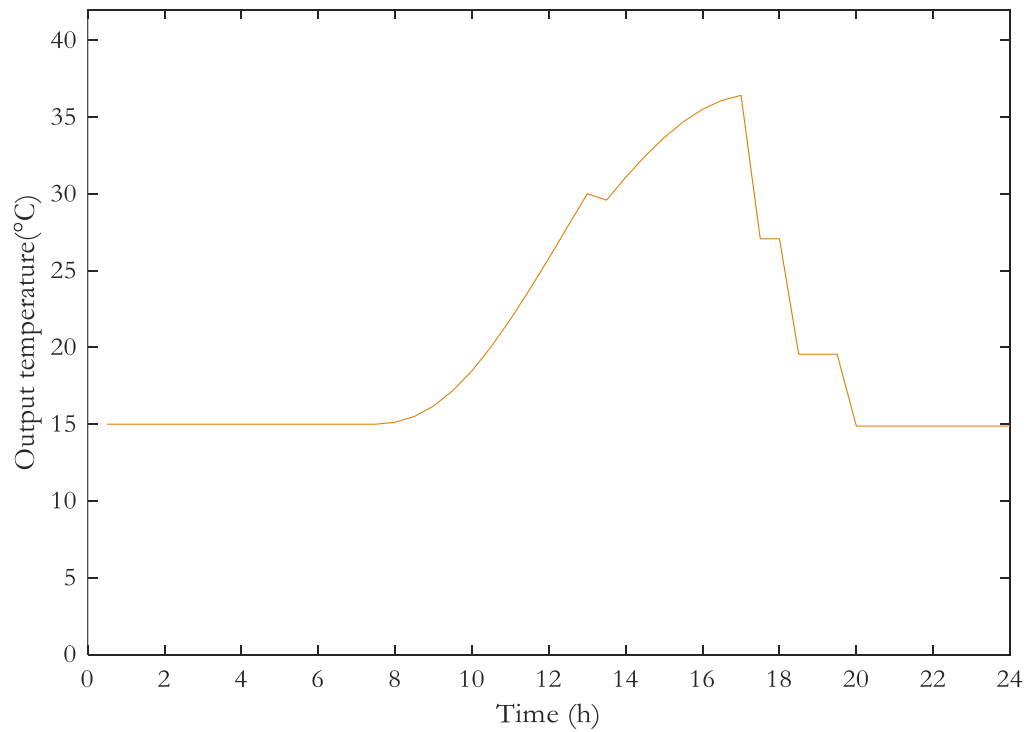Figure 4.27: Hot water storage tank output temperature during winter
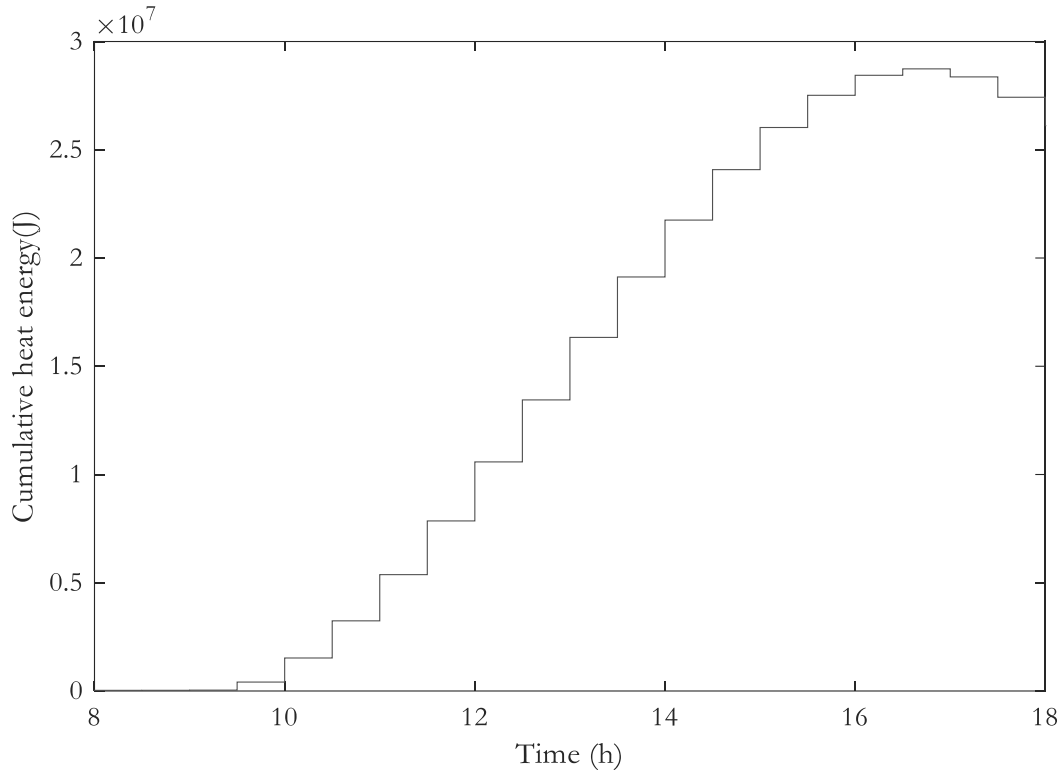
Figure 4.28: Cumulative heat gain of the hot water storage tank during winter

4.3.3. Comparison of the baseline and the optimal switching control model

The developed model for the baseline and the optimal switching of flow used is actual historic data for summer and winter, to successfully simulate the operation thereof.

4.3.3.1. Summer case

The temperature of the PV module without cooling reached a maximum of 46°C, whereas, the optimal switching control model reached a maximum of 25.27°C. The output power of the PV module obtained a maximum of 262W at 13.75% efficiency, due to its high surface temperature. The optimal switching control model obtained 293W at 15.38% efficiency due to applying the optimal switching control model.

The daily amount of energy produced during summer via the baseline is the cumulative sum of all the output power magnitudes at each interval during the day, which equates to

82

2083.2Wh/day, as presented in Fig. 4.10. On the other hand, the optimal switching control model generates 2256.6Wh/day, as seen in Fig. 4.18. However, the output generated by the optimal switching control model is essentially the output of the PV module, therefore not taking the energy consumed by the fluid circulation pump into account, which is rated 24W at 900l/h. However, at the time that the pump supplies the required flow rate of 324 l/h, the power consumption is 8.64W. The fluid circulation pump operates for 13 hours and 30 minutes during the day. Therefore, the energy consumed by the fluid circulation pump is calculated as follows, 8.64W x 13,5hours = 116.64Wh/day. Thus, the output energy of the optimal switching control model is calculated as 2256.6Wh – 116.64Wh = 2139.96Wh/day.

Therefore, the optimal switching control model may generate a marginally higher energy output compared to the baseline. The simulation results yield a 70.78% output energy improvement.

This intervention provides a practical optimal integration of PV and hot water supply for domestic loads. Furthermore, the model presents the potential to improve the lifespan of the PV module.

4.3.3.2 Winter case

The temperature of the PV module during winter, without cooling, reached a maximum of 24°C, whereas, the optimal switching control model reached a maximum of 14.87°C. The output power of the PV module obtained a maximum of 164W at 15.47% efficiency. The optimal switching control model obtained 172W at 16.18% efficiency, due to application of the optimal switching control model.

The daily amount of energy produced during winter via the baseline is the cumulative sum of all the output power magnitudes at each interval during the day, which equates to 1037.10Wh/day, as illustrated in Fig. 4.14. On the other hand, the optimal switching control model generates 1070Wh/day, as observed in Fig. 4.24. However, the output generated by the optimal switching control model is purely the output of the PV module, not taking into account the energy consumed by the fluid circulation pump, rated 24W at 900l/h. However,

83

when the pump supplies the required flow rate of 324l/h, the power consumption is 8.64W. The fluid circulation pump is in operation 10 hours and 30 minutes throughout the day. Therefore, the energy consumed by the fluid circulation pump is calculated as follows, 8.64W x 10,5hours = 90.72Wh/day. Hence, the actual output energy of the optimal switching control model is calculated as, 1070Wh – 90.72Wh = 979.28Wh/day.

4.4. Summary

In this chapter a standard PV system (baseline) and the optimal switching control of flow have been simulated using the SCIP (solving constrained integer programs) solver in the optimization toolbox of MATLAB. The developed model for the baseline and the optimal switching of flow used historic data to successfully simulate the operation thereof.

The optimal switching control of flow shows the potential to optimize the output power of the PV module efficiently during summer. The proposed model yields an output power improvement of 2.65% during summer, whereas a 5.90% deterioration during winter. Therefore, the collector effectively absorbs the heat from the surface of the PV module. The simulation results further demonstrate the proposed model yields a daily heat gain of 9.37×10^7J, 26.03kWh inside the water storage tank during the selected summer day and 2.61×10^7J, 7.25kWh during the selected winter day.

In addition, the PV output power, PV cell temperature and PV cell efficiency with and without cooling presented in this chapter are plotted on the same graph, and illustrated in Appendix B. This was performed for both summer and winter cases, in order to compare the performance of a PV module with and without cooling more clearly.

It should be noted that the heat generated on the surface of the PV module is significantly greater during summer in comparison to winter. Therefore, there will be a higher amount of hot water available during summer in comparison to winter.

This intervention provides a practical and optimal integration of PV and hot water supply for domestic loads. Furthermore, this model displays the potential to improve the lifespan of the PV module.

Chapter V: Economic analysis

5.1. Introduction

The cost effectiveness of a project should consistently be validated, where the proposed model is compared to a standard PV system, known as the baseline. There are economic performance indicators, such as simple payback period (SPP), internal rate of return (IRR), benefits-to-cost ratio (BCR) and life-cycle cost (LCC) [109]. The SPP method is straightforward to understand and to calculate. However, the SPP method does not factor in the instance of depreciating over time due to inflation and other factors. Furthermore, the project lifetime is not taken into account with this method, as the investors will not be fully aware of the profitability of the project.

5.2. Payback period

5.2.1. True payback period analysis

The payback period is defined as the number of years it takes to pay the initial capital investment back from the cash flow that the investment produces. The true PBP was selected to be the economic performance indicator for this study, due to the fact that it takes the project lifetime and time value of money into account. The true PBP can be estimated as the ratio between the present worth (PW) of total cost (PW_{TC}) and the annual average of the PW of total benefits (PW_{TB}). The true PBP method is proposed to compare the optimal switching control model with the standard PV system.

The true PBP, as previously mentioned is estimated by making use of the following equation:

$$"True" PBP = \frac{PW_{TC}}{PW_{TB-av}} \tag{5.1}$$

Where: PW_{TB-av} is the annual average PW_{TB}, calculated with the following equation:

$$PW_{TB-av} = \frac{PW_{TB}}{n} \tag{5.2}$$

Where: PW_{TC} is the total cost of the PW and PW_{TB} are the total benefits of the PW. The PW_{TC} is the algebraic sum of the total cost, for instance, the initial investment costs, and replacement costs. The salvage costs of all components are neglected, due to all the components assumed to be utilized over their lifetime. However, the replacement cost, C_{rep}, is included and calculated as follows [109]:

$$C_{rep} = C_{cap} N_{rep} \tag{5.3}$$

Where : C_{cap} is the initial capital cost of each component and N_{rep} is the number of component replacements over the projects lifetime.

The PW_{TB} is the annual cost savings obtained via the PV system and calculated by using the following equation [110]:

$$PW_{TB} = AB \left[\frac{(1+r)^n - 1}{r(1+r)^n} \right] \tag{5.4}$$

Where : AB is the annual benefit, n is the project lifetime and r is the average inflation rate. The annual average inflation rate data has been acquired from the historic inflation of South Africa, showing an average inflation rate of 5.49%, as seen in Fig. 5.1. By making use of this average inflation rate, an accurate prediction can be made regarding future costs.

86
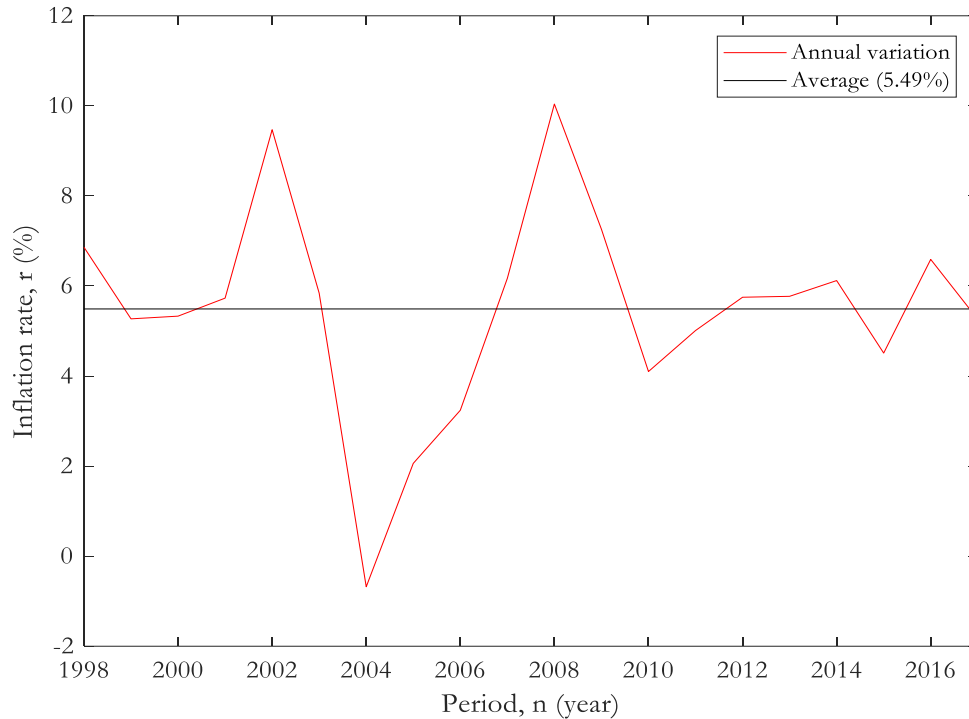
Figure 5.1: The annual average inflation rate of South Africa from 1998 until 2017 (Adapted from Ref. [111])

5.2.2. Initial capital investment

In this sub-section, the initial investment cost of the standard PV system and the optimal switching control model is broken down into component level, where the South African Rand was trading at R12.36 to the United States dollar.

Table 5.1 below, presents prices of the components used for the analysis of the standard PV system [112], where it can be observed that the EnerSol 250W Solar Panel contributes the most towards the initial investment thereof.

Table 5.2 presents the prices of the components for the optimal switching control model [112-115], in which one can observe that the SunScan 1.7m² flat plate collector of the optimal switching control model has the highest cost. It can also be observed that it contains many components, compared to the standard PV system and the initial investment is higher by a factor of 3 compared to the standard PV system.

87

Table 5.1: Bill of quantity of the standard PV system

Component description	Quantity	Net price (R)	Net price (USD)
EnerSol 250 W Solar Panel	1	2,511.60	203.2
Solar aluminium structure	1	1,000	80.91
Labour	-	2,000	161.81
Total initial investment cost	-	5,511.60	445.92

Table 5.2: Bill of quantity of the optimal switching control model

Component description	Quantity	Net price (R)	Net price (USD)
EnerSol 250W Solar Panel	1	2,511.60	203.2
SunScan 1.7m² flat plate collector	-	4,186	338.67
Solar aluminium structure	1	1,500	121.36
150 l GAP ECO electric storage tank	1	2,995.20	242.33
DC50K Solar Circulation Pump and Controller	1	1,006.67	81.45
Labour	-	4,000	323.62
Total initial investment cost	-	16,199.47	1,310.63

5.2.3. Annual energy cost savings

The annual energy cost savings is the cumulative electrical energy generated by the PV module for the standard PV system, as well as the optimal switching control model. Furthermore, the heat gain within the hot water storage tank is included solely for the optimal switching control model, which is calculated using the following equation [50]:

$$C_{gain} = t_s.M.C\sum_{k=0}^{N}(T_{c,o}(k) - T_{c,i}(k)).U(k) \tag{5.1}$$

88

where:

t_s is the sampling time,

M is the mass of the circulation fluid,

C is the specific heat capacity of water,

$T_{c,o}$ and $T_{c,i}$ are the outlet and inlet temperatures of the thermal collector pipes, respectively and $U_{(k)}$ is the switching status of the circulation pump.

The daily cumulative electrical energy generated by the PV module during a typical summer day was 2.08kWh and 1.04kWh during a winter day. These values were obtained from section 4.3.1.1 showing a typical summer day and 4.3.1.2 of a typical winter day.

Further, the daily cumulative electrical energy generated by the optimal switching control model during a typical day in summer was calculated as follows: 2256.6Wh – 116.64Wh = 2.14kWh. Throughout winter, the daily cumulative energy generated can be calculated as follows: 1070Wh – 116.64Wh = 0.98kWh. These values were obtained from section 4.3.2.1, illustrating a typical summer day and 4.3.2.2, a typical winter day. The energy consumed by the circulation pump is 116.64Wh, where the calculation is presented in section 4.3.3.1 and section 4.3.3.2.

The daily cumulative heat gain inside the hot water storage tank of the optimal switching control model during a typical day in summer was 26.03kWh and 7.25kWh during a typical winter day. These values were obtained from section 4.3.2.1, displaying a typical summer day and 4.3.2.2 a typical winter day. The total energy is the sum of the daily cumulative electrical energy generated by the PV module and the heat gain inside the hot water storage tank. During summer, the total energy is calculated as follows, 2.14kWh + 26.03kWh = 28.17kWh. Whereas, a typical day during summer may be calculated as follows, 0.98kWh + 7.25kWh = 8.23kWh.

The annual cost savings for the standard PV system and the optimal switching control model is calculated from Table 5.3, where the electricity tariff is $0.16USD$/kWh.

The annual energy cost for the standard PV system is USD 106.18 and USD 1339.31 for the optimal switching control model.

89

Table 5.3: Annual energy cost savings

Strategy	Energy cost (USD/day)	Energy cost (USD/year)	Saving
Standard PV system			
Standard PV system-summer	2.083 kWh x 0.16 USD/kWh = 0.333	0.333 x 273 days = 90.91	/
Standard PV system-winter	1.037 kWh x 0.16 USD/kWh = 0.166	0.166 x 92 days = 15.27	
Standard PV system-total net cost	/	106.18	
Optimal control			
Optimal control-summer	28.17 kWh x 0.16 USD/kWh = 4.51	4.507 x 273 days = 1231.23	
Optimal control-winter	8.23 kWh x 0.16 USD/kWh = 1.32	1.32 x 92 days = 121.44	
Optimal control-total net cost		1352.67	% 92.15

5.3. Results and discussion

The true payback period calculations for the standard PV system and the optimal switching control model are performed in this section. The operational and maintenance costs are assumed as 1% for both systems, that is, USD 4.46 and USD 13.11 for the standard PV system and optimal switching control model, respectively.

The annual benefit (AB), for the standard PV system, is calculated as USD 106.18 – USD 4.46 = USD 101.72/year and USD 1352.67 – USD 13.11 = USD 1339.56/year for the optimal switching control model. The parameters used to analyse the cost-effectiveness of both the standard PV system and the optimal switching control model are illustrated in Table 5.4.

The true PBP for both the standard PV system and optimal switching control model is calculated and illustrated in Table 5.5, where the project and component lifetime are likewise indicated.

Table 5.4 : Parameters of the Standard PV system and Optimal switching control model

Parameters	Standard PV system	Optimal model
Total initial investment (*USD*)	445.92	1,310.63
Project lifetime, *n* (years)	30	30
PV lifetime (years)	30	30
N_{rep-PV} (-)	0	0
C_{rep-PV} (USD)	0	0
SunScan 1.7m² flat plate collector lifetime (years)	/	20
N_{rep-SC} (-)	/	1
C_{rep-SC} (USD)	/	335.68
Solar Circulation Pump lifetime (years)	/	12
N_{rep-CP} (-)	/	2
C_{rep-CP} (USD)	/	162.9

Table 5.5: True PBP of the Standard PV system and Optimal switching control model

Parameters	Standard PV system	Optimal model
AB (USD)	101.72	1,338.51
PW_{TC}	445.92	1,809.21
PW_{TB}	1,479.92	19,489.25
PW_{TB-av}	123.33	1624.1
"True" PBP (years)	4	2

The results in Table 6.5 present that the total investment should be recovered over the period of 4 years for the standard PV system. In this case, the project lifetime amounts to 30 years, in which the investor has 26 years to generate a profit. However, it takes 2 years to recover the total capital cost with the optimal switching control model. Therefore, the investor has 28 years to generate a profit. The optimal switching control model may generate more energy than the standard PV system. Therefore, the optimal switching control model generates a higher profit over the predicted lifetime, compared to the standard PV system. However, having a higher initial investment cost compared to the standard PV system.

5.4. Summary

In this chapter, the optimal switching control strategy was evaluated. The initial capital costs and energy generated of both the optimal switching control strategy and the standard PV system (baseline) were noted, in order to compare the aforementioned systems.

A payback period analysis was done in order to calculate the time in which each system will be paid back and thereafter generate profit. The analysis presented the total capital cost of the standard PV system may be recovered after 4 years, which provides the investor 26 years to generate profit from their investment. However, the analysis displayed that it takes 2 years to regain the total capital investment for the optimal switching control strategy. The initial capital cost of the optimal switching control strategy is higher by a factor of 3 than the standard PV system, which comes forth as objectional in investing in the optimal switching control strategy. However, when observing both systems over their predicted lifetimes, the optimal switching control strategy generates a significantly higher profit, regardless of its extortionate initial capital cost and is therefore the ultimately efficient system.

Chapter VI: Conclusion and recommendations

6.1. Conclusion

This Chapter summarizes the proposed research conducted in this work, based on the optimal switching control of flow in hybrid PV/T system, cooled by forced water circulation.

The main concern, addressed in this research, was the influence of temperature on the PV module and the associated decrease in efficiency thereof. This research was based on developing an optimal control model to maximize the energy output of the PV module using water circulation to collect the heat and persevering in maintaining the surface temperature as minimal as achievable.

The operating principle of the hybrid PV/T system has been described in Chapter III, followed by the mathematical model for the hybrid system's optimal switching control.

The first and main objective function is to maximize the energy output of the PV module, by controlling the pump switching status, whilst utilizing the heat absorbed via the flat plate collector for domestic applications. The control variable can either be 1 or 0, the upper bound and lower bound constraint of the switch. The second objective function is to minimize the discomfort level within the hot water storage tank, where the discomfort level is the difference between the output temperature of the hot water storage tank and the desired temperature. The discomfort level in this study has a lower priority compared to the first objective function. The objective function and subjected constraints were derived, where the SCIP (solving constrained integer programs) solver in the optimization toolbox of MATLAB was used.

In Chapter IV, the PV system, flat plate collector and hot water storage tank temperature parameter data have been utilized as inputs for the purpose of the simulation. The hourly solar radiation, ambient temperature and hot water demand have furthermore been used as inputs. A baseline was established, representing a standard 250W PV system without cooling during summer and winter for Bloemfontein, Free State. The optimal switching control strategy was evaluated by comparing it with the baseline through simulations, presented in this chapter.

93

The simulation results present that the proposed model yields an output power improvement of 2.65% during the selected summer day, whereas a 5.90% deterioration during winter. The simulation results further show that the proposed model yields a daily heat gain of 9.37×10^7J, being 26.03kWh within the water storage tank during the selected summer day and 2.61×10^7J, being 7.25kWh during the selected winter day.

Chapter V has presented an economic feasibility study of a standard PV system, compared to the optimal switching control model. The payback period (PBP) is used to evaluate the economic performance of both systems, where it takes up to 4 years and 2 years for the investor to generate profit from the standard PV system and the optimal switching control model, respectively. However, when looking at both systems over their predicted lifetime, the optimal switching control strategy generates a higher profit of 92.41%, when the heat gain inside the hot water storage tank is included as energy gain, regardless of its extortionate initial capital cost, and is, therefore, the most efficient system.

The following conclusions can be made from this study:

- The proposed optimal switching control model of a hybrid PV/T system cooled with forced water circulation may make a significant improvement in harvesting energy from the sun and, therefore, reducing the rate of cell degradation and maximizing the life span of the PV module, as revealed from the literature review conducted in chapter II.

- The initial capital cost of the optimal switching control model is extortionate in comparison to the standard PV system. However, it generates a significantly higher profit over its lifetime, compared to the standard PV system.

- There is further heat gain inside the hot water storage tank, which is considered a saving, as a result of less money being lost to heat the water.

6.2. Recommendations

This research was focusing solely on developing an optimal switching control strategy of a hybrid PV/T system, cooled by forced water circulation. In future work, an optimal control

strategy may be developed, in which an optimal mass flow rate at each desired interval may be obtained in the stead of switching a constant flow rate.

The techno-economic implications of using other circulating fluids, other than water, will further be investigated.

Future research may be done on closed loop control techniques, such as model predictive control (MPC). This may minimize the unexpected disturbances as a result of solar radiation, ambient temperature, hot water demand and ambient inlet water temperature.

In this study, a circulation pump was utilized to cool the PV module, which consumes energy. The PV module may be cooled through a domestic thermosyphon system, at which point there is no circulation pump to consume energy and the overall conversion efficiency may be compared to the current hybrid PV/T system.

References

[1] Hu J., Chen W., Yang D., Zhao B., Song H. and Ge B. "Energy performance of ETFE cushion roof integrated photovoltaic/thermal system on hot and cold days." *Applied Energy*, vol. 173, pp. 40-51, March. 2016.

[2] Yau Y.H. and Lim K.S. "Energy analysis of green office buildings in the tropics-Photovoltaic system." *Energy and Buildings*, vol. 126, pp. 177-193, May. 2016.

[3] Wang Y., Zhou S. and Hou H. "Cost and CO_2 reductions of solar photovoltaic power generation in China: Perspectives for 2020." *Renewable and Sustainable Energy Reviews*, vol. 39, pp. 370-380, November. 2014.

[4] Bhubaneswari P., Iniyan S. and Goic R. "A review of solar photovoltaic technologies." *Renewable and Sustainable Energy Reviews,* vol. 15, pp.1625-1636, 2011.

[5] da Silva R.M. and Fernandes J.L.M. "Hybrid photovoltaic/thermal (PV/T) solar systems simulation with Simulink/Matlab." *Solar Energy,* vol. 84, pp.1985-1996, December. 2010.

[6] Elbreki A.M., Alghoul M.A., Al-Shamani A.N., Ammar A.A., Yegani B., Alsanossi, Aboghrara M., Rusaln M.H. and Sopian K. " The role of climatic-design-operational parameters on combined PV/T collector performance: A critical review." *Renewable and Sustainable Energy Reviews,* vol. 57, pp.602-647, January. 2016.

[7] Kumar K., Sharma S.D., Jain L. "Standalone Photovoltaic (PV) Module Outdoor Testing Facility for UAE Climate." Submitted to CSEM-UAE Innovation Centre LLC, 2007.

[8] Sahay A, Sethi V.K, Tiwari A.C and Pandey M. "A review of solar photovoltaic panel cooling systems with special reference to Ground coupled central panel cooling system (GC-CPCS)." *Renewable and Sustainable Energy Reviews*, vol. 42 pp. 306-312, October. 2014.

[9] Royne A, Dey C.J. and Mills D.R. "Cooling of photovoltaic cells under concentrated illumination: a critical review." *Solar Energy Materials and Solar Cells*, vol. 86 pp. 451-483, April. 2003.

[10] Jordehi A.R. "Parameter estimation of solar photovoltaic (PV) cells." *Renewable and Sustainable Energy Reviews*, vol. 61, pp. 354-371, July. 2016.

[11] Duffie J.A., Beckman W.A. "*Solar Engineering of thermal processes.*" John Wiley & Sons, 2013, New York.

[12] Moharram K.A., Abd-Elhady M.S., Kandil H.A. and El-Sherif H. "Enhancing the performance of photovoltaic panels by water cooling." *Ain Shams Engineering Journal,* vol. 4, pp. 869-870, May. 2013.

[13] Hove T. "A method of predicting long-term average performance of photovoltaic systems." *Renewable Energy*, vol. 21, pp. 207-229, 2000.

[14] Siegel M., Klein S., Beckman W. "A simplified method for estimating the monthly average performance of photovoltaic systems." *Solar Energy*, vol. 26, pp. 413-418, July. 1981.

[15] Evans D. "Simplified method for predicting photovoltaic array output." *Solar Energy*, vol. 27, pp. 555-560, 1981.

[16] Cazzaniga R., Clot M.R., Clot P.R. and Tina G.M. "Floating tracking cooling concentrating (FTCC) systems." In *Proc. 0160-8371*, 2012, pp. 514-517.

[17] Chen H.T, Lai S.T, Haung L.Y. "Investigation of heat transfer characteristics in plate-fin heat sink." *Applied Thermal Engineering*, vol. 50, pp. 352-360, January. 2013.

[18] Pang W., Liu Y., Shao S., Gao X. "Empirical study on thermal performance through separating impacts from a hybrid PV/TE system design integrating heat sink." *International Communications in Heat and Mass Transfer*, vol. 60, pp. 9-12, November 2015.

[19] Good C. "Environmental impact assessments of hybrid photovoltaic-thermal (PV/T) systems." *Renewable and Sustainable Energy Reviews*, vol. 55, pp. 234-235, Oct. 2015.

[20] Alzaabi A.A., Badawiyeh N.K., Hantoush H.O. and Hamid A.K. "Electrical/thermal performance of hybrid PV/T system in Sharjah, UAE." *International Journal of Smart Grid and Clean Energy*, vol. 3, pp. 385, Oct 2014.

[21] Sharma S.D., Kitano H. and Sagara K. "Phase Change Materials for Low Temperature Solar Thermal Applications." *Energy*, vol. 29, pp. 31-64, September. 2004.

[22] Solar Electricity and Heat in One Package. Internet: https://solartoday.org/2015/01/solar-electricity-and-heat-in-one-package/, January. 2015.

[23] Mehrotra S., Rawat P., Debbarma M. and Sudhakar K. "Performance of a solar panel with water immersion cooling technique." *International Journal of Science, Environment and Technology*, vol. 3, pp. 1161-1172, June. 2014.

[24] Zhu L., Raman A.P. and Fan S. "Radiative cooling of solar absorbers using a visibly transparent photonic crystal thermal blackbody." *In Proceedings of the National Academy of Sciences*, August. 2015, pp.12282-12287.

[25] Cracker H. Radiative cooling of solar absorbers using a visibly transparent photonic crystal thermal blackbody. Internet: https://gadgtecs.com/2015/09/25/engineers-invent-clear-coating-that-boost-solar-cell-efficiency-by-cooling-them/ , September. 2015.

[26] Mazón-Hernández R. , García-Cascales J. R. , Vera-García F. , Káiser A. S. and Zamora B. "Improving the Electrical Parameters of a Photovoltaic Panel by Means of an Induced or Forced Air Stream." *International Journal of Photoenergy*, pp. 1-10, February. 2013.

[27] Kiflemariam R, Almas M and Lin C. "Modeling Integrated Thermoelectric Generator-Photovoltaic Thermal (TEG-PVT) System." *COMSOL Conference in Boston*, 2014.

[28] Carlotti M., Ruggeri G., Bellina F., Pucci A. "Enhancing optical efficiency of thin-film luminescent solar concentrators by combining energy transfer and stacked design." *Journal of Luminescence*, vol. 171, pp. 215-220, March. 2016.

[29] Vishwanathan B., Reinders A.H.M.E., de Boer D.K.G., Desmet L., Ras A.J.M., Zahn F.H., Debije M.G.. "A comparison of performance of flat and bent photovoltaic luminescent solar concentrators." *Solar energy*, vol. 112, pp. 120-127, February. 2015.

[30] Shaltout M.A.M., Ghettas A., Sabry M. "V-trough concentrators on a photovoltaic full tracking system in a hot desert climate", *Renewable Energy,* vol. 6, pp. 527–532, 1995.

[31] Andrade L.A., Barrozo M.A.S., Vieira L.G.M. "A study on dynamic heating in solar dish concentrators", *Renewable Energy,* vol. 87, pp. 501-508, March. 2016.

[32] Parel T.S., Pistolas C., Danos L. and Markvart T. "Modelling and experimental analysis of the angular distribution of the emitted light from the edge of luminescent solar concentrators", *Optical Materials,* vol. 42, pp. 532-537, April. 2015.

[33] Wu Y., Connelly K., Liu Y., Gu X., Gao Y. and Chen G.Z. "Smart solar concentrators for building integrated photovoltaic façades", *Solar Energy,* vol. 133, pp. 111-118, August. 2016.

[34] Rabl A. "Comparison of solar concentrators", *Solar Energy,* vol. 18, pp. 93-111, August. 1976.

[35] Correia S.F.H., Lima P.P., Andre P.S., Ferreira M.R.S. and Carlos L.A.D. "High-efficiency luminescent solar concentrators for flexible wave guiding photovoltaics", *Solar Energy Materials and Solar Cells,* vol. 138, pp. 51-57, July. 2015.

[36] Akbarzadeh A., Wadowski T. "Heat-pipe-based cooling systems for photovoltaic cells under concentrated solar radiation." *Appl Therm Eng,* vol. 16, pp. 81-87, January. 1996.

[37] Alonso Garcia M.C., Balenzategui J.L. "Estimation of photovoltaic module yearly temperature and performance based on Nominal Operation Cell Temperature calculations." *Renewable Energy,* vol. 29, pp. 1997-2010, October. 2004.

[38] S. Dubey, Tiwari G.N. "Thermal modeling of a combined system of photovoltaic thermal (PV/T) solar water heater." *Solar Energy,* vol. 82, pp. 602-612, July . 2008.

[39] Hashim H., Bomphrey J.J., Min G. "Model for geometry optimisation of thermoelectric devices in a hybrid PV/TE system." *Renewable Energy,* vol. 87, pp. 458-463, March . 2016.

[40] Popovici C.G., Hudisteanu S.V., Mateescu T.D., Chereches N.C. "Efficiency improvement of photovoltaic panels by using air cooled heat sinks." *Energy Procedia,* vol. 85, pp. 425-432, January. 2016.

[41] Verma V., Kane A., and Singh B. "Complementary performance enhancement of PV energy system through thermoelectric generation." *Renewable and Sustainable Energy Reviews,* vol. 58, pp. 1017-1026, May. 2016.

[42] Ali H., Yilbas B.S., and Al-Sulaiman F.A. "Segmented thermoelectric generator: Influence of pin shape configuration on the device performance." *Energy,* vol. 111, pp. 439-452, September. 2016.

[43] Soprani S., Haertel J.H.K., Lazarov B.S., Sigmund O. and Engelbrecht K. "A design approach for integrating thermoelectric devices using topology optimization." *Applied Energy*, vol. 176, pp. 49-64, August. 2016.

[44] Kalogirou S.A., Tripanagnostopoulos Y. "Hybrid PV/T solar systems for domestic hot water and electricity production." *Energy Conversion and Management*, vol. 47, pp. 3368-3382, January. 2006.

[45] Ali H. H., Ahmed M., Abdel-Gaied S.M. "Hybrid PV/T solar systems for domestic hot water and electricity production." *Energy Conversion and Management*, vol. 47, pp. 3368-3382, January. 2006.

[46] Wu S.Y., Zhang Q.L., Xiao L., Guo F.H. "A heat pipe photovoltaic/thermal (PV/T) hybrid system and its performance evaluation." *Energy and Buildings*, vol. 43, pp. 3558-3567, September. 2011.

[47] Michael J.J., Iniyan S., Goic R. "Flat plate solar photovoltaic–thermal (PV/T) systems: A reference guide" *Renewable and Sustainable Energy Reviews*, vol. 51, pp. 62-88, June. 2015.

[48] Hu M., Zheng R., Pei G., Wang Y., Li J. and Ji J."Experimental study of the effect of inclination angle on the thermal performance of heat pipe photovoltaic/thermal (PV/T) systems with wickless heat pipe and wire-meshed heat pipe." *Applied Thermal Engineering* (2016), doi: http://dx.doi.org/10.1016/j.applthermaleng. 2016.06.003

[49] Jouhara H., Szulgowska-Zgrzywa M., Sayegh M.A., Milko J., Danielewicz J., Nannou T.K. and Lester S.P. "The performance of a heat pipe based solar PV/T roof collector and its potential contribution in district heating applications." *Energy*, vol. xxx, pp. 1-9, April. 2016.

[50] Ntsaluba S., Zhu B. and Xia X. "Optimal flow control of a forced circulation solar water heating system with energy storage units and connecting pipes." *Renewable Energy*, vol. 89, pp.111-112, Nov. 2015.

[51] Tang X., Quan Z. and Zhao Y." Experimental investigation of solar panel cooling by a novel micro-heat pipe array." *Energy Power Eng,* vol. 2, pp. 171–174, January.2010.

[52] Sotehi O., Chaker A., Maalouf C. "Hybrid PV/T water solar collector for net zero energy building and fresh water production: A theoretical approach." *Desalination*, vol. 385, pp. 1-11, May. 2016.

[53] Aste N., Leonforte F. and Del Podro C. "Design, modeling and performance monitoring of a photovoltaic–thermal (PVT) water collector." *Solar Energy*, vol. 112, pp. 85-99, February. 2015.

[54] Kroi A., Prabst A., Hamberger S., Spinnler M., Tripanagnostopoulos Y. and Sattelmayer T. "Development of a seawater-proof Hybrid Photovoltaic/Thermal solar collector." *International Conference on Alternative Energy*, vol. 52, pp. 93-103, 2014.

[55] Tonui J.K. and Tripanagnostopoulos Y. "Performance improvement of PV/T solar collectors with natural air flow operation." *Solar Energy*, vol. 82, pp. 1-12, January. 2008.

[56] Tonui J.K. and Tripanagnostopoulos Y. "Improved PV/T solar collectors with heat extraction by forced or natural air circulation." *Renewable Energy*, vol. 32, pp. 623-637, April. 2007.

[57] Tripanagnostopoulos Y., Yianoulis P. and Patrikios D. " Hybrid PV/TC solar system." *Renewable Energy*, vol. 8, pp. 505-508, August. 1996.

[58] Tripanagnostopoulos Y. "Aspects and improvements of hybrid photovoltaic/thermal solar energy systems." *Solar Energy*, vol. 81, pp. 117-1131, September. 2003.

[59] Tripanagnostopoulos Y., Nousia T., Souliotis M. and Yianoulis P. "Hybrid photovoltaic/thermal solar systems." *Solar Energy*, vol. 72, pp. 217-234, March. 2002.

[60] Tripanagnostopoulos Y. "New designs of building integrated solar energy systems." *Energy Procedia*, vol. 57, pp. 2186-2194, 2004.

[61] Rahul S.R. and Hariharan R. " Performance Study of Solar Photovoltaic Thermal Collector Integrated with Cooling System." *International Journal of Emerging Engineering Research and Technology*, vol. 2, pp. 132-145, 2004.

[62] Hosseini R., Hosseini N. and Khorasanizadeh H. "An experimental study of combining a photovoltaic system with a heating system." *Photovoltaic Technology*, pp. 2993-3000, May. 2011.

[63] Tan W.C., Chong K.K. and Tan M.H. "Performance study of water-cooled multiple-channel heat sinks in the application of ultra-high concentrator photovoltaic system." *Solar*

Energy, pp. 314-327, March. 2017.

[63] Huang M.J., Eames P.C. and Norton B. "Thermal regulation of building-integrated photovoltaics using phase change materials." *International Journal of Mass and Heat Transfer*, vol. 47, pp. 2715-2733, June. 2004.

[64] Huang M.J., Eames P.C. and Norton B. "Phase change materials for limiting temperature rise in building integrated photovoltaics." *Solar Energy*, vol. 80, pp. 1121-1130, September. 2006.

[65] da Cunha J.P. and Eames P. "Thermal energy storage for low and medium temperature applications using phase change materials – A review." *Applied Energy*, vol. 177, pp. 227-238, September. 2016.

[66] Liu L., Su D., Tang Y. and Fang G. "Thermal conductivity enhancement of phase change materials for thermal energy storage: A review." *Renewable and Sustainable Energy Reviews*, vol. 62, pp. 305-317, September. 2016.

[67] Su D., Jia Y., Alva G., Liu L and Fang G. "Comparative analyses on dynamic performances of photovoltaic–thermal solar collectors integrated with phase change materials." *Energy Conversion and Management*, vol. 131, pp. 79-89, January. 2017.

[68] Wang T., Wang S., Luo R., Zhu C., Akiyama T. and Zhang Z. "Microencapsulation of phase change materials with binary cores and calcium carbonate shell for thermal energy storage." *Applied Energy*, vol. 171, pp. 113-119, June. 2016.

[69] Hachem F., Abdulhay B., Ramadan M., El Hage H., El Rab M.G. and Khaled M. "Improving the performance of photovoltaic cells using pure and combined phase-change materials - Experiments and transient energy balance." *Renewable Energy*, vol. 107, pp. 567-575, February. 2017.

[70] Hasan A., Sarwar J., Alnoman H. and Abdelbaqi S. "Yearly energy performance of a photovoltaic-phase change material (PV-PCM) system in hot climate." *Solar Energy*, vol. 146, pp. 417-429, Apr. 2017.

[71] Sardarabadi M., Passandideh-Fard M., Maghrebi M.J. and Ghazikhani M. "Experimental study of using both ZnO/ water nanofluid and phase-change material (PCM) in photovoltaic thermal systems." *Solar Energy Materials and Solar Cells*, vol. 161, pp. 62-69, Nov. 2016.

[72] Chandel S.S. and Agarwal T. "Review of cooling techniques using phase-change materials for enhancing efficiency of photovoltaic power systems." *Renewable and Sustainable Energy Reviews*, vol. 73, pp. 1342-1351, March. 2017.

[73] Su D., Jia Y., Alva G., Liu L and Fang G. "Comparative analysis on dynamic performances of photovoltaic–thermal solar collectors integrated with phase change materials." *Energy Conversion and Management*, vol. 131, pp. 79-89, November. 2016.

[74] Chinamhora T., Cheng G., Tham Y. and Irshad W." PV Panel Cooling System for Malaysian Climate Conditions.", *International Conference on Energy and Sustainability*, April 27, 2013, Karachi, Pakistan.

[75] Zhu L., Boehm R.F., Wang Y., Halford C. and Sun Y. "Water immersion cooling of PV cells in a high concentration system." *Solar Energy Materials and Solar Cells*, vol. 95, pp. 538-545, February. 2011.

[76] Abrahamyan Y.A., Serago V.I., Aroutiounian V.M., Stafeev V.I., Karamian G.G., Martoyan G.A. and Mouradyan A.A. "The efficiency of solar cells immersed in liquid dielectrics." *Solar Energy Materials and Solar Cells*, vol. 73, pp. 367-375, August. 2002.

[77] Wang Y., Fang Z., Zhu L., Huang Q., Zhang Y. and Zhang Z. "The performance of silicon solar cells operated in liquids." *Applied Energy*, vol. 86, pp. 1037-1042, August. 2009.

[78] Rosa-Clot M., Rosa-Clot P., Tina G.M. and Scandura P.F. "Submerged photovoltaic solar panel: SP2." *Renewable Energy*, vol. 35, pp. 1862-1865, August. 2010.

[79] Han X., Wang Y. and Zhu L. "Electrical and thermal performance of silicon concentrator solar cells immersed in dielectric liquids." *Applied Energy*, vol. 88, pp. 4481-4489, December. 2011.

[80] Sun Y., Wang Y., Zhu L, Yin B., Xiang H. and Huang Q. "Direct liquid-immersion cooling of concentrator silicon solar cells in a linear concentrating photovoltaic receiver." *Energy*, vol. 65, pp. 264-271, February. 2014.

[81] Xiang H., Wang Y., Zhu L., Han X., Sun Y. and Zhao Z. "3D numerical simulation on heat transfer performance of a cylindrical liquid immersion solar receiver." *Energy Conversion and Management*, vol. 64, pp. 97-105, December. 2012.

[82] Arpin A. K., Losego M.D., Cloud A.N., Ning H., Mallek J., Sergeant N. P., Zhu L., Yu Z., Kalanyan B¸, Parsons G.N., Girolami G.S., Abelson J.R., Fan S. and Braun P.V. "Three-dimensional self-assembled photonic crystals with high temperature stability for thermal emission modification." *Nature Communications*, pp. 1-6, October. 2013.

[83] Zhu L, Raman A., Wang K.X., Anoma M.A. and Fan S. "Radiative cooling of solar cells." *Optica*, vol. 1, pp. 32-38, July. 2014.

[84] Cao C. , Li H. , Feng G. , Zhang R. and Huang K. "Research on PV/T – Air Source Heat Pump Integrated Heating System in Severe Cold Region." *Procedia Engineering*, vol. 146, pp. 410-414, August. 2016.

[85] Tiwari A., Sodha M.S. , Chandra A and Joshi J.C. "Performance evaluation of photovoltaic thermal solar air collector for composite climate of India." *Solar Energy Materials and Solar Cells*, vol. 90, pp. 175-189, January. 2006.

[86] Mojumder J.C., Ong H.C., Chong W.T., Izadyar N. and Shamshirband S. "The intelligent forecasting of the performances in PV/T collectors based on soft computing method". *Renewable and Sustainable Energy Reviews*, in press http://dx.doi.org/10.1016/j.rser.2016.11.225.

[87] Kasaeian A., Khanjari Y., Golzari S., Mahian O and Wongwises S. "Effects of Forced Convection on the Performance of a Photovoltaic Thermal System: An Experimental study." *Experimental Thermal and Fluid Science*, Feb. 2017.

[88] Saygin H., Nowzari R., Mirzaei N., and Aldabbagh L.B.Y. "Performance evaluation of a modified PV/T solar collector: A case study in design and analysis of experiment: An Experimental study." *Solar Energy*, vol. 141, pp. 210-221, Dec. 2016.

[89] Senthil Kumar R., Puya Priyadharshini N. and Natarajan E. "Experimental and Numerical Analysis of Photovoltaic Solar Panel using Thermoelectric Cooling." *Indian Journal of Science and Technology*, vol. 8, pp. 1-9, December. 2015.

[90] Wang S., Shi J., Chen H., Schafer S.R., Munir M., Stecker G., Pan W., Lee J.J. and Chen C.L. "Cooling design and evaluation for photovoltaic cells within constrained space in a CPV/CSP hybrid solar system." *Applied Thermal Engineering*, vol. 110, pp. 369-381, Jan. 2017.

[91] Borkar D.S., Prayagi S.V. and Gotmare J. "Performance Evaluation of Photovoltaic Solar Panel Using Thermoelectric Cooling." *International Journal of Engineering Research*, vol. 3, pp. 536-539, September. 2014.

[92] Benghanem M, Al-Mashraqi A.A. and Daffalla K.O. "Performance of solar cells using thermoelectric module in hot sites." *Renewable Energy*, vol. 89, pp. 51-59, December. 2015.

[93] Najafi H and Woodbury K. "Feasibility Study of Using Thermoelectric Cooling Modules for Active Cooling of Photovoltaic Panels." *ASME Proceedings*, vol. 6, pp. 1743-1751, November. 2012.

[94] Ahadi S, Hoseini H.R. and Faez R. "Using thermoelectric devices in photovoltaic cells in order to increase efficiency." *Indian Journal of Science and Research*, vol. 2, pp. 20-26, 2014.

[95] Najafi H and Woodbury K. "Optimization of a cooling system based on Peltier effect for photovoltaic cells." *Solar Energy*, vol. 91, pp. 152-160, May.2013.

[96] Shukla A., Kant K., Sharma A. and Biwole P.H. "Cooling methodologies of photovoltaic module for enhancing electrical efficiency: A review." *Solar Energy Materials and Solar Cells*, vol. 160, pp. 275-286, Feb. 2017.

[97] van Sark W.G.J.H.M. "Feasability of photovoltaic-thermoelectric hybrid modules." *Applied Energy*, vol. 88, pp. 2785-2790, August.2011.

[98] Yang D and Yin H. "Energy Conversion Efficiency of a Novel Hybrid Solar System for Photovoltaic, Thermoelectric, and Heat Utilization." *IEEE Transactions on Energy Conversion*, vol. 26, pp. 662-670, March.2011.

[99] Kane A., Verma V., Singh B. "Optimization of thermoelectric cooling technology for an active cooling of photovoltaic panel". *Renewable and Sustainable Energy Reviews*, in press http://dx.doi.org/10.1016/j.rser.2016.11.114

[100] Irshad K., Habib K., Basrawi F. and Saha B.B. "Study of a thermoelectric air duct system assisted by photovoltaic wall for space cooling in tropical climate." *Energy*, vol. 119, pp. 504-522, Jan. 2017.

[101] Enescu D. and Spertino F. "Applications of hybrid photovoltaic modules with thermoelectric cooling.". *8th International Conference on Sustainability in Energy and Buildings*, SEB-16, 11-13 September. 2016.

[102] Kusakana K. and Vermaak H.J. "Hybrid diesel generator/renewable energy system performance modelling." *Renewable Energy* 67 (2014):97-102.

[103] Riffonneau Y., Bacha S., Barreul F and Ploix S. "Optimal Power Flow Management for Grid Connected PV Systems with Batteries." *IEEE Transactions on Sustainable Energy*, vol. 2, pp. 302-312, July. 2011.

[104]Alteragy.co.za, 'South Africa: EnerSol Solar Panel 250W', 2017, [Online]. Available: https://www.alternagy.co.za/shop/enersol-solar-panel-250w/ [Accessed: 02- March- 2018]

[105] Ge Z., Wang H., Wang H., Zhang S and Guan X. "Exergy Analysis of Flat Plate Collectors." *Entropy*, vol. 16, pp. 2549-2567, May. 2014.

[106] Sichilalu S., Mathaba T and Xia X. "Optimal control of a wind–PV-hybrid powered heat pump water heater." *Applied Energy* 185 (2017):1173-1184.

[107] "ZKSJ PUMP-Circulation Pump Manufacturer", Circulation Pump-DC50K, 2017. [Online]. Available: https://zksjpump.com/product/dc50k/. [Accessed: 15- Apr- 2018].

[108] Sauran.net. (2017) *Station Details - Southern African Universities Radiometric Network*. [online] Available at http://www.sauran.net/ShowStation.aspx?station=7 [Accessed 15 Nov.2017].

[109] Ogunjuyigbe A.S.O., Ayodele T.R. and Akinola O.A. "Optimal allocation and sizing of PV/wind/split-diesel/battery hybrid energy system for minimizing life cycle cost, carbon emission and dump energy of remote residential building." *Applied Energy* 171(2016):71-153.

[110] Capehart BL, Kennedy WJ, Turner WC. Guide to energy management. 5th ed. Indian Trail, United States: The Fairmont Press, Inc.; 2008.

[111] T. Media, "Historic inflation South Africa – historic CPI inflation South Africa", Inflation.eu, 2017. [Online]. Available: http://www.inflation.eu/inflation-rates/south-africa/historic-inflation/cpi-inflation-south-africa.aspx. [Accessed: 16- Jan-2018].

[112] PriceCheck, " Enersol 250W Solar Panel ", 2018. [Online]. Available: http://www.pricecheck.co.za/offers/95902374/Enersol+250W+Solar+Panel.[Accessed: 17- April- 2018].

[113] Sustainable, "Flat Plate Collectors ", 2018. [Online]. Available: http://www.sustainable.co.za/water-heating/solar-heating-collectors/flat-plate-collectors.html.[Accessed: 18- April- 2018].

[114] PriceCheck, "Gap 150l Eco Green Solar Ready Geyser ", 2018. [Online]. Available: https: //www.pricecheck.co.za/offers/87715384. [Accessed: 18- April- 2018].

[115] ZKSJ PUMP, "Circulation Pump DC50K ", 2018. [Online]. Available: https://zksjpump.com/product/dc50k/.[Accessed: 18- April- 2018].

Appendixes

Appendix A: Exogenous data (30-minute averaged)

Appendix A1: Summer input data

Time	Direct normal irradiance (W/m²)	Ambient air temperature (°C)	Inlet water temperature (°C)	Hot water consumption (l)
00:00	0	21.96	25	0
00:30	0	20.94	25	0
01:00	0	20.86	25	0
01:30	0	20.32	25	0
02:00	0	20.39	25	0
02:30	0	20.46	25	0
03:00	0	21.04	24	0
03:30	0	20.62	24	0
04:00	0	20.22	24	0
04:30	0	18.88	24	0
05:00	0	18.2	24	0
05:30	0	17.19	24	0
06:00	36.467	18.05	24	0
06:30	77.6371	17.77	24	0
07:00	160.288	18.29	23	0
07:30	262.911	19.46	23	0
08:00	449.131	21.58	23	0
08:30	576.487	24.69	23	0
09:00	752.366	27.49	23	0

108

09:30	744.271	26.89	23	0
10:00	936.704	27.43	23	0
10:30	952.619	27.93	23	0
11:00	1063.29	28.34	23	0
11:30	1127.9	29.65	23	0
12:00	1140.56	30.12	24	0
12:30	1174.31	30.24	24	0
13:00	1121.5	30.5	24	91
13:30	1096.57	30.39	24	0
14:00	1056.41	31.3	24	0
14:30	1026.3	32.08	24	0
15:00	929.177	32.51	24	0
15:30	837.918	32.12	24	0
16:00	708.317	32.32	24	0
16:30	618.933	32.34	24	0
17:00	491.122	32.44	24	0
17:30	359.921	32.45	25	0
18:00	232.078	32.13	25	0
18:30	113.173	30.71	25	120
19:00	21.175	28.86	25	0
19:30	0	27.17	25	120
20:00	0	25.86	25	0
20:30	0	25.71	25	0
21:00	0	23.21	25	104
21:30	0	22.25	25	0
22:00	0	21.46	25	0
22:30	0	20.89	25	0
23:00	0	20.24	25	0
23:30	0	19.84	25	0

Appendix A2: Winter Input Data

Time	Direct normal irradiance (W/m²)	Ambient air temperature (°C)	Inlet water temperature (°C)	Hot water consumption (l)
00:00	0	10.04	15	0
00:30	0	9.55	15	0
01:00	0	9.24	15	0
01:30	0	9.35	15	0
02:00	0	8.94	15	0
02:30	0	8.37	15	0
03:00	0	7.839	15	0
03:30	0	6.25	14	0
04:00	0	4.865	14	0
04:30	0	5.235	14	0
05:00	0	4.613	14	0
05:30	0	4.057	14	0
06:00	0	4.971	14	0
06:30	0	4.562	13	0
07:00	0	5.201	13	0
07:30	40.256	4.872	13	0
08:00	117.074	4.489	13	0
08:30	213.085	6.863	13	0
09:00	310.381	8.47	13	0
09:30	405.021	12.06	13	0
10:00	488.506	13.99	13	0
10:30	555.914	13.79	13	0
11:00	604.2	14.84	13	0
11:30	637.29	15.76	13	0
12:00	653.092	16.7	14	0

116

12:30	654.919	17	14	0
13:00	637.945	17.34	14	70
13:30	607.54	18.02	14	0
14:00	555.746	18.8	14	0
14:30	494.613	18.9	14	0
15:00	419.061	19.33	14	0
15:30	331.196	19.19	14	0
16:00	234.224	18.81	14	0
16:30	133.297	18.07	14	0
17:00	49.1995	17.11	14	120
17:30	0.402176	15.46	14	0
18:00	0	14.91	15	120
18:30	0	13.86	15	0
19:00	0	13	15	0
19:30	0	11.89	15	100
20:00	0	12.16	15	0
20:30	0	10.93	15	0
21:00	0	10.35	15	0
21:30	0	10.13	15	0
22:00	0	9.86	15	0
22:30	0	9.98	15	0
23:00	0	9.58	15	0
23:30	0	8.51	15	0

Appendix B: Performance comparison between baseline and optimal switching control

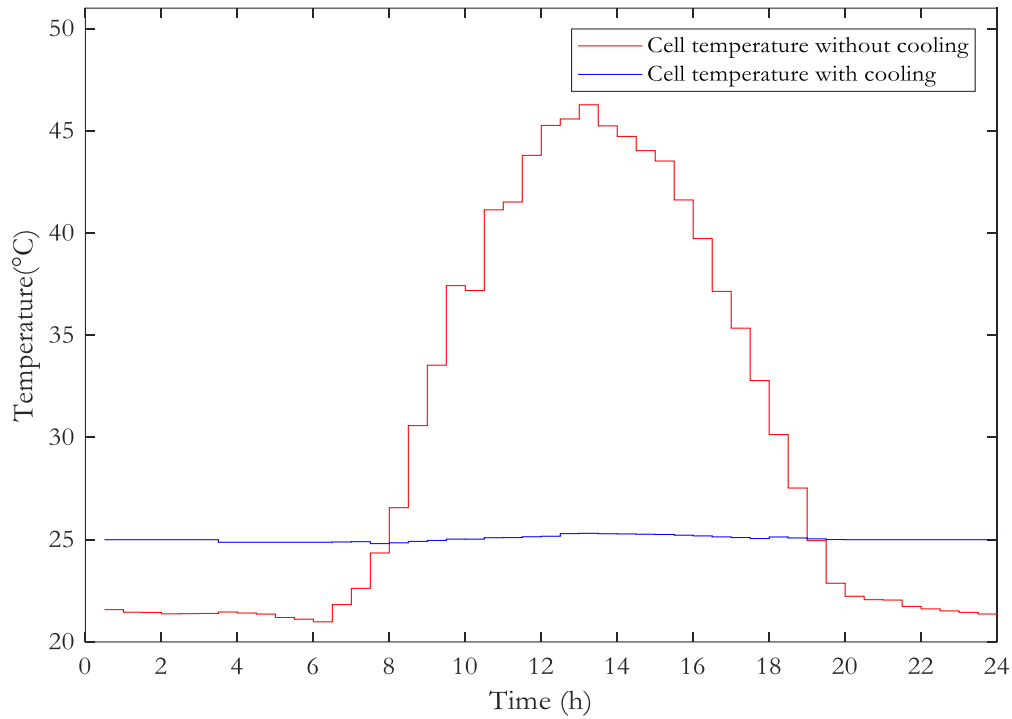## Appendix B1: Summer performance
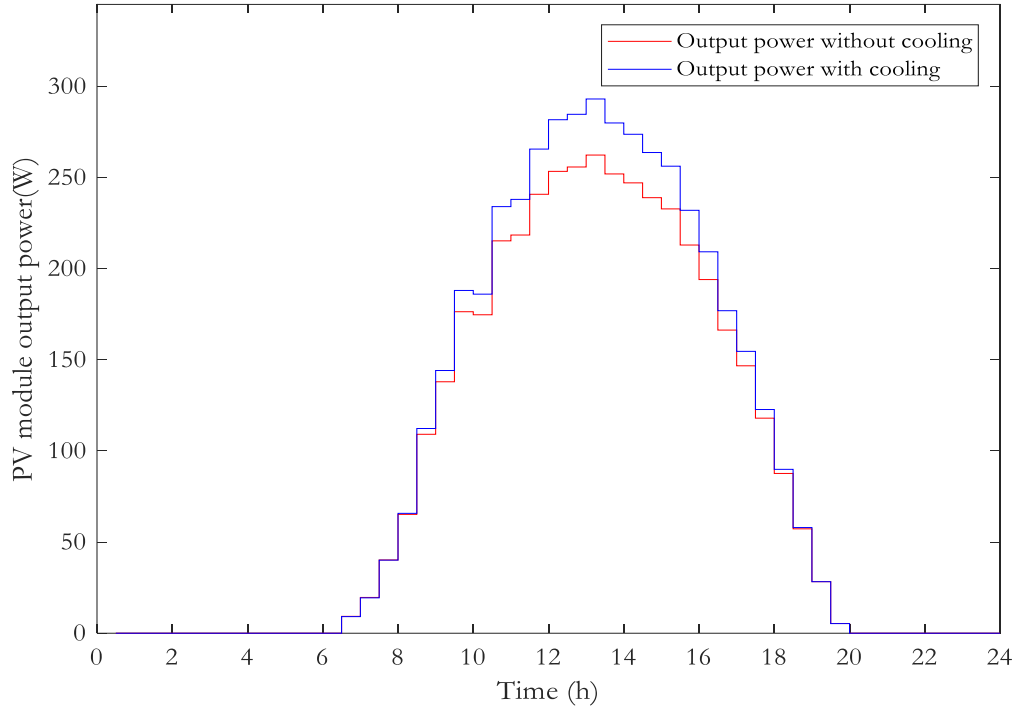

Figure B1-1: PV cell temperature comparison during summer
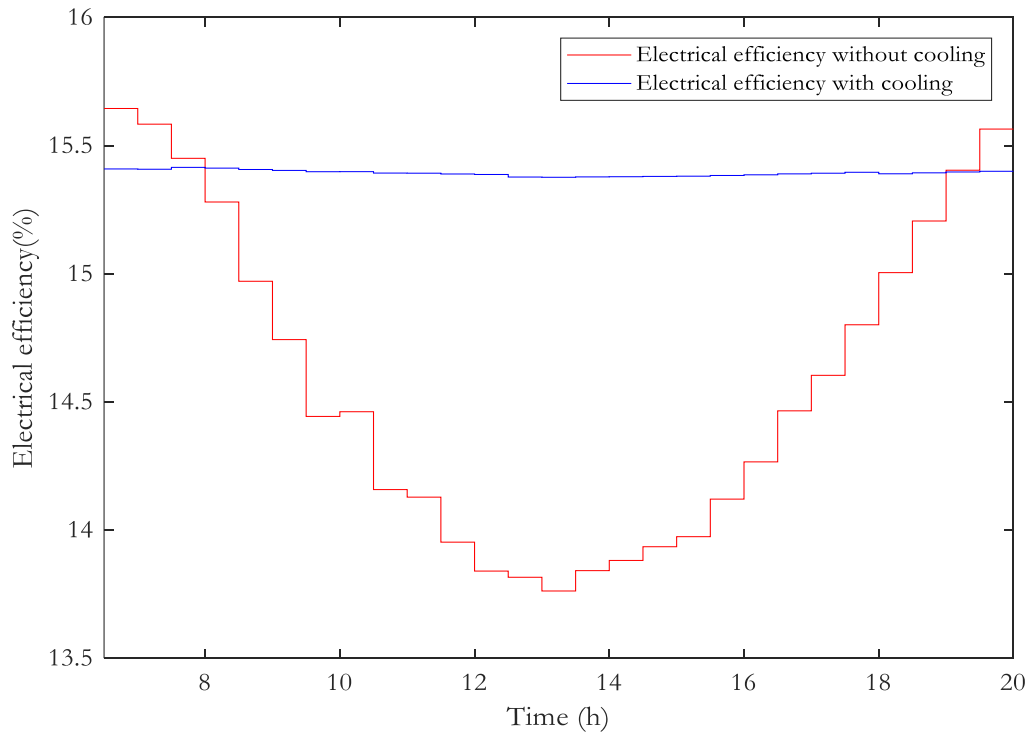
Figure B1-2: PV output power comparison during summer

Figure B1-3: PV electrical efficiency comparison during summe
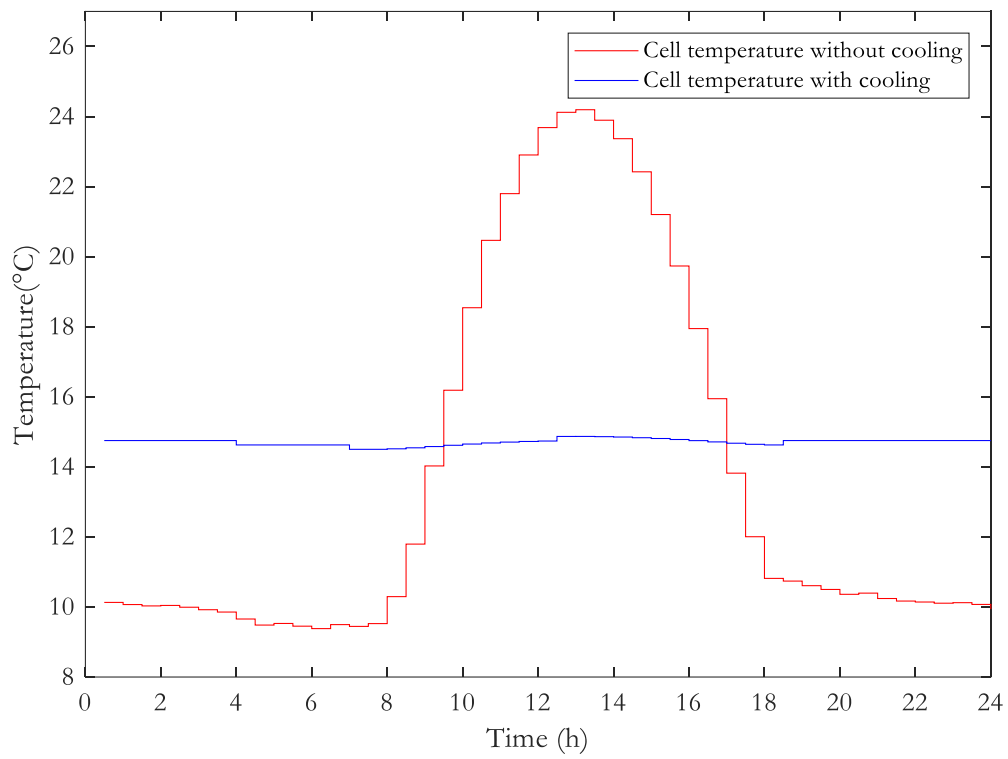
119

Appendix B2: Winter performance

Figure B2-1: PV cell temperature comparison during winter
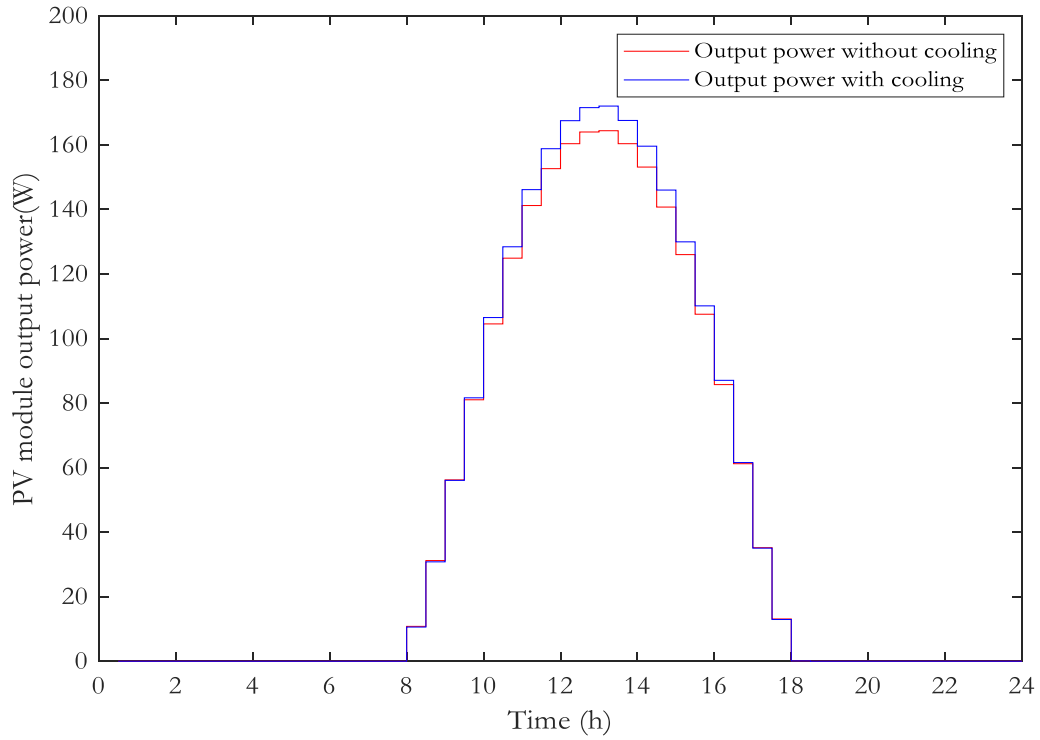
120

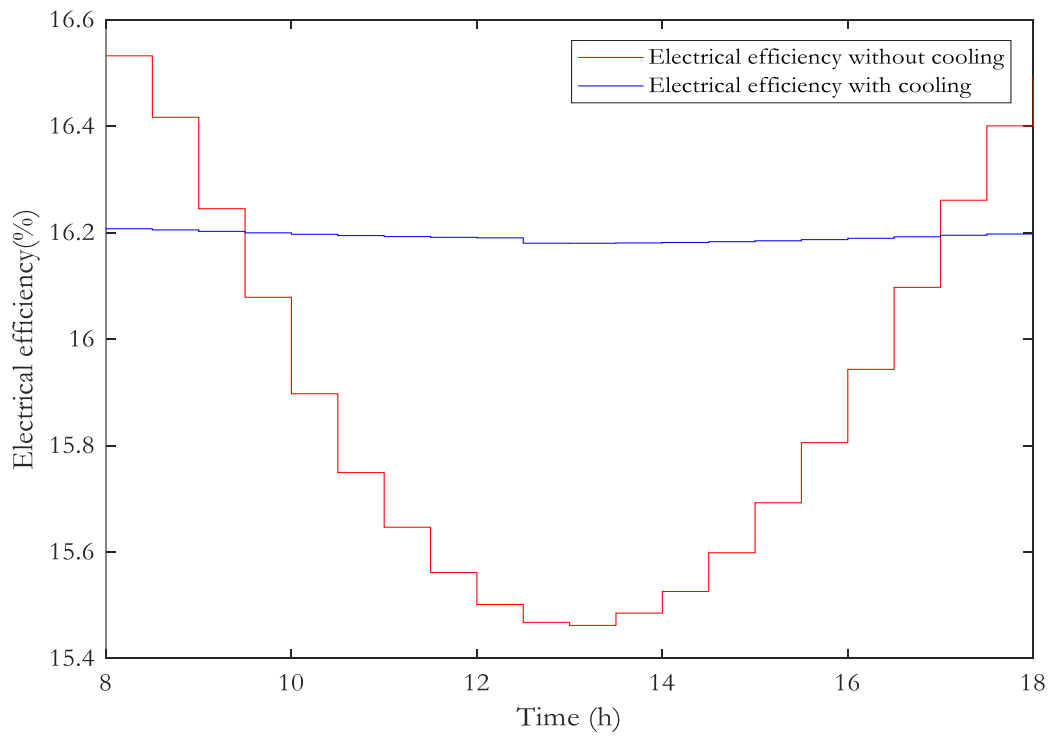Figure B2-2: PV output power comparison during winter

Figure B2-3: PV electrical efficiency comparison during winter

121